Abstract

NICHOLSON, MARK ANDREW. Thermal Loading and Uncertainty Analysis of High Level Waste in Yucca Mountain. (Under the direction of Man-Sung Yim).

Based on the current discharge rate of nuclear reactors the total inventory of SNF in the U.S. will exceed the current design capacity of the Yucca Mountain repository by 2010. This leaves no room for future SNF discharged from the current nuclear fleet or reactors that potentially will be built. Expansion of the Yucca Mountain repository would provide a large economical benefit as siting and developing a second repository would be a drawn out, divisive and expensive process. The goal of this work is to analyze the thermal loading of SNF into Yucca Mountain in order to investigate the feasibility of repository capacity increase without exceeding the thermal limitations set by the DOE. To examine the feasibility of repository capacity expansion, the concept of variable drift spacing using uniform loading and the concept of variable drift thermal loading using a non-uniform following were investigated. To support the work, a thermal analysis model, SRTA, was employed to describe the temperature changes in the rock around the waste packages against thermal design limits as a function of spent fuel characteristics and composition. Results indicated that, by implementing the scheme of variable drift spacing or variable drift thermal loading, the capacity of the repository could be increased from the legislative limit of 70,000 MTU without violating the thermal limits of the drift wall (200˚C) and the limit midway between the drifts (96˚C). By implementing different loading criteria it was found that the capacity of the repository could be increased by as much as 48% based on the mean estimate. This thesis does not include capacity increases that could result from extending the repository

footprint, the number of levels in the repository or the appropriateness of the thermal design limits.

Thermal Loading and Uncertainty Analysis of High Level Waste in Yucca Mountain

by
Mark Andrew Nicholson

A thesis submitted to the Graduate Faculty of
North Carolina State University
in partial fulfillment of the
requirements for the Degree of
Master of Science

Nuclear Engineering

Raleigh, North Carolina

2007

Approved By:

Dr. Man-Sung Yim (Chair of Advisory Committee)	Dr. J. Michael Doster

Dr. Jeffrey Ray Thompson

Dedication

I would like to thank God for all the blessings he has bestowed upon my family and me. Alisa thank you for all your love, patience, and support. Also thank you for our two beautiful daughters. I would also like to thank my family for supporting me through my academic years.

Biography

Mark Andrew Nicholson received a Bachelors of Science in Nuclear Engineering from North Carolina State University (NCSU) in May 2002. After which he began work with Scientech, LLC (Energy*Solutions*, LLC) working in the Decontamination and Decommissioning division. Mark returned in the spring of 2005 to get his Masters in Nuclear Engineering.

Acknowledgements

I would like to thank my advisors Drs. Yim, Doster, and Thompson. I would like to also thank Dr. Jun Li for helping me and being there to answer questions when I needed help. Without their help this work would not have been possible. Dr. McNelis thank you for your help throughout my thesis work. I would also like to thank Judith Cuta of Pacific Northwest Laboratory for helping me with COBRA-SFS.

Table of Contents

List of Figures

List of Tables

List of Abbreviations

Abbreviation		Definition
APD	–	Areal Power Density
ATW	–	Accelerator-driven Transmutation of Waste
BWR	–	Boiling Water Reactor
CB	–	Crystal Ball
DHLW	–	Defense High-Level Waste
DOE	–	Department of Energy
HTOM	–	High-Temperature Operating Mode
LBNL	–	Lawrence Berkeley National Laboratory
LLNL	–	Lawrence Livermore National Lab
LTOM	–	Low Temperature Operating Mode
MTU	–	Metric Tons Uranium: the weight of spent nuclear fuel (SNF) after irradiation
NWPA	–	Nuclear Waste Policy Act of 1982
PWR	–	Pressurized Water Reactor
SNF	–	Spent Nuclear Fuel
SNL	–	Sandia National Laboratory
SRTA	–	Simplified Repository Thermal Analysis
TPA	–	Total-System Performance Assessment

1 Introduction

Siting a high level nuclear waste repository entails high economic, social, and political costs. Given the difficulty in siting the Yucca Mountain repository and the already identified need for additional capacity, the concept of expanding the capacity of the Yucca Mountain repository is of significant interest to the nuclear industry and the Department of Energy (DOE). As the capacity of the repository is limited by the decay heat inventory of the spent nuclear fuel in relation to the thermal design limits, expanding the capacity requires appropriate schemes for decay heat and spent fuel loading management.

The United States is faced with the disposal of waste from all commercial nuclear power plants since the first nuclear reactor went online. The nuclear waste from these reactors is a large concern for the commercial industry as the waste is currently being stored onsite. Most nuclear plants have started using dry storage as a means to store the spent fuel as the storage in the spent fuel pools is reaching capacity.

In 1983 the Nuclear Waste Policy Act of 1982 (NWPA) was signed, approving the development of a high-level nuclear waste repository. In December 1984, the DOE selected nine locations in six states as candidates for potential repository sites. The NWPA was amended in 1987 by congress that gave direction for the DOE to pursue only Yucca Mountain that is located on federally protected land within the boundaries of the Nevada Test Site in Nye County (Figure 1.1).

There were several reasons for choosing Yucca Mountain as the site suitable for the repository. Reasons for choosing Yucca Mountain included (DOE 2007):

- Remote location of the site. The closest inhabitant is 14 miles away.
- The geological makeup of the site. The geology is comprised of layers of volcanic rock call "Tuff."
- Located in a fairly arid climate that receives, on average, less than 7.5 inches of water a year.
- No natural geologic resources of value.

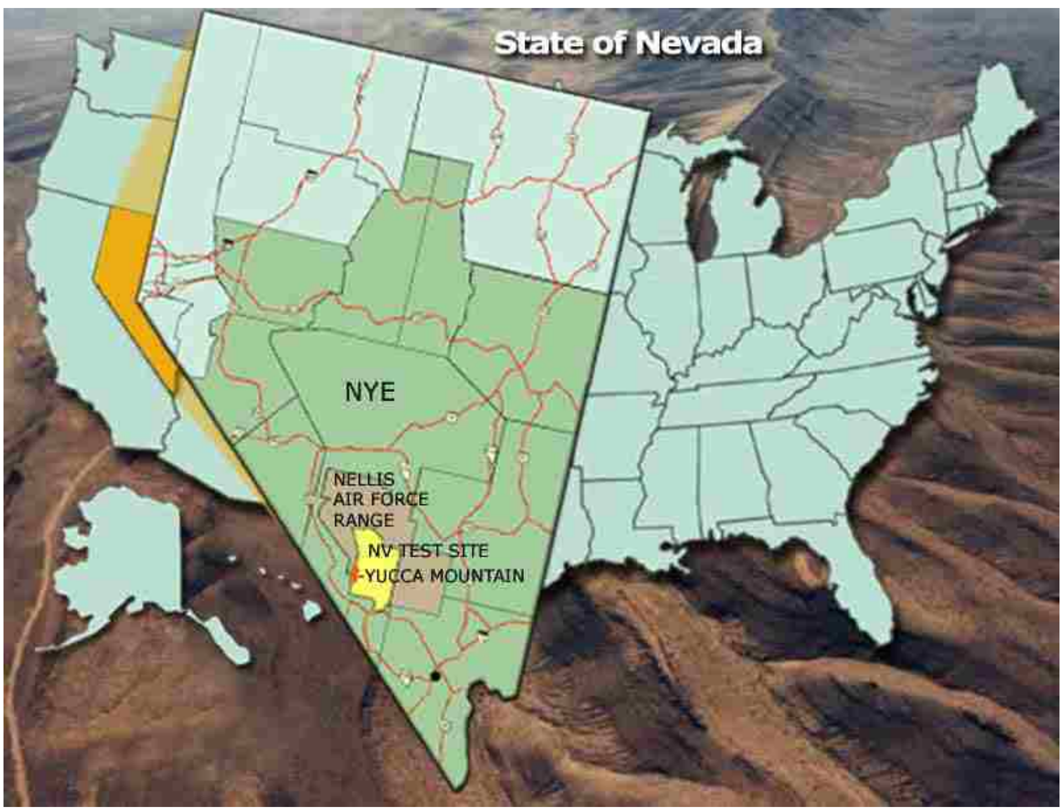

Figure 1.1: Location of Yucca Mountain (DOE 2007)

Under the amended NWPA, 70,000 metric tons of uranium (MTU) would be allowed to be stored at the Yucca Mountain repository. Of this total mass, the DOE will use ten percent of the capacity for the military/defense waste while the remaining 63,000 MTU is slated for commercial spent nuclear fuel (SNF). At the current discharge rate of nuclear fuel it is expected that by 2010 the planned capacity of 63,000 MTU of commercial SNF will have been reached, as seen in Table 1.1 (Stahala, 57).

Table 1.1: Cumulative SNF Discharged by Year

Year	**Cumulative SNF Discharged (MTU)**
2003	49,800
2004	51,700
2005	54,200
2006	55,800
2007	57,800
2008	59,600
2009	61,400
2010	63,400

As the nuclear industry is faced with the fact that the repository will reach capacity by 2010, it is essential to analyze how spent fuel is loaded into the repository. The current Yucca Mountain repository is based on a single level, fixed drift spacing design for a fixed area or footprint. Studies performed to date investigating the capacity of Yucca Mountain often assume that the loading of spent fuel is uniform throughout the repository and use the concept of a linear loading with areal power density (APD) as the metric. However, use of linear loading or APD can be problematic with the various cooling times involved. The temperature within the repository at any point in time is controlled by the integral of the heat deposited in the repository. The integral of the decay heat varies as a function of pre-loading cooling periods even for a fixed linear loading. A meaningful repository capacity analysis requires the use of a computer model that describes the time-dependent temperature distributions in the rock from the dissipation of the heat throughout the repository system.

If variations from the current Yucca Mountain repository design are to be considered, expanding the capacity of the repository would be pursued in several ways including: (1) increase the footprint size; (2) implement multiple-levels in the repository for the given footprint; (3) allow the drift distance to vary within thermal limits; and, (4) allow non-uniform loading of wastes into the drifts within thermal limits. Options (1) and (2) have been investigated by other researchers (EPRI, 2006).

The goal of this thesis is to analyze the thermal loading of SNF into Yucca Mountain in order to investigate the feasibility of increasing the repositories capacity without exceeding the thermal limitations set by the DOE. Specifically, options (3) and (4) were investigated for possible expansion of the Yucca Mountain repository capacity. To support the work, a thermal analysis model was employed to describe the temperature changes in the rock around the waste packages against the thermal design limits as a function of spent fuel characteristics and composition.

1.1 Objectives

The purpose of this work is to examine the effect of adopting variable drift spacing and using non-uniform drift loading of SNF on the capacity of the Yucca Mountain repository. A computer model was utilized for efficient repository heat transfer calculations and sensitivity and uncertainty analyses were performed to identify key parameters and to estimate the uncertainty in the results and understand how the repository capacity estimation would be affected by the uncertainty.

1.2 Tasks

Literature research was conducted to review and build upon previous related work. To properly analyze the thermal impact of SNF to the Tuff rock at Yucca Mountain, design parameters had to be determined from literature. Additionally, uncertainties in these parameters were researched in order to conduct a Monte Carlo uncertainty analysis of the repository rock heat transfer calculations.

The loading of spent fuel casks was also analyzed for both uniform and non-uniform (e.g. regionalized) loading to determine if the cask loading strategy has any effect on compliance with the thermal design limits for the Yucca Mountain repository. From the analysis of spent fuel cask loading it will determined if the thermal limits of the repository have been affected or not.

A nominal range sensitivity analysis was performed to determine which input parameters had the greatest impact on the thermal analysis. A five percent increase from the mean input values was assumed for this analysis. Based on this analysis and the design specifications it would be determined which parameters played an important role in the model. It was noted that certain parameters by design are constant such as the waste package spacing with no need for consideration in uncertainty analysis.

The final task for this project was to study the effects of implementing variable drift spacing and variable drift thermal loading on the Yucca Mountain repository capacity. The capacity increase of the repository was investigated based on the mean as well as the ninety-fifth percentile estimates. Additionally, a sensitivity analysis was performed on the effect of reducing input parameter uncertainty on repository capacity estimates.

2 Literature Review

In the next several sections, the work of a number of researchers, who analyzed the thermal loading of Yucca Mountain in order to examine the temperature distribution in the repository rock as well as to investigate whether the capacity of the repository could be increased, is reported. In the works cited, the researchers assumed that the repository was loaded uniformly throughout the drifts.

2.1 Argonne National Lab

The SINDA/G software (Gaski 1987) was used by Argonne National Laboratories to investigate the separation of spent nuclear waste to determine if repository capacity could be increased. SINDA/G is a thermal analyzer software package based on a finite difference method. Thermal convection from surface water infiltration through the porous rock was also included in the model. One of the proposed scenarios was to reprocess the spent fuel and remove the elements responsible for the decay heat that causes thermal limits to be reached. Five elements were considered in the separation process, i.e., Plutonium (Pu), Americium (Am), Cesium (Cs), Strontium (Sr), and Curium (Cm). Cs and Sr would be stored for 200-300 years while Pu, Am, and Cm would either be transmuted to a stable isotope or recycled for further power production in nuclear reactors. They found that by reducing the amount of waste and decay heat the capacity of the repository could be increased by as much as three times (Wigeland 2006).

2.2 Bechtel SAIC

Bechtel SAIC has investigated the thermohydrologic model of the repository using the TOUGHREACT code (Xu, et al. 2004) developed by Lawrence Berkley National Lab (LBNL). The model uses thermal-hydrologic-chemical seepage, which simulates the composition of water that could seep into the drifts and the composition of the gaseous phase. This study of the seepage of water includes the model of fractures in the Tuff rock where water flow can occur (Bechtel 2005).

Bechtel has also studied the impact of ventilation during the preclosure period. The investigation included how the decay heat affects the performance of both waste packages and the emplacement drift. The ventilation model they used simulated the heat transfer processes in and around a waste emplacement drift and predicted the heat removal by ventilation during the preclosure period. They estimated that eighty-eight percent of the heat would be removed during the preclosure period (Bechtel 2004).

2.3 Electric Power Research Institute

The Electric Power Research Institute (EPRI) has been involved in the analysis of increasing the capacity of the repository. EPRI has proposed several different layouts for the repository that would expand the footprint of the mountain. Figure 2.1 shows one scenario of increasing the footprint of the repository (EPRI 2006).

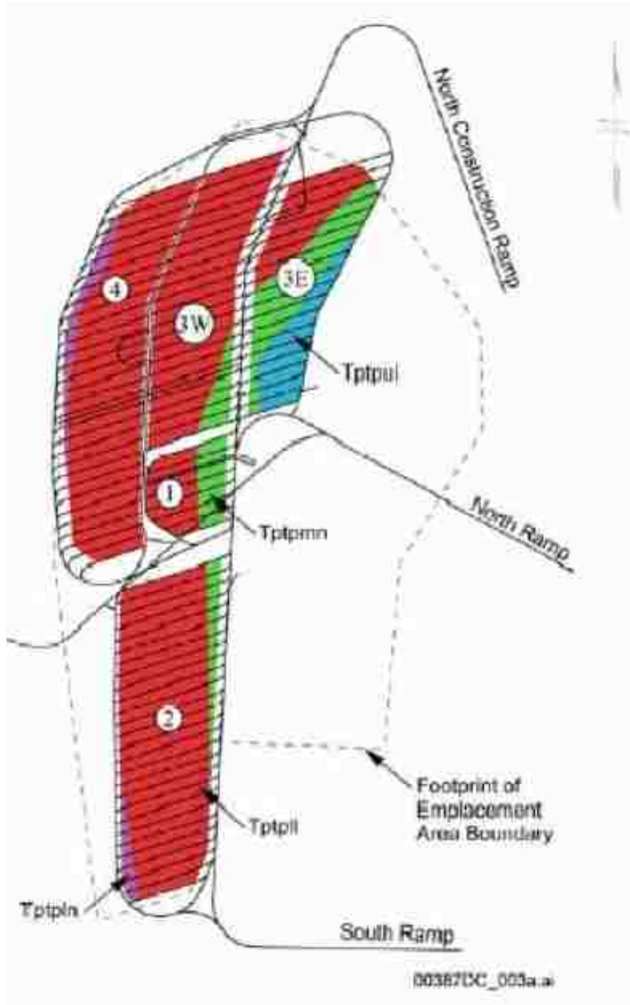

Figure 2.1: Proposed Repository Layout

A multi-level repository has also been proposed that would also increase the capacity to a large degree. For this multi-level design a relaxing of the thermal limit between the drifts for a 200-300 year period was also proposed. The computer code used by EPRI for the analysis was TOUGH2. The TOUGH2 code is a general-purpose numerical simulation program for multi-phase fluid and heat flow in porous and fractured media. By using this code they found for the primary block (original footprint) of the three-layer scheme that the capacity could be increased by two to three times (Ibid).

As a result of these analyses, EPRI estimated that the capacity could be increased at least four times the legislative limit to approximately 260,000 MTU. EPRI also hypothesized that with additional characterization of the repository that the capacity could be increased by nine times to approximately 570,000 MTU. Based on the increase in capacity there would be enough storage for the existing fleet and the expansion of the new nuclear fleet for at least several decades (Ibid).

2.4 Lawrence Berkley National Lab

The TOUGH computer code (Pruess et al. 1999) has been developed by Lawrence Berkley National Lab (LBNL) to determine the multi-phase fluid and heat flow in porous and fractured media. TOUGH code is based on an integral finite difference method for space discretization, and first-order fully implicit time differencing. The TOUGH2 code was developed for geothermal reservoir, nuclear waste disposal, unsaturated zone hydrology, and geologic storage of CO_2 (LBNL 2007).

University of California, Berkeley in conjunction with LBNL has studied the expansion of the repository resulting from the implementation of an accelerator-driven transmutation of waste (ATW) fuel cycle. They found that the number of waste packages could be reduced by a factor of ten through transmutation of nuclear waste (Cheon 2005).

LBNL has also studied the moisture conditions in the fractured rock in the repository. This study showed the effect of natural convection of moisture from high temperature locations to low temperature locations. Their simulation showed the significance of in-drift natural convection on the thermal-hydrological conditions in the fractured rock (Birkholzer 2006).

2.5 Lawrence Livermore National Lab

Lawrence Livermore National Lab (LLNL) used a multiscale thermohydrologic model to predict the thermal-hydrologic conditions in emplacement drifts and the surrounding Tuff rock. The NUFT code that was developed at LLNL was used to simulate a low-temperature operating mode (LTOM) of an expanded footprint (Glascoe 2004). Another study analyzed the impact of buoyant gas-phase flow inside the repository due to water infiltration into the repository. This study was important in showing the failure scenario of a waste package due to corrosion (Buscheck 2000).

2.6 Sandia National Laboratory

Sandia National Laboratory (SNL) developed a method for determining equivalent thermal loads for each type of spent fuel planned for emplacement in a proposed nuclear waste repository. The study included determining the thermal loading of commercial spent fuel and defense high-level waste (DHLW). This work is of importance due to the fact that the characterization of the DHLW was not previously known (Mansure 1991).

SNL has also studied natural convection of a LTOM repository design. The purpose of their study was to model different waste packages and determine the dominant mode of heat transfer. They found that thermal radiation was the dominant mode of heat transfer inside the drift and natural convection affected the variation in surface temperature on the hot waste packages (Itamura 2003).

3 Methods and Approaches

3.1 Computer Codes and Tools

To perform the tasks described in Chapter 2, several computer codes were implemented in this research. A list of codes used for this research follows:

- COBRA-SFS (Michener 1995)
    - Code used to analyze the thermal-hydraulic behavior of multi-assembly spent fuel storage systems.
    - The code is based on a finite difference approach to predict flow and temperature distributions of cask and fuel assemblies under natural and forced convection.
- COMSOL 3.3a (COMSOL 2007)
    - Based on three dimensional finite element approach
- Simplified Repository Thermal Analysis (SRTA) Code (Li, et al. 2007)
    - Based on three dimensional analytical solution
- Crystal Ball (Decisioneering 2007)
    - Monte Carlo simulation software package

3.2 Design Conditions

The design of the Yucca Mountain repository is a complex system and the thermal analysis of the repository can be a rather difficult undertaking. In order to analyze the thermal loading of the repository certain assumptions, which will be described in Section 3.3, were made. The SRTA code is based on an analytical solution that simplifies the thermal analysis.

The code is also based on a conduction model that uses a heat loss factor, which takes into account the loss of heat during the forced ventilation/convection period of the repository or otherwise known as the preclosure period.

The DOE has specified certain design limits in order to achieve the structural integrity of the repository. The limits that cannot be exceeded are the temperatures at various locations in the repository. These limits are based on studies done by the DOE that will be further discussed in Section 3.5.

3.3 Assumptions

The repository design analyzed in this work is based on a high-temperature operating mode (HTOM). The waste packages are spaced so that heat from radioactive decay will boil water in the surrounding rock. This water will vaporize and migrate away from the emplacement drifts to a point between the drifts where the temperature is less than the boiling point. At this point the vapor between the drifts will condense and flow through the system without ever contacting the waste packages that would lead to corrosion and eventual failure of the spent fuel cask. Figure 3.1 illustrates how water passes through the repository system.

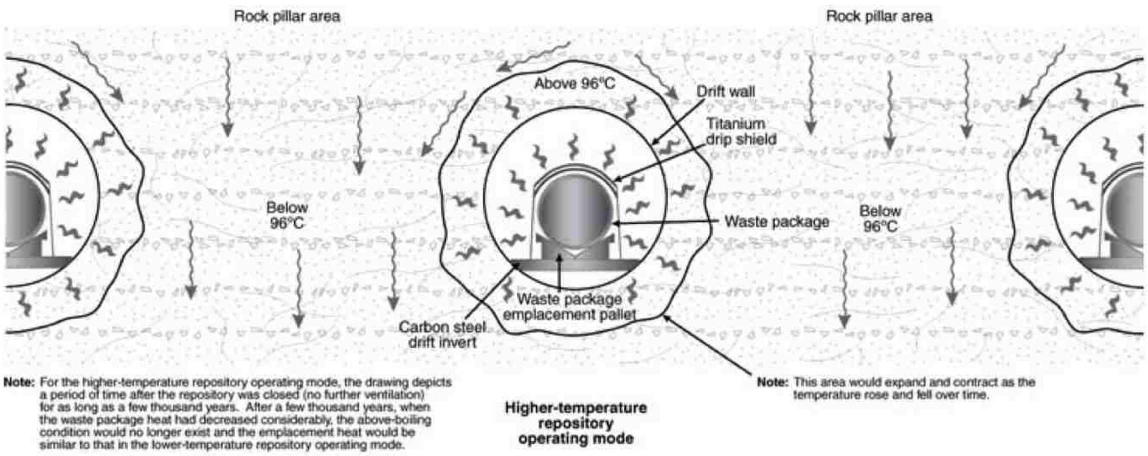

Figure 3.1: Repository Design (Wigeland, 5)

Assumptions that were made in the thermal analysis model are given in Table 3.1. The cooling time before the waste is emplaced inside the repository is very important to the thermal analysis since the decay of SNF is exponential. For example, during this twenty-five year period of interim storage, the estimated decay heat reduction was over ninety percent. Ventilation is also an important design aspect of the repository. The rate of ventilation plays a large role when analyzing the amount of heat removed from the waste packages in the drift.

Two models for calculating the temperature distribution for the repository were used; the SRTA code and COMSOL Multiphysics. The SRTA code is based purely on conduction while the COMSOL model is based on conduction and convection. SRTA utilizes a parameter known as the heat loss factor. This parameter takes into account the amount of heat removed from the system during the preclosure period.

Table 3.1: Model Assumptions

Interim Storage[1]	25 years
Forced Ventilation[2]	50-75 years
Volumetric Ventilation rate[3]	15 m^3/s
Heat Loss Factor[4]	70%[4] & 88%[5]

1 – Wigeland, 4
2 – Wigeland, 5
3 – DOE 2002a
4 – NRC 2002
5 – Bechtel, 108

The repository outline (see Figure 3.2), for this analysis is a fixed footprint area in the size of 4.9 square kilometers (NRC 2002). Throughout the thermal analysis the design criterion set by the DOE will be followed as closely as possible. Certain aspects such as the distance between drifts can be modified from its original distance of 81 meters. Decreasing the distance between drifts will increase the amount of SNF that can be stored in the mountain. Likewise, if the mass of the waste package (MTU/package) were increased, the capacity would also be increased. Both scenarios will be investigated to study how different techniques can increase the capacity of the repository.

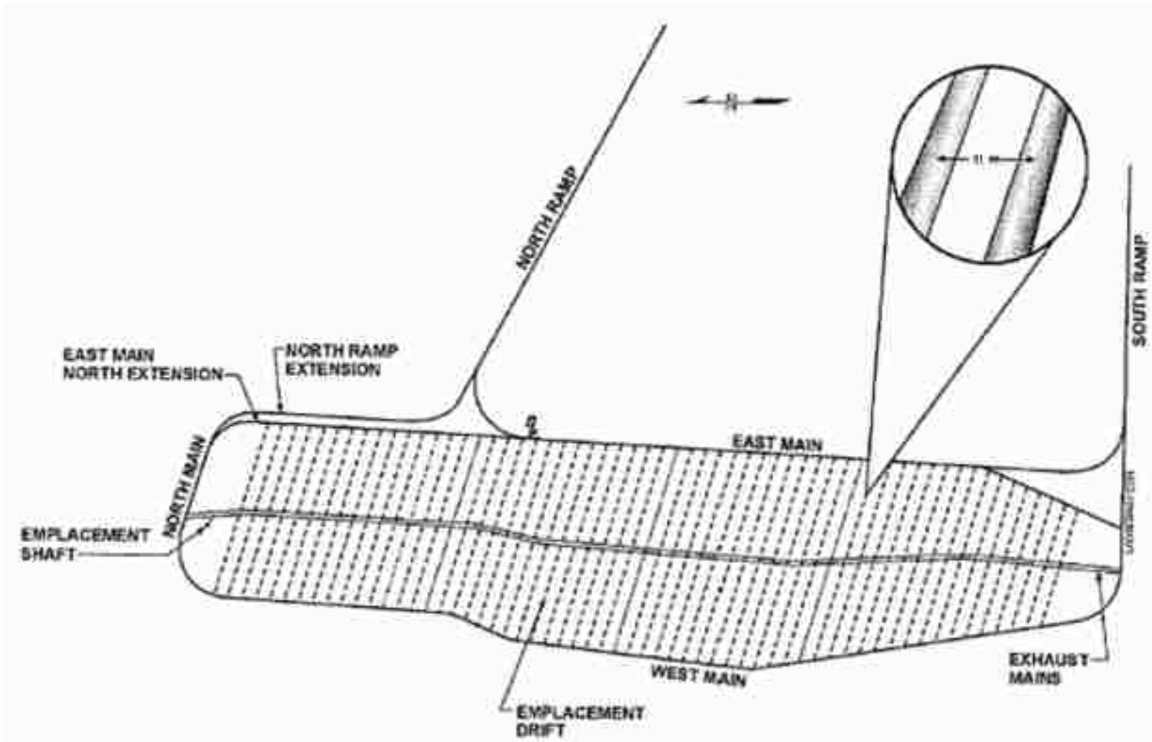

Figure 3.2: Yucca Mountain Repository Footprint

3.4 Loading

The concept of non-uniform loading involves administratively separating the fuel basket of a shipping cask into two or more regions and loading fuel with different burnup, cooling times and enrichments into these regions. Assuming that these loaded casks are directly disposed of at the Yucca Mountain, understanding how regionalized loading patterns might affect the repository thermal design limits, if at all, is of interest. Although the non-uniform loading would not affect the total heat flux coming out of cask surfaces, the spent fuel clad surface temperature is expected to be affected by the loading pattern. Current thermal limit is that the peak clad temperature can not exceed 350˚C.

COBRA-SFS (Spent Fuel Storage) was used to analyze the temperature inside the fuel cask under different conditions. Four different loading cases were analyzed for ambient temperatures of 17.2˚C and 200˚C on the outside of the cask. The peak clad temperature was analyzed in order to investigate if the thermal limit of the clad was violated.

As far as how should the SNF casks be loaded into the proposed repository at Yucca Mountain, current designs assume that the heat load inside the drifts is uniform throughout the repository. However, the fuel burnup varies throughout the total population of spent fuel assemblies. It is proposed for this work that a non-uniform loading of the repository can be utilized if deemed necessary.

The way in which non-uniformity was applied was to analyze loading schemes based on five different scenarios that are discussed in Section 7.2. Non-uniform loading is based on a homogeneous linear heat load for the individual drift and heterogeneous loading of the drifts throughout the repository. Appendix C provides the linear heat load for each of the loading schemes. From this non-uniform loading, the thermal analysis was used to determine whether the amount of waste per package could be increased thus increasing the storage capacity of the repository. The undesirable effects of non-uniform loading could cause unexpected hot spots and moisture to be present in the drifts that have a lower decay heat at an earlier time. Presence of a drift that has a high decay heat located near a drift of low decay heat causes a shift in the location where the moisture can pass through the system as illustrated in Figure 3.1. This can lead to an undesirable outcome as moisture could reach the drift of lower decay heat possibly causing failure of the waste packages due to corrosion at an earlier time.

Uniform loading based on the adoption of variable drift spacing was also analyzed for possible benefits of increased capacity.

3.5 Thermal Limits

There are thermal design criteria set by the DOE for the Yucca Mountain repository. Table 3.2 gives the three thermal criteria that must not be exceeded. The cladding thermal criterion minimizes the thermal creep in the cladding, which serves as a secondary containment so that radioactive material release is minimized in case the spent fuel cask fails. The drift wall temperature limit was set to avoid stresses in the Tuff rock. The Tuff rock has mineral crystobalite that is dispersed in the rock and changes phase and expands by five percent when temperatures are between 200˚C and 250˚C (Johnson 1998). The temperature criteria between the drifts was chosen so that water, below the boiling point, would be allowed to pass through the rock system so that saturation in the geological system does not occur.

Table 3.2: Repository Thermal Limits

SNF cladding temperatures:	≤ 350˚C
Drift wall temperature:	≤ 200˚C
Mid-drift temperatures:	≤ 96˚C

4 Decay Heat Model

The decay heat model used in this work is based on a multivariable regression analysis that was developed by Mike Stahala (Stahala 2006). ORIGEN-ARP was used in conjunction with SAS 9.1 to fit the multivariable regression (Ibid).

4.1 Stahala Model

Stahala's model is split into seven time regions ranging from one to ten thousand years (Table 4.1-Table 4.4). To account for effects of enrichment, irradiation days, and burnup on the decay heat of SNF, constants (D_1 and β) were transformed into polynomial functions (Stahala, 32-33). These functions include burnup, irradiation days, and enrichment as can be seen in Equations (4.1) through (4.3).

$$Q(t) = e^{D_1} \cdot t^{-\beta} * (burnup / 33{,}000) \quad (W / MTU) \tag{4.1}$$

$$\begin{aligned} D_1 = {} & \alpha_1 + \alpha_2 \cdot \ln\left(\frac{burnup}{33000}\right) + \alpha_3 \cdot IrradiationDays + \alpha_4 \cdot enrichment + \\ & \alpha_5 \cdot \ln\left(\frac{burnup}{33000}\right) \cdot IrradiationDays + \alpha_6 \cdot \ln\left(\frac{burnup}{33000}\right) \cdot enrichment + \\ & \alpha_7 \cdot IrradiationDays \cdot Enrichment + \alpha_8 \cdot \ln\left(\frac{burnup}{33000}\right)^2 + \alpha_9 \cdot IrradiationDays^2 \\ & + \alpha_{10} \cdot enrichment^2 \end{aligned} \tag{4.2}$$

$$\beta = \gamma_1 + \gamma_2 \cdot \ln\left(\frac{burnup}{33000}\right) + \gamma_3 \cdot IrradiationDays + \gamma_4 \cdot enrichment +$$
$$\gamma_5 \cdot \ln\left(\frac{burnup}{33000}\right) \cdot IrradiationDays + \gamma_6 \cdot \ln\left(\frac{burnup}{33000}\right) \cdot enrichment + \quad (4.3)$$
$$\gamma_7 \cdot IrradiationDays \cdot Enrichment + \gamma_8 \cdot \ln\left(\frac{burnup}{33000}\right)^2 + \gamma_9 \cdot IrradiationDays^2$$
$$+ \gamma_{10} \cdot enrichment^2$$

Each time region has distinct values of α_i and γ_i. These values are based on the type of assembly (BWR or PWR) as well as burnup values. Table 4.1 through Table 4.4 give the values at each of the time regions.

Table 4.1: PWR SNF, Burnup Greater than 10,000 MWd/MTU

	Time Regions (Years)						
	1-8	**8-49**	**49-74**	**74-150**	**150-300**	**300-1500**	**1500-10000**
α_1	10.25023	8.355097	9.678154	9.540531	7.937692	9.338127	7.989349
α_2	0.16978	0.840270	1.463955	1.619106	0.680299	-0.801864	-0.653556
α_3	-0.00103	-0.000086	-0.000057	0.000033	0.000301	0.000153	0.000077
α_4	-0.08375	-0.117771	-0.081999	0.110681	0.162211	0.039567	-0.094851
α_5	0.00009	-0.000004	-0.000002	0.000034	0.000112	0.000043	0.000015
α_6	-0.00458	-0.115912	-0.307055	-0.375121	-0.008816	0.389129	0.329830
α_7	-0.00001	0.000002	0.000000	-0.000010	-0.000019	-0.000006	-0.000004
α_8	0.03856	0.323765	0.711786	0.889675	0.325840	-0.867962	-0.719298
α_9	0.00000	0.000000	0.000000	0.000000	0.000000	0.000000	0.000000
α_{10}	0.00632	0.010781	0.015174	0.004219	-0.013763	-0.016375	-0.005921
γ_1	1.41811	0.489392	0.846595	0.818513	0.498310	0.727457	0.556041
γ_2	-0.14328	0.201370	0.371920	0.408705	0.223544	-0.032594	-0.016553
γ_3	-0.00047	-0.000028	-0.000018	0.000003	0.000056	0.000032	0.000021
γ_4	0.00173	-0.025549	-0.016584	0.027626	0.038554	0.017103	-0.000927
γ_5	0.00005	-0.000005	-0.000005	0.000004	0.000019	0.000008	0.000004
γ_6	0.01728	-0.032595	-0.085043	-0.101081	-0.028822	0.040335	0.033854
γ_7	-0.00001	0.000001	0.000001	-0.000002	-0.000003	-0.000001	-0.000001
γ_8	-0.05534	0.078263	0.184688	0.226197	0.115358	-0.089342	-0.074370
γ_9	0.00000	0.000000	0.000000	0.000000	0.000000	0.000000	0.000000
γ_{10}	0.00003	0.002538	0.003817	0.001317	-0.002278	-0.002761	-0.001387

Table 4.2: PWR SNF, Burnup Less than 10,000 MWd/MTU

	Time Regions (Years)						
	1-8	**8-49**	**49-74**	**74-150**	**150-300**	**300-1500**	**1500-10000**
α_1	10.22298	7.408246	6.859312	4.680701	7.391454	14.8867	10.67194
α_2	0.12504	-0.287601	-1.525997	-2.847634	0.062953	4.4869	2.34838
α_3	-0.00115	-0.000027	-0.000029	-0.000050	0.000165	0.0002	0.00012
α_4	-0.09312	0.163038	0.787007	1.404643	0.083539	-1.3110	-1.01190
α_5	0.00005	0.000026	0.000022	0.000028	0.000073	0.0001	0.00004
α_6	-0.01397	0.020915	0.088262	0.077636	-0.124461	-0.1452	-0.09638
α_7	-0.00001	0.000001	0.000002	-0.000006	-0.000018	0.0000	0.00000
α_8	0.01070	-0.033557	-0.177765	-0.337769	-0.019319	0.5295	0.27571
α_9	0.00000	0.000000	0.000000	0.000000	0.000000	0.0000	0.00000
α_{10}	0.00720	-0.012485	-0.058016	-0.102213	-0.007048	0.0821	0.06904
γ_1	1.56088	0.204601	0.058783	-0.440929	0.082482	1.3752	0.82539
γ_2	0.03370	-0.114245	-0.447213	-0.752950	-0.182871	0.5842	0.30656
γ_3	-0.00055	-0.000024	-0.000023	-0.000028	0.000015	0.0000	0.00001
γ_4	-0.03569	0.064688	0.232200	0.375353	0.115849	-0.1275	-0.09025
γ_5	0.00002	-0.000002	-0.000003	-0.000002	0.000007	0.0000	0.00000
γ_6	-0.00534	0.008642	0.026851	0.024772	-0.015862	-0.0187	-0.01279
γ_7	-0.00001	0.000001	0.000001	-0.000001	-0.000003	0.0000	0.00000
γ_8	0.00284	-0.013122	-0.051884	-0.088867	-0.026591	0.0683	0.03572
γ_9	0.00000	0.000000	0.000000	0.000000	0.000000	0.0000	0.00000
γ_{10}	0.00311	-0.004823	-0.017044	-0.027292	-0.008596	0.0070	0.00543

Table 4.3: BWR SNF, Burnup Greater than 10,000 MWd/MTU

	Time Regions (Years)						
	1-8	**8-49**	**49-74**	**74-150**	**150-300**	**300-1500**	**1500-10000**
α_1	10.25149	8.400158	9.817396	9.709196	7.941068	9.126785	7.876528
α_2	0.16923	0.865227	1.556822	1.731366	0.712889	-0.910927	-0.771827
α_3	-0.00103	-0.000086	-0.000062	0.000028	0.000318	0.000160	0.000076
α_4	-0.08444	-0.127824	-0.109054	0.089415	0.180505	0.069097	-0.081438
α_5	0.00009	-0.000004	-0.000005	0.000027	0.000110	0.000047	0.000016
α_6	-0.00524	-0.118637	-0.312477	-0.375814	-0.006016	0.381057	0.328661
α_7	-0.00001	0.000002	0.000000	-0.000010	-0.000019	-0.000006	-0.000004
α_8	0.03999	0.319416	0.699496	0.863702	0.339016	-0.828049	-0.721295
α_9	0.00000	0.000000	0.000000	0.000000	0.000000	0.000000	0.000000
α_{10}	0.00634	0.011594	0.017600	0.006272	-0.015754	-0.018368	-0.006724
γ_1	1.41190	0.503076	0.885973	0.864889	0.511995	0.704230	0.545043
γ_2	-0.14907	0.206494	0.395570	0.436978	0.236018	-0.044235	-0.030350
γ_3	-0.00047	-0.000028	-0.000019	0.000001	0.000059	0.000033	0.000022
γ_4	0.00368	-0.027813	-0.023522	0.021952	0.040774	0.021301	0.001146
γ_5	0.00005	-0.000005	-0.000005	0.000002	0.000019	0.000008	0.000004
γ_6	0.01833	-0.032578	-0.085770	-0.100740	-0.027748	0.039540	0.033943
γ_7	-0.00001	0.000001	0.000001	-0.000002	-0.000004	-0.000001	-0.000001
γ_8	-0.05581	0.075370	0.179641	0.217993	0.114818	-0.085017	-0.075807
γ_9	0.00000	0.000000	0.000000	0.000000	0.000000	0.000000	0.000000
γ_{10}	-0.00013	0.002718	0.004441	0.001861	-0.002540	-0.003036	-0.001496

Table 4.4: BWR SNF, Burnup Less than 10,000 MWd/MTU

	Time Regions (Years)						
	1-8	**8-49**	**49-74**	**74-150**	**150-300**	**300-1500**	**1500-10000**
α_1	10.23037	7.441953	6.926482	5.087464	7.69886	14.55158	10.66535
α_2	0.12252	-0.228984	-1.384585	-2.421957	0.23938	4.07107	2.24751
α_3	-0.00114	-0.000037	-0.000029	-0.000044	0.00018	0.00019	0.00012
α_4	-0.09590	0.149611	0.787302	1.328281	-0.00016	-1.24929	-0.99890
α_5	0.00005	0.000026	0.000022	0.000028	0.00007	0.00006	0.00004
α_6	-0.01406	0.017357	0.077726	0.041692	-0.14220	-0.11683	-0.08634
α_7	-0.00001	0.000002	0.000002	-0.000006	-0.00002	0.00000	0.00000
α_8	0.00989	-0.025647	-0.154352	-0.275980	-0.00386	0.45669	0.25863
α_9	0.00000	0.000000	0.000000	0.000000	0.00000	0.00000	0.00000
α_{10}	0.00742	-0.011774	-0.058711	-0.097053	0.00070	0.07803	0.06710
γ_1	1.56107	0.215331	0.075295	-0.346942	0.15959	1.33830	0.83402
γ_2	0.03222	-0.092873	-0.406715	-0.647305	-0.12459	0.53777	0.30323
γ_3	-0.00055	-0.000027	-0.000023	-0.000027	0.00002	0.00002	0.00001
γ_4	-0.03693	0.060488	0.233179	0.358891	0.09725	-0.12034	-0.08984
γ_5	0.00002	-0.000003	-0.000003	-0.000002	0.00001	0.00000	0.00000
γ_6	-0.00531	0.007445	0.023987	0.016090	-0.02110	-0.01577	-0.01238
γ_7	-0.00001	0.000001	0.000001	-0.000001	0.00000	0.00000	0.00000
γ_8	0.00262	-0.010004	-0.044947	-0.073119	-0.01975	0.05962	0.03460
γ_9	0.00000	0.000000	0.000000	0.000000	0.00000	0.00000	0.00000
γ_{10}	0.00326	-0.004594	-0.017299	-0.026217	-0.00695	0.00659	0.00528

4.2 DOE Database

The total inventory of SNF was compiled by the DOE into a Microsoft Access database (DOE 2002b). This database provides detailed information on every commercial spent fuel assembly ever irradiated and discharged through 2002. Key parameters that were used in the DOE database to analyze the decay heat inventory of the SNF are given in Table 4.5.

Table 4.5: Key DOE Database Parameters

FF_REACTORID	–	The reactor ID number
FF_INITENR	–	The initial enrichment for each assembly (in weight percent)
FF_MAXBURN	–	The final burnup for each assembly (in megawatt days thermal per metric ton of uranium)
FF_ASSMTYPE	–	The assembly type used to distinguish between PWR and BWR.
CY_CYUPDATE	–	The cycle start date
CY_CYDNDATE	–	Cycle shutdown date (the discharge date)

4.2.1 Burnup Inventory

The burnup inventory of all SNF assemblies is an important factor to look at when considering what type of heat source would be present once the SNF is emplaced into the mountain. Figure 4.1 and Figure 4.2 show the frequency of burnup for both PWR and BWR respectively for DOE SNF inventory through 2002. When comparing these two figures it can be seen that the PWR burnup inventory has higher burnup values when compared to the BWR inventory. However, some of the BWR assemblies have the highest burnup values at around 66,000 MWd/MTU. These high burnup values are due to recent improvements in the fuel cycle.

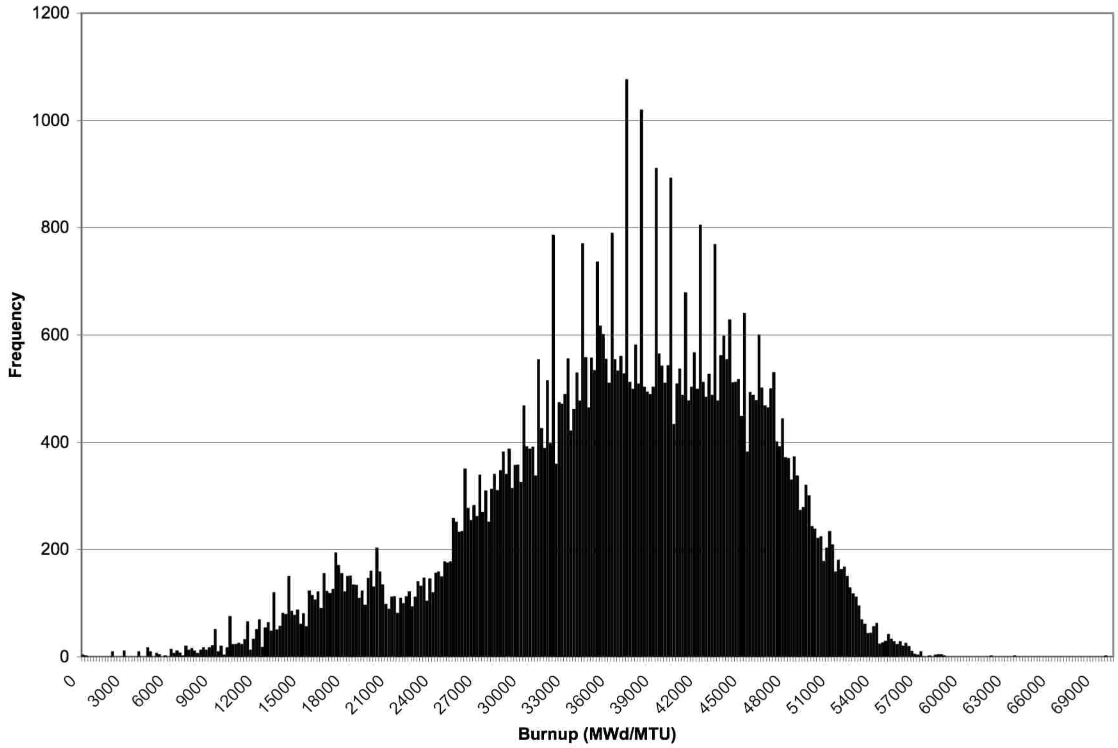

Figure 4.1: PWR Burnup Inventory Through 2002

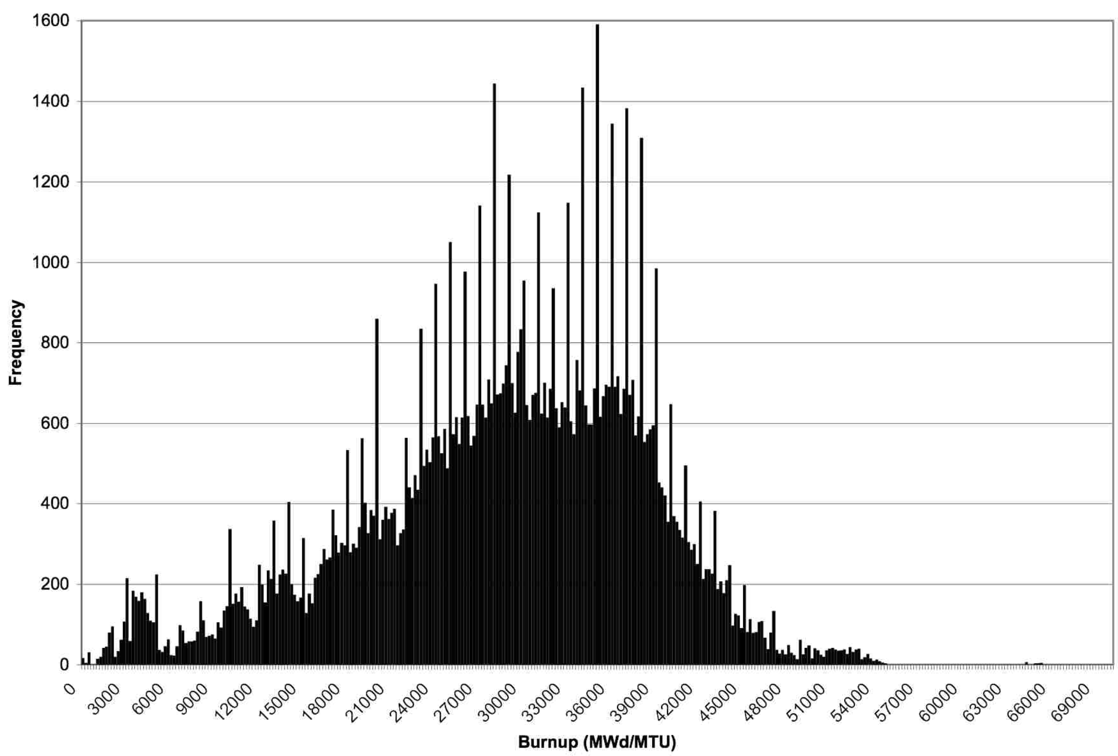

Figure 4.2: BWR Burnup Inventory Through 2002

4.2.2 Decay Heat Inventory

The decay heat inventory of the commercial SNF is a very important parameter because it takes into account factors such as burnup, days irradiated, enrichment, and time to emplacement (or cooling time). These four factors were used in calculating the decay heat by the use of Stahala's model. Burnup of the SNF does not give a true representation of the amount of heat that is deposited into the mountain. One must look at the time to which the fuel is emplaced since the age of fuel varies and the decay heat drops dramatically in the first 25 years.

Figure 4.3 and Figure 4.4 show the decay heat inventory assuming an emplacement time of 2017. The PWR inventory contains higher decay heat values than the BWR inventory. The decay heat for the entire inventory was analyzed and an assembly based on the average decay heat for both PWR and BWR was found and was utilized in the uniform loading case.

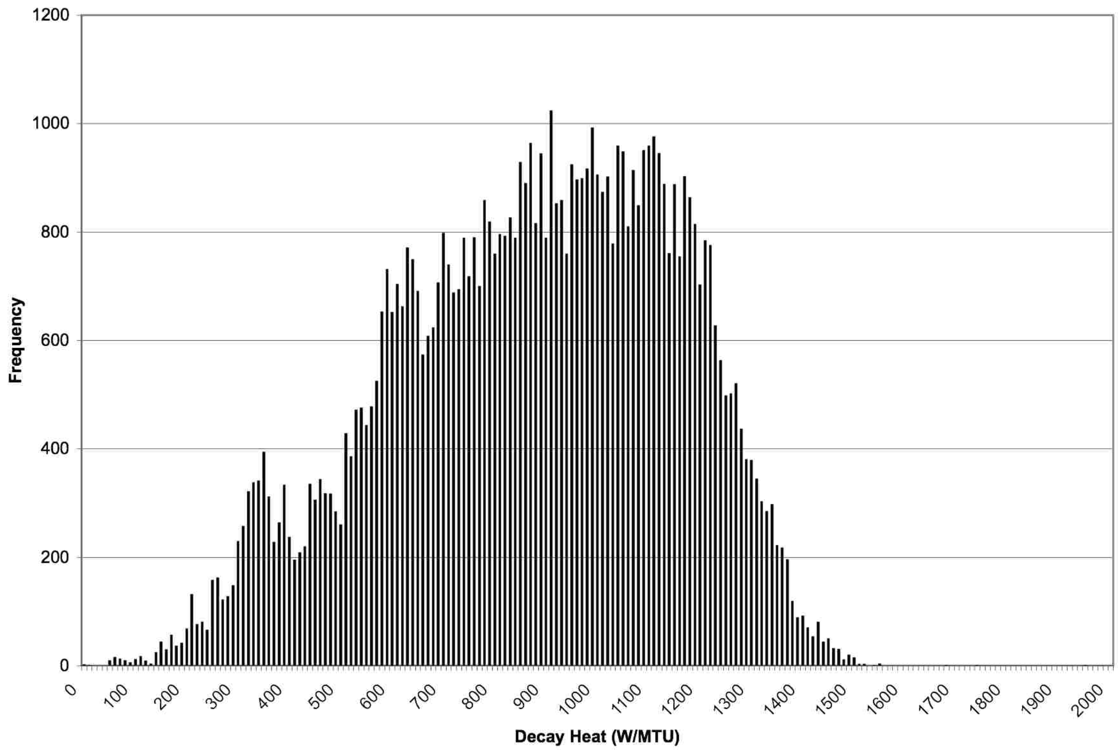

Figure 4.3: PWR Decay Heat Inventory at Emplacement Time of 2017

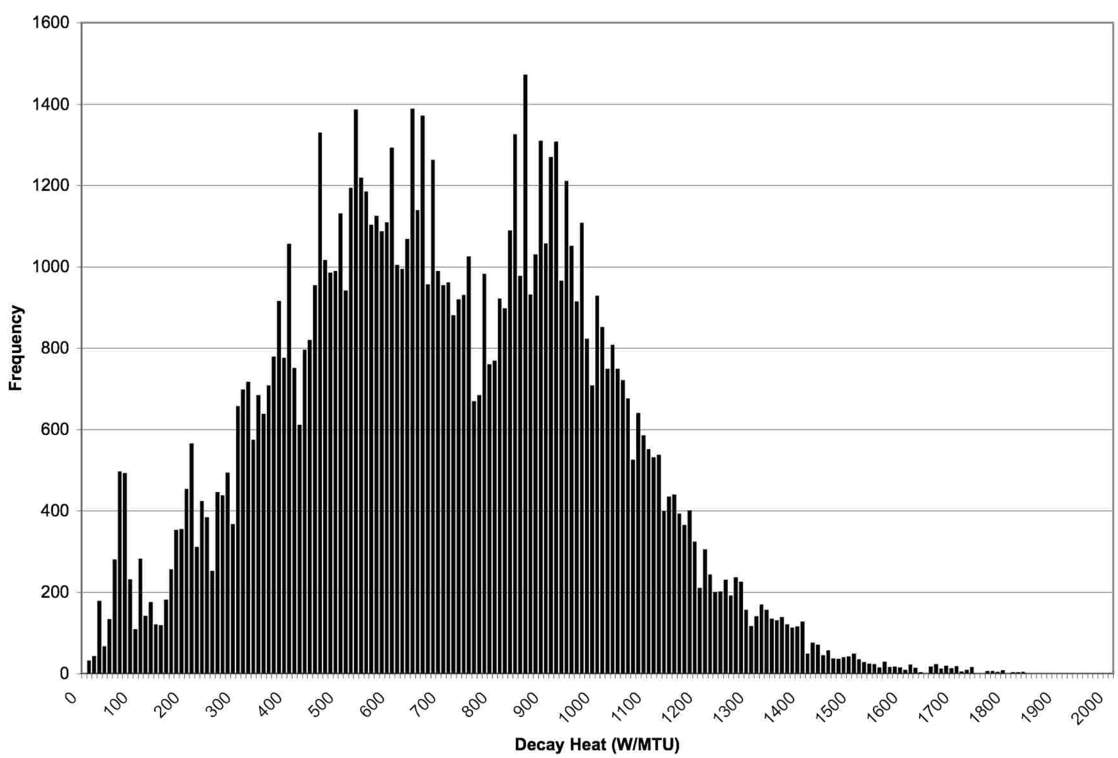

Figure 4.4: BWR Decay Heat Inventory at Emplacement Time of 2017

5 COBRA-SFS

COBRA-SFS (Michener 1995) is a code that is used to analyze the thermal-hydraulic behavior of multi-assembly spent fuel storage systems. The code is based on a finite difference approach to predict flow and temperature distributions of cask and fuel assemblies under natural and forced convection. This code is derived from the family of COBRA codes, which has been validated against data on commercial spent fuel data (Ibid).

A TN-24P cask manufactured by Transnuclear Inc. was modeled to investigate the temperature profiles of the spent fuel cask. COBRA-SFS was used to analyze the potential benefits of loading a cask nonuniformly. Figure 5.1 gives a representation of a non-uniform loaded fuel cask with low burnup assemblies on the inside and high burnup assemblies on the outside. It will be shown that nonuniform loading plays a very important role in the peak cladding temperature.

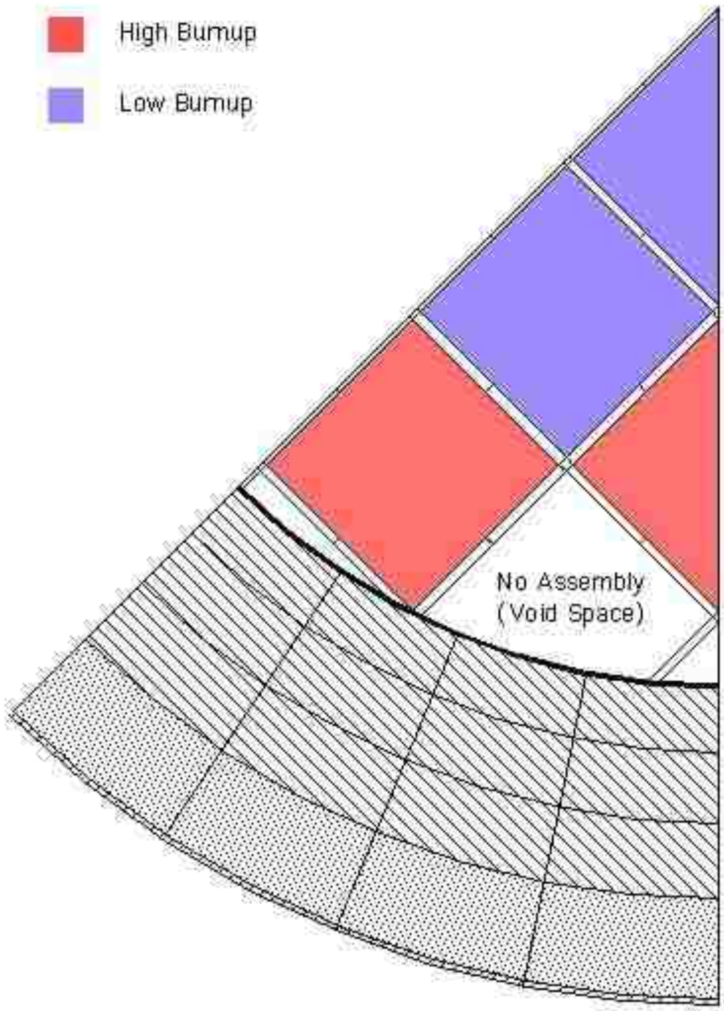

Figure 5.1: Non-uniform Loaded Fuel Cask

5.1 Model Description

COBRA-SFS was used to model a cask using the design specifications for the TN-24P fuel cask that are given in Table 5.1. Appendix A provides the input file for COBRA-SFS for which the loading of the spent fuel cask was analyzed. Note that the case in Appendix A is for uniform heat load for a one-eighth spent fuel cask as specified in OPER.8 (found in Appendix A). The 1/8th core can be seen in Figure 5.2.

Table 5.1: TN-24P Cask Design Specifications

1.	Type:	Prototype Metal Storage Cask
2.	Manufacturer/Vendor:	Transnuclear Inc.
3.	Capacity (assemblies):	
	a. Intact SNF	24 PWR
	b. Consolidated Fuel Rods (@2 assys/can)	42 PWR
4.	Weight (tons)	
	a. Loaded	100
	b. Empty	82.3
5.	Dimensions:	
	a. Overall Length (in)	199.3
	b. Overall Cross Section (in)	89.8
	c. Cavity Length (in)	163.4
	e. Wall Thickness (in)	16.25
	f. Cooling Fin Length (in)	--
	g. Lid Thickness (in)	15.4
	h. Bottom Thickness (in)	11.0
	i. Basket Length (in)	162.2
	j. Basket Cross Section (in)	N/A
	k. Thickness of Basket Spears (in)	0.4
6.	Neutron Shield:	
	a. Number of Rods	N/A
	b. Rod Diameter (in)	N/A
	c. Side Thickness (in)	4.2
	d. Lid Thickness (in)	4.2
	e. Bottom Thickness (in)	None
7.	Materials of Construction:	
	a. Cask Body	Forged Steel
	b. Basket	Al/B
	c. Neutron Shield	Polyethylene Resin (sides) Granular Polypropylene (lid)
8.	Cavity Atmosphere:	Helium

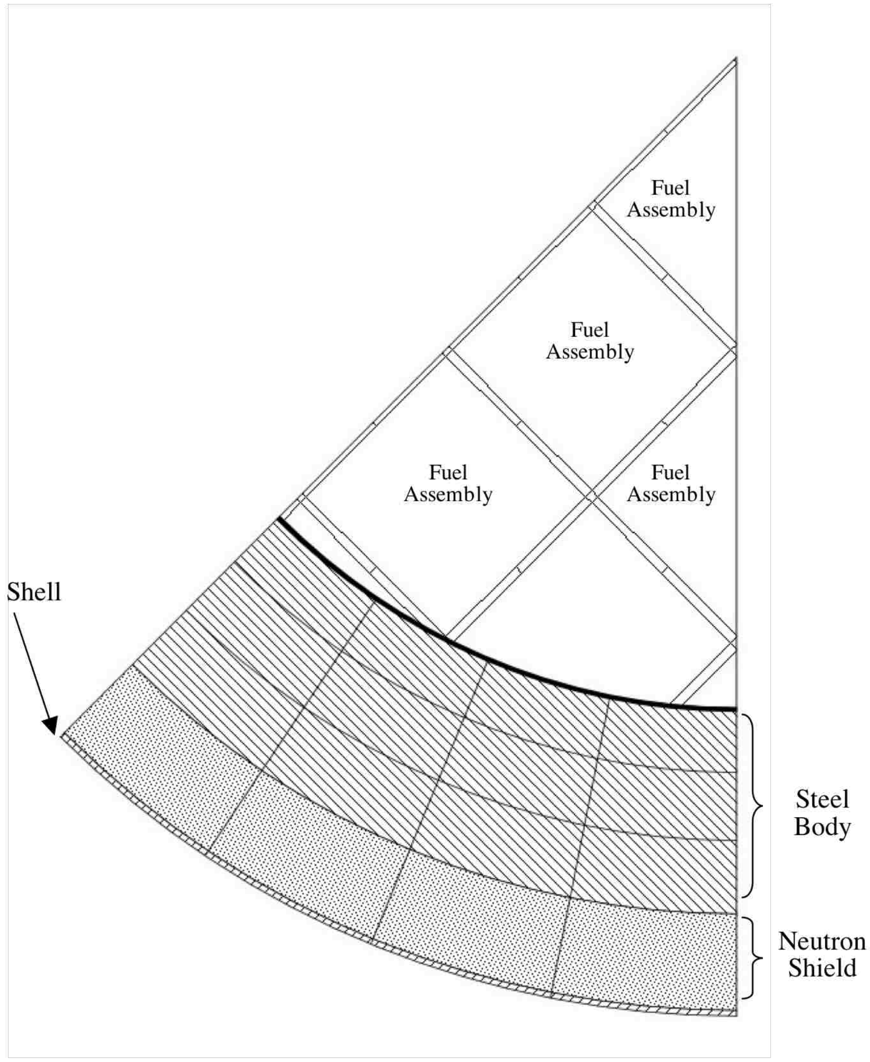

Figure 5.2: One-eight Section of TN-24P Cask Model

COBRA-SFS is based on English units. In order to convert watts/MTU to MBtu/(hr·ft^3) the following parameters must be used in the conversion:

- 460.9 kg of Uranium per 15 x 15 PWR assembly
- Fuel rod diameter: 0.422 in
- Fuel rod length: 12 ft =144 in
- Number of rods per 15 x 15 fuel assembly: 225

The above dimensions for the 15 x 15 PWR assembly gives the total volume of the assembly as:

$$\pi\left(\frac{0.422in}{2}\right)^2 * 144in * 225 = 4531.69in^3 = 2.6225ft^3 \tag{5.1}$$

The conversion of decay heat is given as:

$$\frac{MBtu}{hr-ft^3} = \left(\frac{watts}{MTU}\right)\left(\frac{0.4609MTU}{PWR\cdot assembly}\right)\left(\frac{\frac{J}{s}}{watt}\right)\left(\frac{3600s}{hr}\right)\left(\frac{PWR\cdot assembly}{2.6225ft^3}\right) \times\left(\frac{9.47817\left(10^{-4}\right)Btu}{J}\right)\left(\frac{MBtu}{1\times10^6 Btu}\right) \tag{5.2}$$

The decay heat used for the COBRA-SFS analysis was based on a cooling period of seven years for a given burnup of 50,000 MWd/MTU with a decay heat of 2393.5 W/MTU. The decay heat used for the COBRA-SFS analysis was 0.0014354 MBtu/(hr·ft^3). This corresponding decay heat correlates to a total of 1 kW per assembly giving the total wattage for the TN-24P cask as 24 kW. The minimum time before SNF can be emplaced into the repository is twenty-five years. The decay heat corresponding to this time period is 1324 W/MTU (7.93974x10^{-4} MBtu/(hr·ft^3) with the total wattage of the cask being 13.175 kW (or 0.549 kW per assembly in the uniform case).

In terms of how regionalized loading within the cask is conceptualized, this study assumes that 50% and 75% of the assembly power for the uniform case is applied. The cask with a total power of 24 kW is assumed to have 1 kW per assembly for the uniform case. For the case of the cask with a power of 13.175 kW the power of each assembly is approximately 0.549 kW for uniform loading. Taking 50% and 75% of assembly power for the uniform case, when the total power of the cask is 24 kW or 1 kW per assembly, gives 0.5 kW and 0.75 kW for the non-uniform case respectively. Therefore, for a non-uniform case when 50% of the uniform assembly power is taken, the cask is loaded with 0.5 kW on the inside/outside and 1.5 kW on the outside/inside. Similarly, by taking 75% of the uniform assembly power the cask is loaded with 0.75 kW on the inside/outside or 1.25 kW on the outside/inside. The case for the 13.175 kW cask is done in similar fashion with 50% and 75% of the uniform loading power of 0.549 kW.

5.2 COBRA-SFS Results

Taking into account that the maximum heat load was emplaced into the TN-24P cask one can see how the temperatures for the peak clad temperatures are affected. To see the effect of changing the ambient temperature on the cladding temperature, the ambient temperature surrounding the cask was varied. In one case it was assumed that the fuel cask was stored outside of Yucca Mountain for a period of time during which the mean annual temperature was 17.2˚C (DOE 2007). Another scenario for 200˚C was analyzed to show the increase in clad temperature due to a higher ambient temperature on the outside of the cask. This higher temperature scenario corresponds to the temperature limit of the drift wall. In reality, since there will be forced ventilation for an extended period (50-75 years for this study), the temperatures inside the drift will be significantly lower than the temperature limit of the drift wall.

5.2.1 Cask Load of 24 Kilowatt

In Figure 5.3 the cask with the highest clad temperature is the cask loaded with 1.5 kW assemblies on the inside and 0.5 kW loaded on the outside. There is little difference in the two casks that have the lower heat load assemblies on the inside.

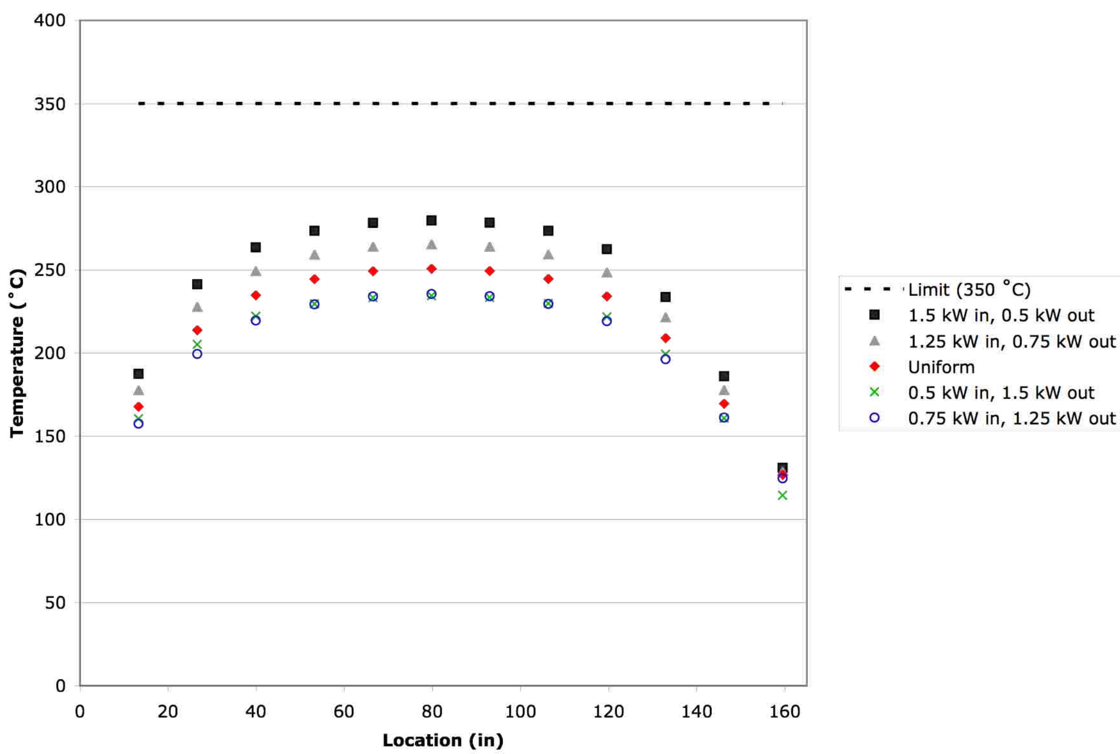

Figure 5.3: Peak Clad Temperature (Ambient Temperature 17.2˚C): Cooled 7 Years

In Figure 5.4 the results show a shift towards and beyond peak clad temperature limit of 350˚C. The thermal limit of all loading patterns except for the 0.5 and 0.75 kW assemblies on the inside are violated. By the time most of the fuel is emplaced into the repository there has been a significant amount of decay. The following section discusses the scenario in which the fuel has cooled for twenty-five years before the cask is emplaced in the repository.

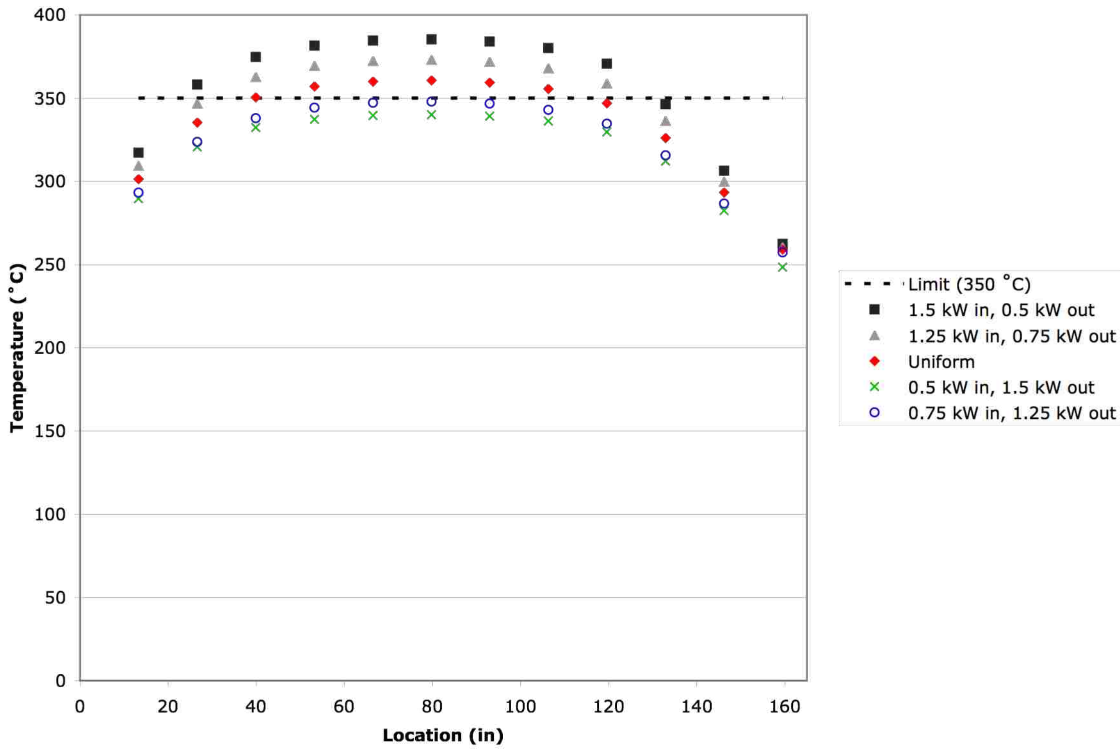

Figure 5.4: Peak Clad Temperature (Ambient Temperature: 200˚C): Cooled 7 Years

5.2.2 Cask Load of 13.175 Kilowatt

The different loading cases in Figure 5.5 and Figure 5.6 show that after twenty-five years of cooling the temperature is greatly reduced compared to the loading cases for seven years. From this it can be concluded that there is no concern with respect to the cladding surface temperature with the use of non-uniform loading of SNF in the cask.

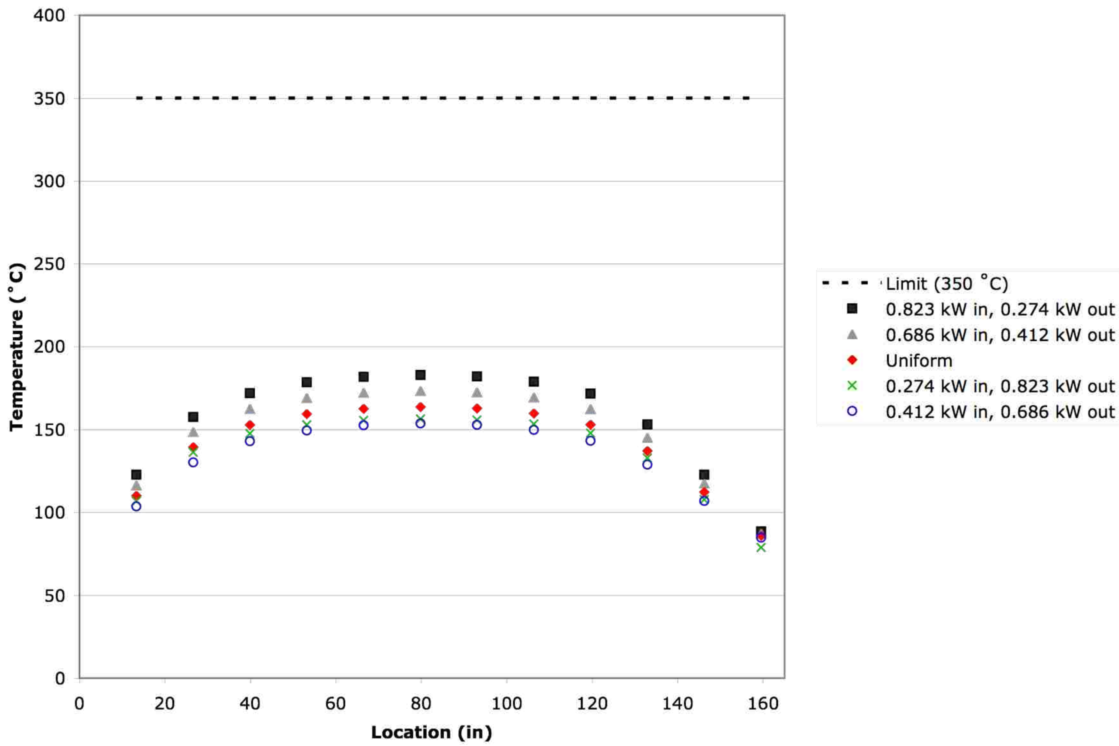

Figure 5.5: Peak Clad Temperature (Ambient Temperature 17.2˚C): Cooled 25 Years

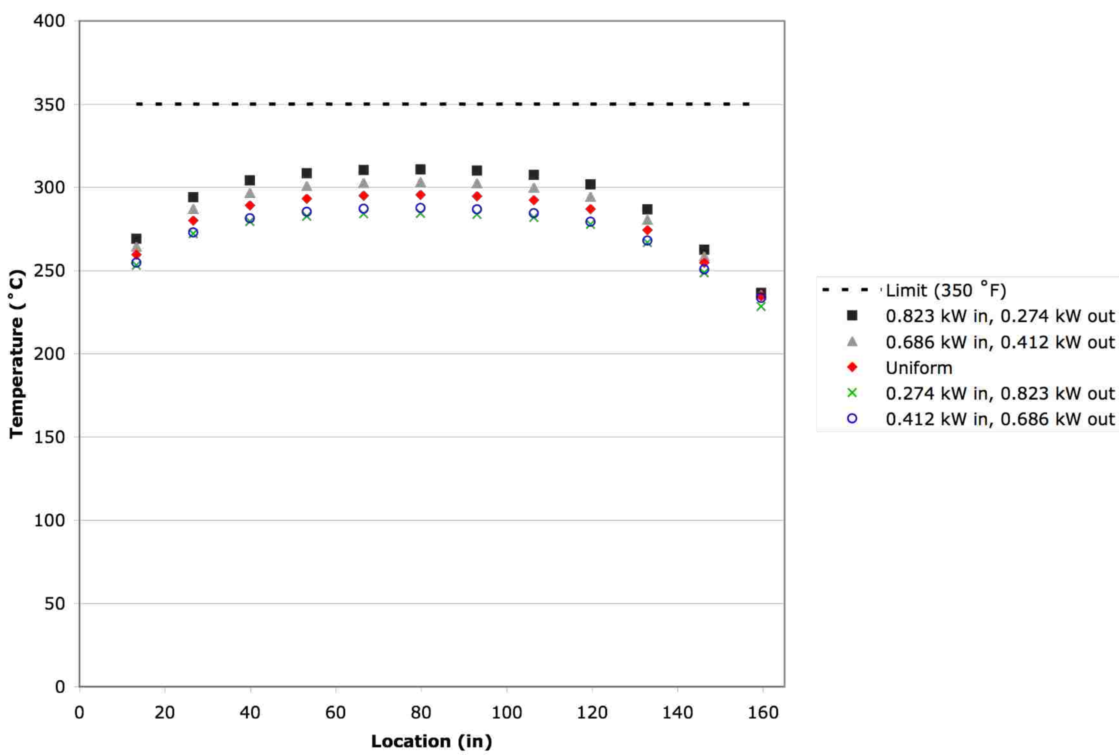

Figure 5.6: Peak Clad Temperature (Ambient Temperature 200˚C): Cooled 25 Years

6 Simplified Repository Thermal Analysis Code

Due to a large number of calculations involved, an efficient computational model for a repository thermal analysis was needed. The thermal analysis model selected was based on its ability to calculate repository-horizon average rock temperatures by using an analytic solution model to the heat conduction equation. It was assumed that the modeled repository has line sources laid out parallel to each other covering the entire proposed repository (NRC 2002). The model treats each line source independently with different heat loads. The analytical solution was originally derived by Claesson and Probert (Claesson 1996). The SRTA code was modified to include four running modes. The first two modes in the following list were used to analyze the temperature in the repository.

1. Variable burnup data
2. Variable drift spacing
3. Variable spent fuel age
4. Variable waste package payload

6.1 The SRTA Model

The analytical solution derived by Claesson and Probert to solve for a temperature at any given point is given as:

$$\Delta T(x,y,z,t)=\int_0^t \frac{\alpha q''_{rep}(t')}{4k\sqrt{\pi}}\frac{1}{\sqrt{4\alpha(t-t')}}\left[erf\left(\frac{L-x}{\sqrt{4\alpha(t-t')}}\right)+erf\left(\frac{L+x}{\sqrt{4\alpha(t-t')}}\right)\right]$$
$$\left[erf\left(\frac{B-y}{\sqrt{4\alpha(t-t')}}\right)+erf\left(\frac{B+y}{\sqrt{4\alpha(t-t')}}\right)\right]\left[\exp\left(\frac{-z^2}{4\alpha(t-t')}\right)-\exp\left(\frac{-(z-2H)^2}{4\alpha(t-t')}\right)\right]dt' \tag{6.1}$$

where:

$\Delta T(x,y,z,t)$	–	increase in temperature at time t at point (x, y, z) in the semi-infinite medium due to one line source [˚C]
$q''_{rep}(t)$	–	time-dependent repository heat flux [W/m^2]
α	–	thermal diffusivity of the semi-infinite medium [m^2/s]
k	–	thermal conductivity of the semi-infinite medium [W/(m-˚C)]
L	–	half length of a line source [m]
B	–	half width of a line source [m]
H	–	depth of a line source below the ground surface [m]
t	–	actual time after activation of heat flux [s]
t'	–	time of integration [s]
x,y,z	–	location of interest [m]

The SRTA code uses an input file called variable.dat that contains all of the data used in the temperature analysis. Table 6.1 gives the various parameters used in the calculations.

Table 6.1: SRTA Input Variables

Parameter Description:	Units:	Code Parameters:	Mean Value:	Source:
Density of Tuff Rock	Kg/m^3	rho	2593	DOE 2004
Specific Heat of Tuff Rock	J/(kg-K)	Cp	930	DOE 2004
Thermal Conductivity of Tuff Rock	W/(m-K)	cond	2.603	DOE 2004
Conductivity of Natural Convection	W/(m-˚C)	conde_n	0.9	NRC 2002
Factor for ventilation heat losses	-	hloss_fact	0.88	Bechtel 2004
Thermal Conductivity Of Drip Shield	W/(m-˚C)	condds	20	DOE 2001
Thermal Conductivity Of Backfill	W/(m-˚C)	condbf	-	-
Emissivity of Drip Shield	-	emissds	0.64	Michels 1949
Emissivity of Waste Package	-	emisswp	0.87	NRC 2002
Waste Package Diameter	m	wpdia	1.644	NRC 2002
Waste Package Length	m	wplength	5.275	NRC 2002
Emplacement Backfill Thickness	m	bfthick	0	NRC 2002
Drip Shield Thickness	m	dsthick	0.02	NRC 2002
Drip Shield Diameter	m	ds_idia	2.75	NRC 2002
Emplacement Drift Diameter	m	driftdia	5	NRC 2002

Table 6.1 continued: SRTA Input Variables

Parameter Description:	Units:	Code Parameters:	Mean Value:	Source:
Circumferential Fraction Not Covered By Floor	-	frac_inv	0.75	NRC 2002
Waste Package Payload	MTU	wppayload	7.89	NRC 2002
Time Of Backfill Emplaced	Yr	timeofbackfill	50-300	
Number Of Weights For Gauss Legendre Integration	-	npoints	20	NRC 2002
Ambient Repository Temperature	˚C	ambreptemp	20	NRC 2002
Elevation of Repository Horizon	m	elevrep	1072	NRC 2002
Elevation of Ground Surface	m	elevgs	1400	NRC 2002
Inner Waste Package Thickness	m	tss	0.05	NRC 2002
Outer Waste Package Thickness	m	tcs	0.02	NRC 2002
Thermal Conductivity of Inner Overpack	W/(m-˚C)	akss	16.62	DOE 2001
Thermal Conductivity of Outer Overpack	W/(m-˚C)	akcs	15.49	DOE 2001
Waste Package Length	m	alengthwp		NRC 2002
Effective Thermal Conductivity Of Basket Spent Fuel in Waste Package	W/(m-˚C)	aksf	1.00	NRC 2002
Emplacement Drift Spacing	m	driftspace	81	NRC 2002
WPSpacing Along Emplacement Drift	m	wpspace	6.1392	NRC 2002
Repository Drift Angle	radians	angle	-0.304	NRC 2002

6.2 Benchmarking Simplified Repository Thermal Analysis (SRTA) Code

The SRTA code was adapted from the Total-System Performance Assessment (TPA) code (NRC 2002) that was developed by the Nuclear Regulatory Commission. For the verification of the SRTA code, COMSOL Multiphysics (COMSOL Inc. 2007) was chosen as the tool for comparison. COMSOL is used industry wide for research, engineering, and design applications.

The main purpose of SRTA is to analyze the temperature at any given point in the Yucca Mountain repository. As this code utilizes an analytical solution to solve for the temperature in the repository, the time taken to solve the problem is greatly reduced.

The SRTA code is based on a pure conduction model. In order to account for heat loss during the preclosure period a parameter called the heat loss factor is used during the time that the drifts are ventilated. This heat loss factor accounts for the total heat removed during the time of convective heat transfer.

COMSOL Multiphysics is a multi-dimensional finite element analysis and solver package that can be used for various engineering applications. The general heat transfer module with transient analysis was chosen to model a single drift inside of the repository. COMSOL can be a very memory intensive program when the problem contains a high degree of meshing. Due to the complexity and huge memory requirement for COMSOL to simulate the whole repository, several assumptions were made to simplify the model setup. Symmetry conditions were assumed at the vertical planes passing the center of the center drift and midways at both sides of the center drift. This is based on the observation that if the repository is uniformly loaded with the spent fuels, the location of highest temperature point should be the center of the loaded area in the repository. Considering the large distances from the repository loading plane to both the surface and the ground water table (~300 m), symmetry condition was also assumed at the horizontal plane passing the center of the center drift (those dash lines in Figure 6.1). The boundaries at the ground surface and at the water table were assumed at constant temperature.

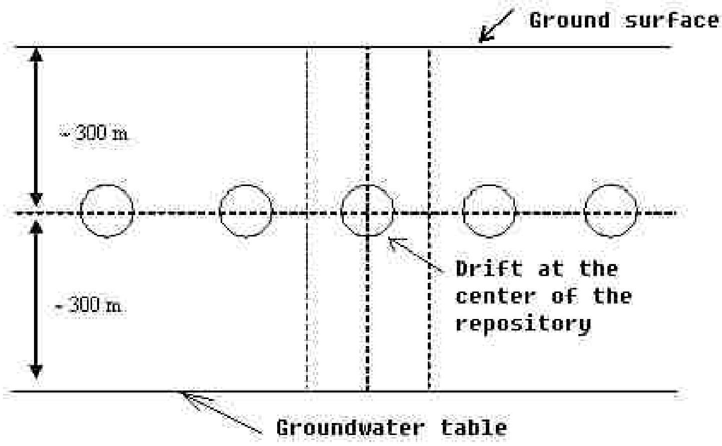

Figure 6.1: Conceptual model in COMSOL for the verification of the SRTA code

Figure 6.2 shows an example of the meshing scheme that was used in the COMSOL model.

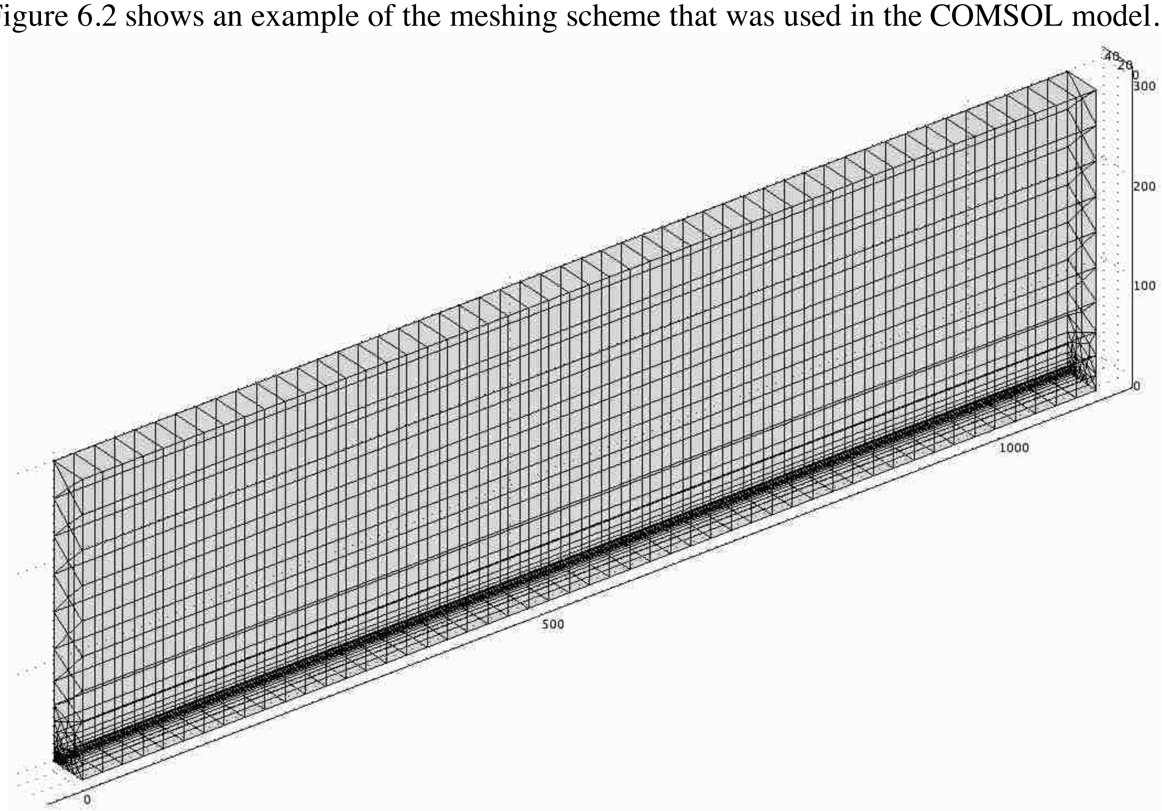

Figure 6.2: Swept Meshing

6.2.1 COMSOL Input

In order to benchmark the SRTA code it was necessary to have consistency between the COMSOL and SRTA models. A three dimensional COMSOL model was used based on a cylindrical heat source with air and Tuff rock regions. Figure 6.3 and Figure 6.4 gives a representation of the drift geometry used in the COMSOL model. A quarter symmetry scheme was used to simplify the temperature analysis of the COMSOL model.

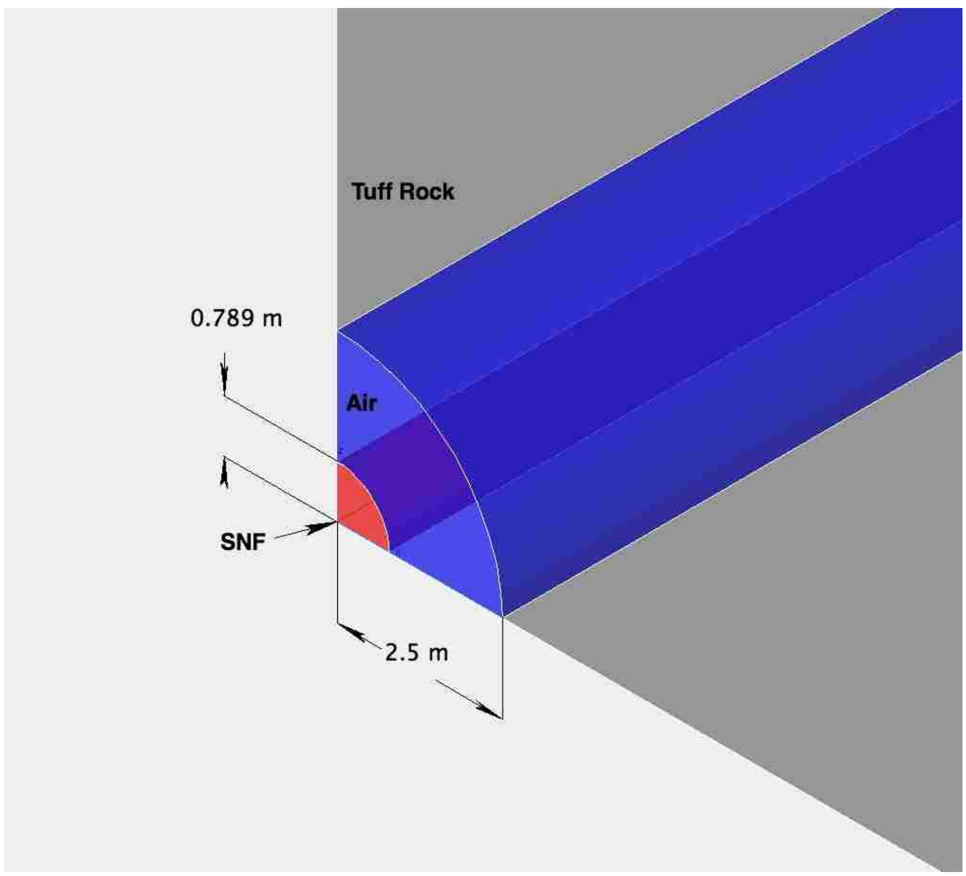

Figure 6.3: COMSOL Drift Geometry

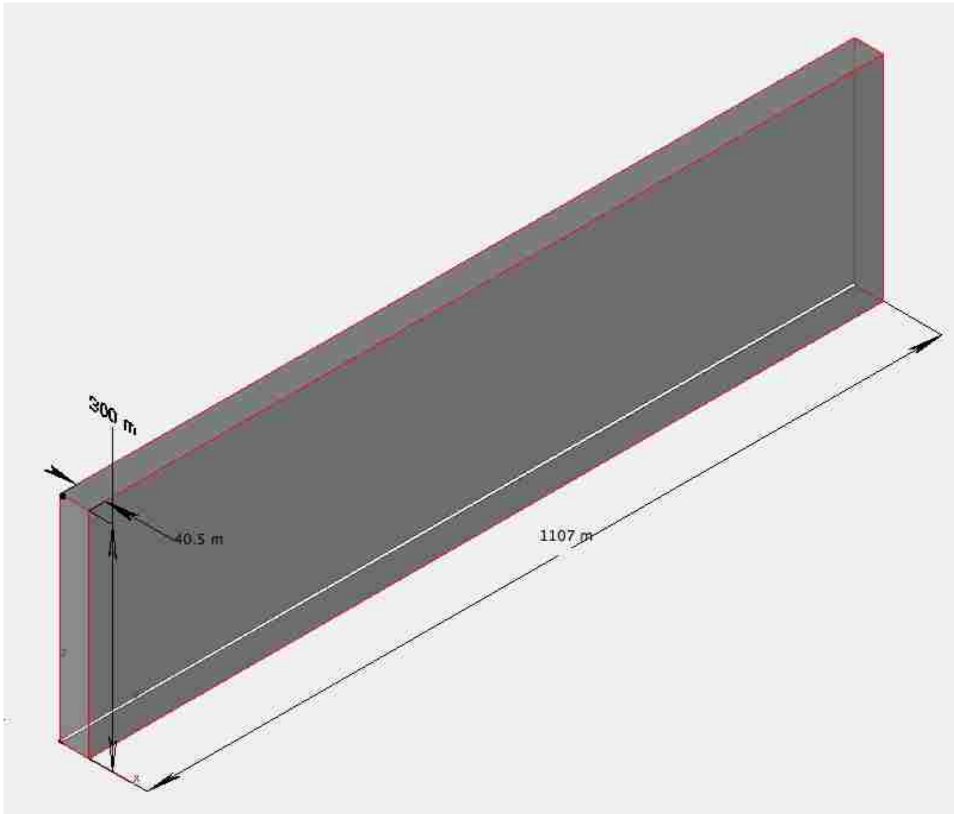

Figure 6.4: COMSOL Quarter Symmetry

In the SRTA and COMSOL models the burnup was taken to be 50,000 MWd/MTU for the entire repository. In both of the codes, the decay heat inventory of SNFs was determined by using the correlation model described in Section 4.

Table 6.2 provides the material input values used in both codes. Additionally, Table 6.3 provides key values for both dimension and other important parameters. These values were kept consistent in both codes in order to obtain a valid benchmark.

Table 6.2: Material Input Values

Material Properties	Value
Density of Rock:	2593 [kg/m^3]
Specific Heat of Rock:	930 [J/(kg·K)]
Rock Thermal Conductivity:	2.603 [W/(m·K)

Table 6.3: Parameter Input Values

Dimensions and Parameters	Value
Burnup:	50000 [MWd/MTU]
Enrichment:	4.4% (weight percent)
Days Irradiated:	600 days
Ambient Temperature:	20 [˚C]
Length of Drift:	1107 [m]
Drift Diameter:	5 [m]
Waste Package Diameter:	1.579 [m]
Ventilation rate:	15 [m^3/s]
Heat Loss Factor:	70% & 88%

The time of interest for analyzing the temperature distribution in the repository starts at the time of SNF emplacement (25 year cooling period) until after the peak temperature occurs between the drifts. As will be seen in the following figures there exists some obvious discontinuities in the plots, this is due to the fact that the decay heat model is split into seven different time regions in order to provide a best-fit line.

In COMSOL the artificial diffusion model was utilized to stabilize oscillations that occur when modeling a convection-dominated problem. Streamline diffusion was applied in the COMSOL model. Streamline diffusion refers to all diffusion occurring along the advection direction. A tuning parameter is required for artificial diffusion. This tuning parameter controls the amount of artificial diffusion being added to the system. A conservative tuning parameter was chosen for this model as can be seen in Table 6.4.

Table 6.4: Diffusion

Diffusion Type	Tuning Parameter Value
Streamline – Petrov-Galerkin/Compensated	0.25

6.2.2 Boundary Conditions

Conduction and convection COMSOL models were analyzed for the comparison with the SRTA code. Sections 6.2.2.1 and 6.2.2.2 describe the boundary conditions used in the modeling of the two different cases.

6.2.2.1 Conduction Model Boundary Conditions

The boundary condition on the top layer of the model is set to a temperature of 20˚C Equation (6.2).

$$T = T_0 \tag{6.2}$$

The boundary conditions for the four sides and bottom (based on Figure 6.4) were set as thermally insulated (Equation (6.3)). The thermal insulation boundary condition specifies the domain that is well insulated and takes advantage of symmetry. The gradient across the boundary is set to be zero and the temperature on one side of the boundary is equal to the temperature on the other side. Because there is no temperature difference across the boundary, heat cannot transfer across it.

$$\mathbf{n} \cdot \left(k \nabla T \right) = 0 \tag{6.3}$$

6.2.2.2 Convection Model Boundary Conditions

Similar to the conduction model the top layer has a temperature boundary condition of 20˚C and the sides and bottom as thermally insulated. The difference between the two models is that the air regions shown in Figure 6.3 have different boundary conditions other than being thermally insulated. The boundary at the beginning of the air region has a temperature boundary condition of 17.2˚C and the boundary at the end of the drift for the air region has a convective flux boundary condition.

The convective flux boundary condition at the end of the drift assumes that all energy passing through boundary does so through convective flux. This condition first assumes that any heat flux due to conduction across the boundary is zero as given in Equation (6.4).

$$\mathbf{n} \cdot \left(-k\nabla T\right) = 0 \tag{6.4}$$

Therefore the convective flux terms is:

$$q \cdot \mathbf{n} = \left(\rho C_p u T\right) \cdot \mathbf{n} \tag{6.5}$$

6.2.3 Ventilation Heat Loss Factor

The heat loss factor takes into account the amount of heat removed from the system during the preclosure period. Two different time periods were examined in both the SRTA and COMSOL models. As of the writing of this thesis, the time period for which forced ventilation occurs has not been finalized. Fifty years and seventy-five years were analyzed in order to compare the effect of extend periods of ventilation. The original heat loss factor assumed by the DOE was 70%. A recent engineering study for the Yucca Mountain repository determined that the value of heat loss factor is 88% (Bechtel 2004).

Figure 6.5 and Figure 6.6 provides a comparison between the SRTA and COMSOL conduction models for the 50 and 75 year preclosure period respectively. The data is presented on semi-log plots since the time period covers a large range of values; this scaling reduces the time period to a more manageable range. The convection model obtained from COMSOL was also analyzed in order to compare the heat loss factor and ventilation rate.

The temperature at the drift wall during the preclosure period increases more than the temperature between the drifts. This is due to the fact that most of the heat is removed due to ventilation of the drift during this time. Once the ventilation is turned off a sharp increase in temperature occurs at the drift wall since heat is no longer being removed. The temperature between the drift shows a slow increase in temperature with time since it takes time for heat to conduct to the Tuff rock in this region. Over time the decay heat of the SNF decreases as well as the temperature. Once the heat sinks (the water table and the ground surface) start dissipating the heat, the temperature begins to decrease.

Given the preclosure periods of fifty and seventy-five years it is intuitive that the temperatures at the drift wall and between the drift will be lower with the 75 year preclosure period since the drifts are ventilated for longer periods of time and the decay heat also decreases with time. A 70% ventilation heat loss factor for the SRTA code at fifty years is more conservative than the COMSOL convection model however; when a heat loss factor of 88% was analyzed the SRTA code was in agreement with COMSOL convection model.

The SRTA model is conservative for the drift wall and between drift temperatures when compared to the COMSOL conduction model. Moreover, the COMSOL convection model has much lower values when compared to both conduction models.

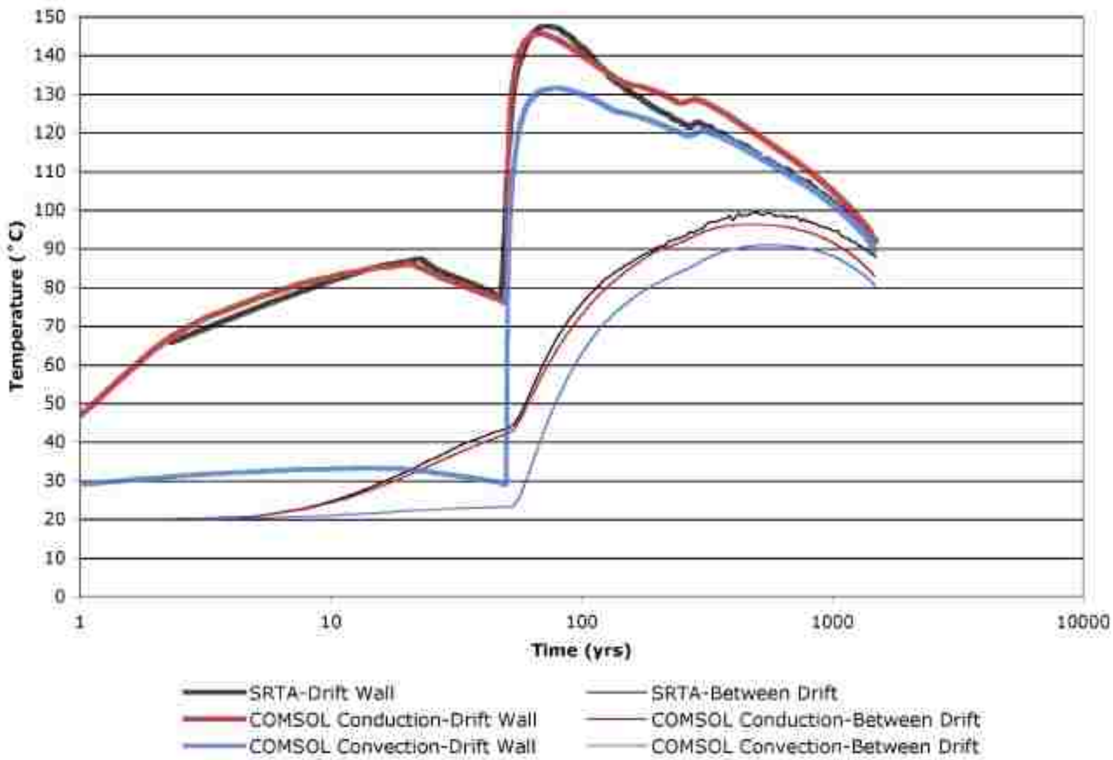

Figure 6.5: SRTA vs. COMSOL 50 Years Ventilation, 70% Heat Loss Factor

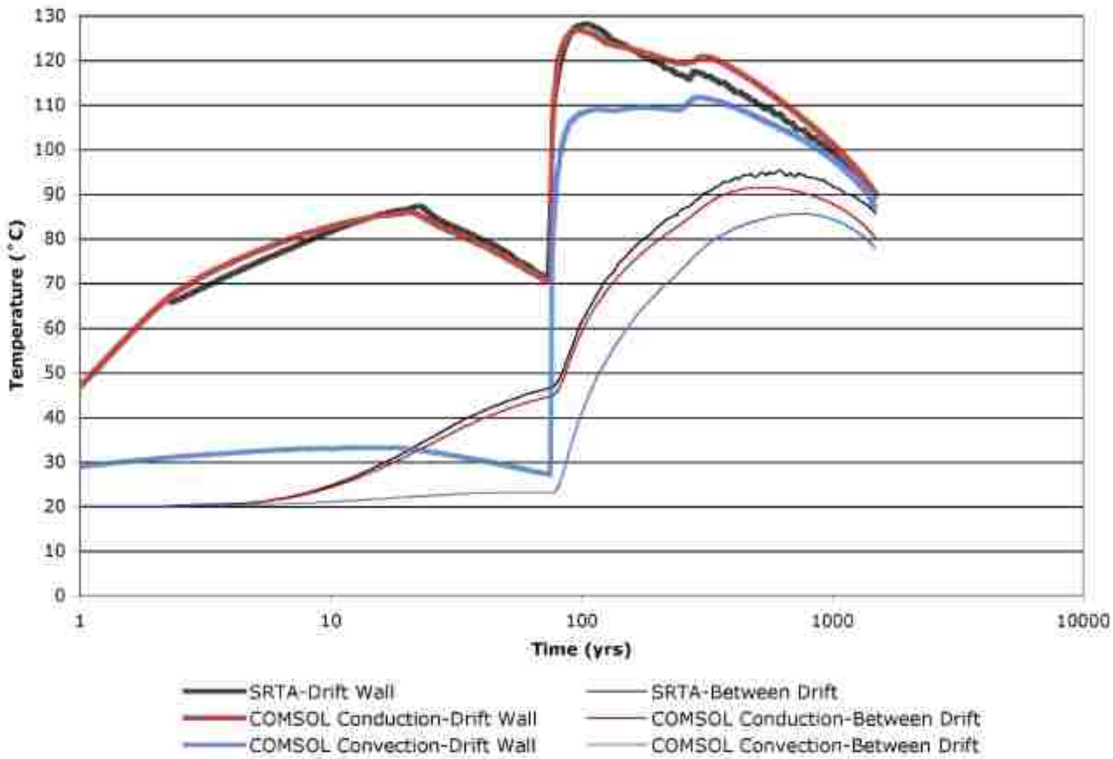

Figure 6.6: SRTA vs. COMSOL 75 Years Ventilation, 70% Heat Loss Factor

Calculation results showed that the SRTA model with a heat loss factor of 70% is very conservative when compared with the COMSOL convection model. A heat loss factor of 88% was also analyzed for both the conduction models. This 88% heat loss factor is the currently accepted value for the Yucca Mountain repository (Bechtel 2004).

Figure 6.7 and Figure 6.8 show the results of peak rock temperature changes over time when the 88% heat loss factor was adopted. Again the SRTA code predicted higher peak rock temperatures compared to the results from the COMSOL model.

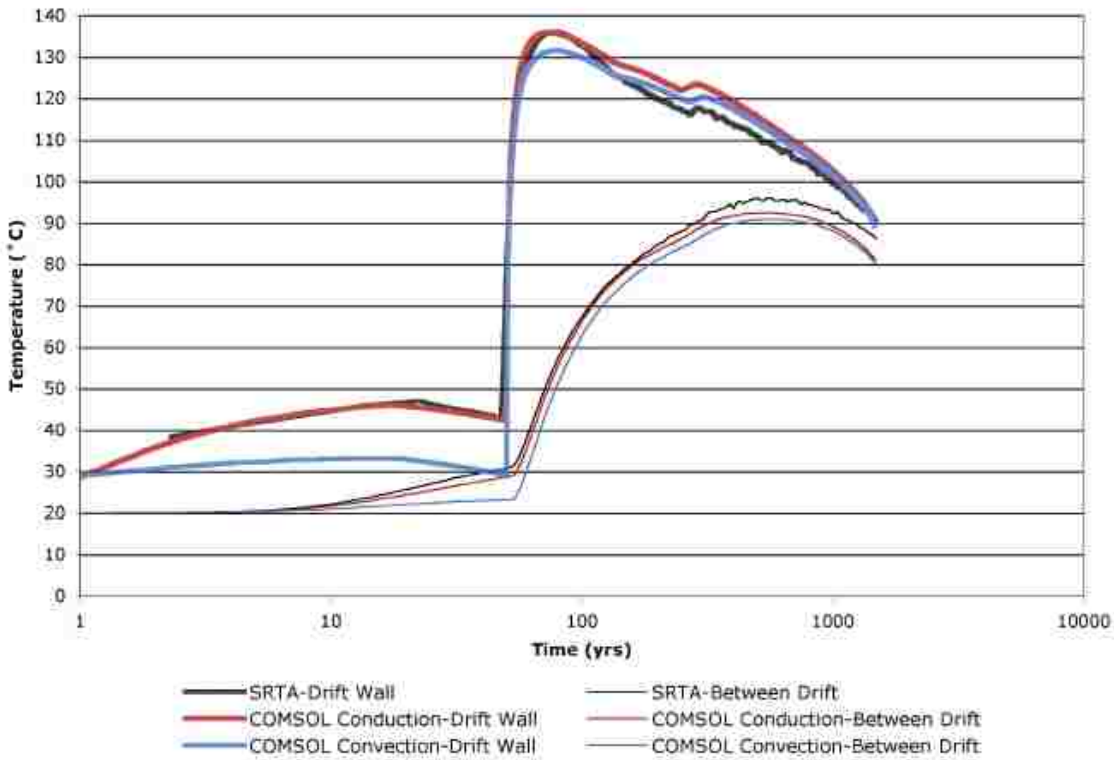

Figure 6.7: SRTA vs. COMSOL 50 Years Ventilation, 88% Heat Loss Factor

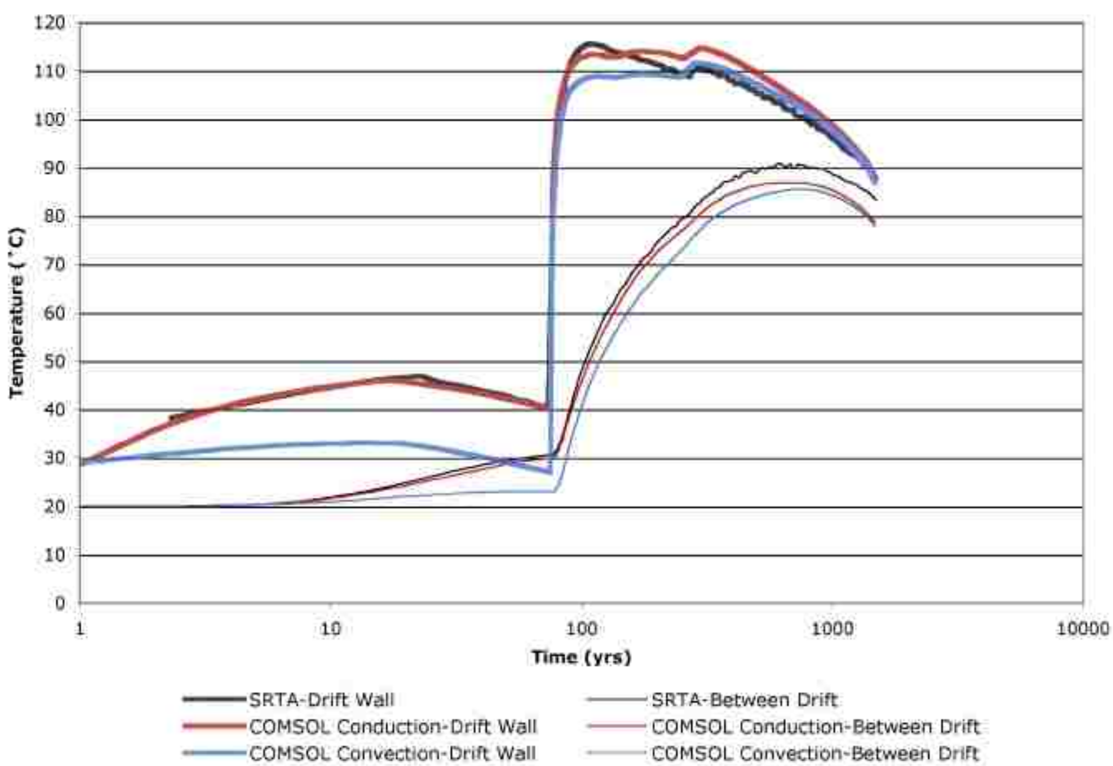

Figure 6.8: SRTA vs. COMSOL 75 Years Ventilation, 88% Heat Loss Factor

6.2.4 Benchmark Results

The benchmark of the SRTA code is important in order to verify the results of the temperature analyses. Based on the results of Section 6.2.3 the SRTA code gives results similar to the conduction and convection models in COMSOL. It was beyond the scope of this research to validate the SRTA code. But verification of SRTA was necessary for this research and the COMSOL code, a well established computer model, was used for that purpose.

The benchmark cases given in Figure 6.5 through Figure 6.8 shows that the SRTA code gives a conservative approach to analyzing the temperatures in the repository in comparison to the results from COMSOL. The values at the drift wall and between the drift for the SRTA model were greater when compared to COMSOL model. The drift wall never approached the temperature limit of 200˚C set by the NRC. Additionally, the temperature between the drifts given from the SRTA approached but did not exceed the limit of 96˚C.

The results obtained from SRTA and the COMSOL conduction model were in better agreement with those from the COMSOL convection model (based on the air flow of $15m^3/s$). This further supports the use of 88% as the value of the heat loss factor as opposed to using 70% in the remainder of the calculations for this research.

6.3 Sensitivity Investigation of Input Parameters

A related topic of importance in this investigation was the effect of uncertainty. As the modeling exercise relies on the use of computational models, uncertainties are unavoidable and understanding the uncertainty in the interpretation of the results is important. In order to gain a better understanding of how the parameters affect the SRTA model results and to identify major parameters of importance, a sensitivity analysis was performed. The sensitivity analysis was based on a nominal range sensitivity analysis. Based on the values given in Table 6.1 a five percent increase in the mean was taken to find the temperature at the drift wall and between the drift for a preclosure period of fifty years. Table 6.5 provides the peak rock temperatures predicted as the base case without the changes in input values from the base value.

Table 6.5: Peak Rock Temperature as the Base Case (50 Years)

Drift Wall (˚C)	**Between Drift (˚C)**
104.36	78.86

Table 6.6: Sensitivity Analysis-5% Increase (50 Years)

Parameters	Drift Wall (˚C)	Between Drift (˚C)
rho	103.32	77.71
Cp	103.32	77.71
cond	101.33	77.56
cond_n	104.36	78.86
hloss_fact	102.48	78.34
condds	104.36	78.86
condbf	104.36	78.86
emissds	104.36	78.86
emisswp	104.36	78.86
wpdia	104.36	78.86
wplength	104.36	78.86
dsthick	104.36	78.86
ds_idia	104.36	78.86
driftdia	104.02	78.88
frac_inv	104.36	78.86
ambreptemp	105.36	79.86
elevrep	104.36	78.46
elevgs	104.36	78.96
tss	104.36	78.86
tcs	104.36	78.86
akss	104.36	78.86
akcs	104.36	78.86
aksf	104.36	78.86
wpspace	100.33	76.05
condfloor	104.36	78.86
emissrw	104.36	78.86

The sensitivity analysis showed (see Table 6.6) that some of the input parameters do have a larger impact than others. The three main contributors were the density, specific heat, and thermal conductivity of the Tuff rock. The waste package spacing can play an important role in the determination of rock temperatures. However this parameter was not included in the uncertainty analysis as the parameters is fixed by design and does contain any variability (DOE 1999).

6.4 Uncertainty of Input Parameters

The SRTA code utilizes an input file comprised of different physical properties of the repository design. Uncertainties of these parameters were characterized by various studies as summarized in Table 6.7. It was noted that all of the parameters' uncertainty were represented by the normal distribution. Certain input values have large uncertainties that can account for a large uncertainty in the temperature analysis.

Crystal Ball 7 (CB 7) (Decisioneering 2007) was used to run a Monte Carlo simulation of the SRTA code. The values in Table 6.7 were used to support the Monte Carlo analysis. Full details of the assumptions utilized in CB 7 are supplied in Appendix B along with graphs of the distributions.

Table 6.7: Uncertainty in Input Values

Code Parameters:	Units	Initial Value (the mean)	Standard Deviations	Distribution	Source
akcs	W/(m-°C)	15.49	4.21	Normal	DOE 2001
akss	W/(m-°C)	16.62	2.10	Normal	DOE 2001
cond	W/(m-K)	2.603	0.341	Normal	DOE 2004
condds	W/(m-°C)	20.00	0.77	Normal	DOE 2001
Cp	J/(kg-K)	930	170	Normal	DOE 2004
driftdia	m	5.0	0.089	Normal	Bechtel 2004
emissds	-	0.64	0.05	Normal	Michels 1949
emisswp	-	0.87	0.02	Normal	Bechtel 2004
hloss_fact	-	0.88	0.01	Normal	Bechtel 2004
rho	Kg/m^3	2593	138	Normal	DOE 2004
wpdia	m	1.644	0.089	Normal	Bechtel 2004

7 Analysis of Capacity Expansion through Variable Drift Spacing and Variable Drift Thermal Loading

Studies performed to date investigating the capacity of Yucca Mountain typically assume that the loading of SNF is uniform throughout the repository (i.e., drift thermal loading is constant throughout the repository with a fixed drift distance). In this study, it is assumed that variable drift spacing or variable drift thermal loading is allowed. As the results of analysis involve uncertainties, uncertainty analysis was performed to better interpret the results. In terms of how to use the results of uncertainty analysis, both the mean and the 95th percentile estimates were used for discussions.

7.1 Variable Drift Spacing

One method to increasing the capacity of the repository is to change the spacing between the drifts. For the case of variable drift spacing, it was assumed that available repository footprint is 4.9km^2 (1,165 acres – the default input value in NRC's TPA code) (NRC 2002) and that the rock temperature at the midway between the drifts is the limiting criterion and that, by adjusting the distance, an optimum distance between the drift within the thermal limit can be found for the given decay heat load using uniform loading.

The decay heat inventory was determined by assuming that the repository was fully loaded with an average PWR (64.5%) and BWR (35.5%) SNF. The DOE database that was discussed in Section 4.2 was analyzed for the decay heat of the entire SNF inventory. Based on this analysis and the projected SNF inventory (Table 1.1) an assembly, characteristic of the total average inventory of the U.S. SNF, was selected as given in Table 7.1. The characteristics of SNFs were assumed to have: a burnup of 39,136 and 31949.5 MWd/MTU for PWRs and BWRs, respectively; irradiation days of 366 and 571 days for PWRs and BWRs, respectively; initial enrichment of 3.094 and 3.004 for PWRs and BWRs, respectively; and a cooling period of 25 years. The time to which the repository is to be closed after the initial emplacement of SNF has yet to be determined. Two time periods of 50 and 75 years were examined in order to study the benefits of longer periods of ventilation.

Table 7.1: Characteristic Fuel Assembly for PWR and BWR

	PWR	**BWR**
Years Cooled:	25	25
Blend:	0.645	0.355
Burnup (MWd/MTU:	39136	31949.5
Days Irradiated:	366	571
Enrichment:	3.094	3.004

7.1.1 Peak Temperatures at Drift Wall and at the Midway between the Drifts

Current design specifications (NRC 2002) state that the drifts must be 81 meters apart. Based on the results of SRTA analysis (as shown in Table 7.2) for the case of using the current drift spacing of 81m, it can be noted that the thermal limits are not exceeded even at the ninety-fifth percentile. This indicate a margin in the current drift spacing design and that the capacity of the mountain could be increased by decreasing the drift spacing. The thermal limit at the drift wall was far less than the limit of 200˚C however, the drift wall was very close to the limit of 96˚C. From this it is concluded that the temperature between the drifts is the most limiting.

Table 7.2: Results of SRTA Analysis Results for the Base Case (81 m drift spacing), Preclosure period of 50 Years

	Temperature (˚C)				
Location:	**Mean**	**Standard Deviation**	**Min/Max**	**90th %ile**	**95th %ile**
Drift Wall	106	10	78/164	119	124
Between Drift	80	7	60/129	90	93

7.1.2 Repository Capacity with the Implementation of Variable Drift Spacing

Table 7.3 demonstrates how the capacity of the repository could be increased by changing the distance between the drifts. The linear heat load for the variable drift spacing is 1.22 kW/m. Based on the between drift thermal limit of 96˚C the SRTA calculations estimated that the spacing between the drifts could be reduced to 63 meters. This implies that the total capacity of the mountain could be increased by 37.1%. This increase in capacity would mean that the repository would not be filled until the year 2023 based on the current nuclear fleets discharge rate of approximately 2000 MTU/year. Based on the analysis for the ninety-fifth percentile the capacity can be increased by 9.8% and the repository filled by 2013.

Table 7.3: Increase in Capacity Due to the Implementation of Variable Drift Spacing (50 Years)-Based on the Mean Estimates (1.22 kW/m)

Drift Spacing [m]	Drift Wall [˚C]	Between Drift [˚C]	Total MTU	Increase in MTU
81	104.36	78.86	70000	-
63	110	96	95942	37.1%

Table 7.4: Increase in Capacity Due to the Implementation of Variable Drift Spacing (50 Years)-Based on the 95th %ile Estimates (1.22 kW/m)

Drift Spacing [m]	Drift Wall [˚C]	Between Drift [˚C]	Total MTU	Increase in MTU
78.5	124	96	76833	9.8%

A preclosure period of seventy-five years was also studied. Table 7.5 provides the results of SRTA analysis along with uncertainty estimates for the base case (with the standard drift spacing of 81 meters). The thermal limits at the ninety-fifth percentile were not exceeded. The estimated midway between the drifts temperature was 7˚C below the thermal limit of 96˚C.

Table 7.5: Results of SRTA Analysis Results for the Base Case (81 m drift spacing), Preclosure period of 75 Years (1.22 kW/m)

	Temperature (˚C)				
Location:	**Mean**	**Standard Deviation**	**Min/Max**	**90th %ile**	**95th %ile**
Drift Wall	92	8	71/146	103	107
Between Drift	77	7	58/130	86	89

Based on this analysis and the information in Table 7.6 the capacity of the repository could be increased by 42.6% when the parameters are based on the peak of the mean. This would extend the life of the repository from 2010 to 2025. For the analysis based on the ninety-fifth percentile the capacity can be increased by 15% and the repository closing around 2015.

Table 7.6: Increase in Capacity Due to the Implementation of Variable Drift Spacing (Preclosure period of 75 Years)-Based on the Mean Estimates (1.22 kW/m)

Drift Spacing [m]	Drift Wall [˚C]	Between Drift [˚C]	Total MTU	Increase in MTU
81	89.03	74.69	70000	-
60.5	106	96	99809	42.6%

Table 7.7: Increase in Capacity Due to the Implementation of Variable Drift Spacing (Preclosure period of 75 Years)-Based on the 95th %ile Estimates (1.22 kW/m)

Drift Spacing [m]	Drift Wall [˚C]	Between Drift [˚C]	Total MTU	Increase in MTU
75	111	96	80565	15%

7.1.3 Main Contributors of Uncertainty in the Analysis of the Variable Drift Spacing Case

Rank correlation coefficients indicate the relationship between the ranks of model inputs and output. Thus, rank correlation provides a measure of degree to which the input parameters change with the output of interest, in this case, peak rock temperatures. Positive coefficients indicate that an increase in the input parameter is associated with a positive increase in the temperature. Negative coefficients imply the opposite situation. The absolute value of the rank correlation means a stronger relationship between the parameters and the temperature.

Figure 7.1 through Figure 7.4 contain the uncertainty parameters and the contribution they have in the calculation of the temperature of the drift wall and between the drifts. There are three main contributors that have the most effect on the SRTA model and these are the material properties of the Tuff rock. Thermal conductivity, specific heat, and density of Tuff rock are the main parameters to uncertainty in the model. The order of the importance of these parameters varies depending on the output of interest, i.e., the drift wall temperature or the rock temperature at the midway between the drifts.

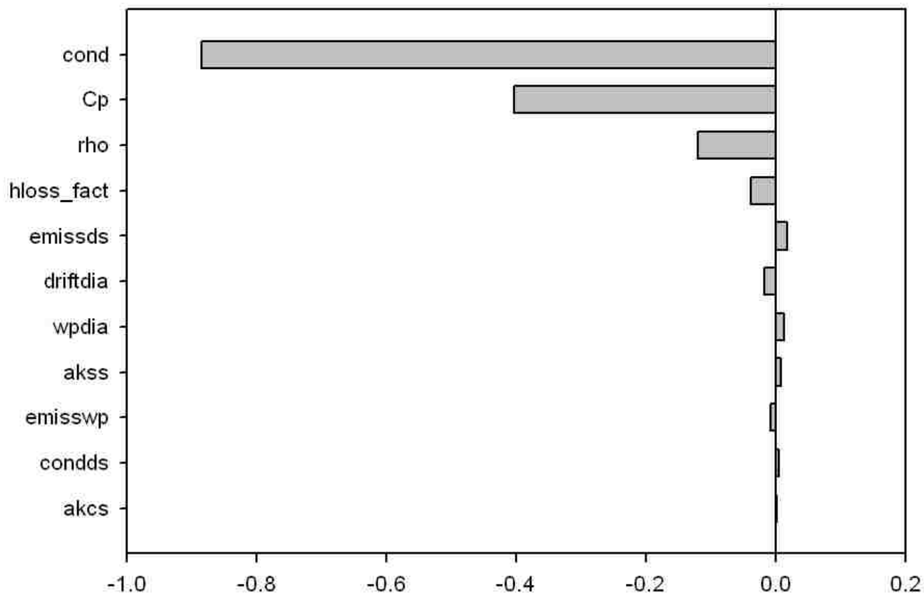

Figure 7.1: Results of Rank Correlation Analysis for Drift Wall Temperature (With Uniform Loading for 50 Year Preclosure Period)

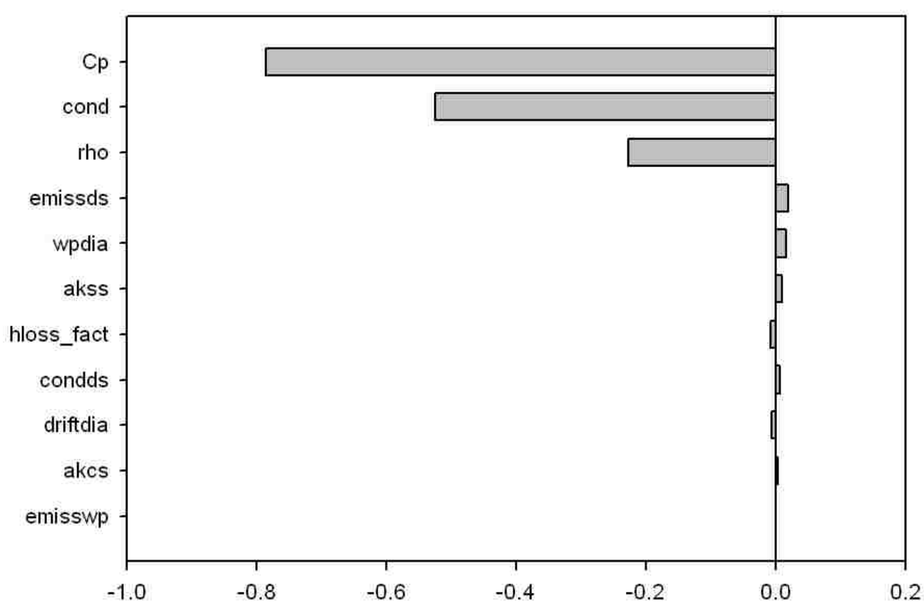

Figure 7.2: Results of Rank Correlation Analysis for Between Drift Temperature (With Uniform Loading for 50 Year Preclosure Period)

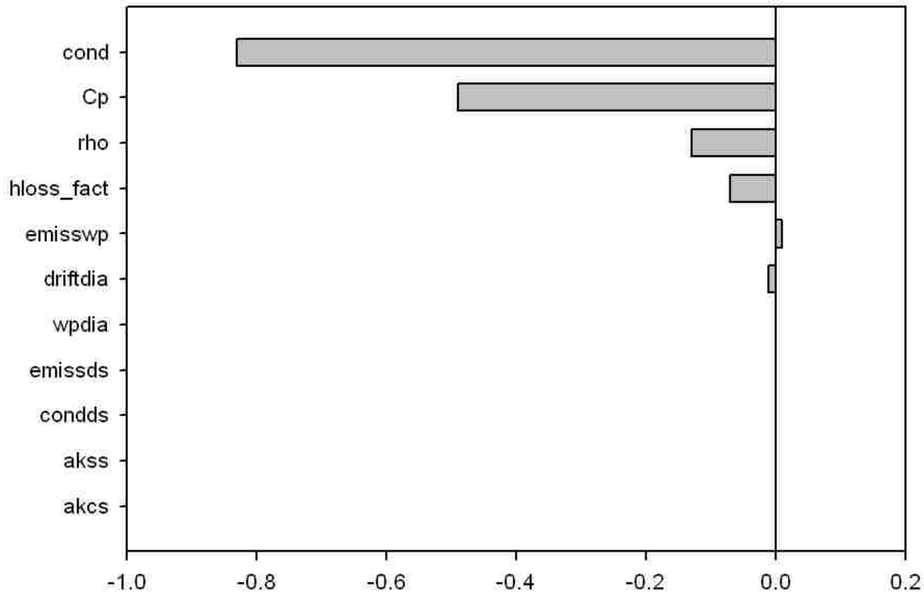

Figure 7.3: Results of Rank Correlation Analysis for Drift Wall Temperature (With Uniform Loading for 75 Year Preclosure Period)

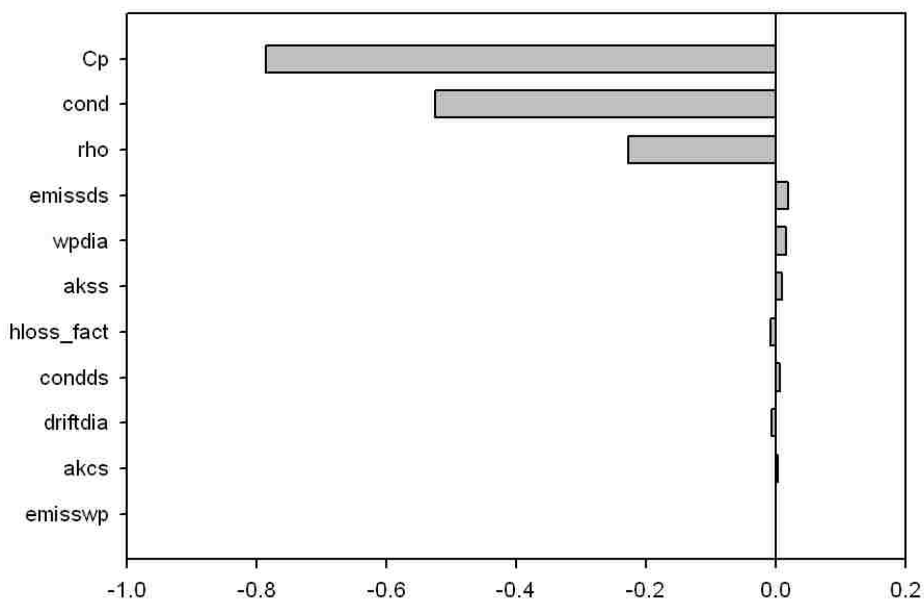

Figure 7.4: Results of Rank Correlation Analysis for Between Drift Temperature (With Uniform Loading for 75 Year Preclosure Period)

7.2 Variable Drift Thermal Loading

As variable drift thermal loading option assumes that each drift accommodates different types of spent fuel in terms of decay heat, a more realistic representation of the decay heat inventory is necessary. To support this study, the existing inventory of SNF generated until 2002 based on the DOE/RW-859 database (DOE 2002b) was used. The database includes a total of about 160,000 fuel assemblies that corresponds to about 46,757 MTU. This 46,757 MTU became the basis for variable thermal loading study (Li, 2-3).

The footprint size used to accommodate these 46,757 MTU was about 759.60 acres (3.07 km2). The total number of drifts available in this footprint size was 35. Based on the inventory of SNF there is an infinite number of ways to load the repository. Five different loading schemes based on different uniform line strengths for thirty-five drifts were analyzed. These scenarios can be explained as given below. Due to the limitations in the computer model, SRTA, the heat flux from each drift was approximated by the drift average value. The average decay heat load of each drift was calculated for each respective scenario to be used as input to the SRTA code. The linear heat load can be found in Appendix C for each of the five loading schemes.

Loading Scheme 1 starts with a low linear heat load at the center of the repository and gradually increases to a higher linear heat load toward the edge (south end) of the repository. Loading Scheme 2 through 5 is loaded with alternating linear heat loads of varying strengths. The loading starts with a high linear heat load for the first drift and a low linear heat load for the second drift and continues alternating between high and low heat loads until thirty-five drifts are full. As can be seen in Appendix C the linear heat loads vary in strength from one loading scheme to another.

7.2.1 Peak Temperatures at Drift Wall and at the Midway between the Drifts

7.2.1.1 Base Case with the Preclosure Period of 50 Years

For the base case, it was assumed that each waste package contained 7.89 Metric Tons of Uranium (MTU). The input values were constant for the base case. The input values used for the base case are shown in Table 6.1. The five loading schemes were analyzed for this base case to see if the thermal design limits would be exceeded with any of the loading schemes.

Table 7.8 provides the calculation results with a preclosure period of fifty years. Based on the temperature at the point midway between the drift, the best loading scheme is expected to be Scheme 1 or 2. The temperature at the drift wall for loading Scheme 2 also is very low. Therefore, the thermal loading of drifts for Scheme 2 can be increased in order to increase the capacity of the repository.

Table 7.8: Results of SRTA Calculations for the Variable Drift Thermal Loading Schemes (Base Case Input Values with 50 Year Preclosure Period)

Scheme:	1	2	3	4	5
Peak drift wall temperature (°C)	127.1	101.0	100.4	122.5	135.3
Location of the peak drift wall temperature	Drift #33	Drift #10	Drift #4	Drift #2	Drift #1
Peak rock temperature between drift (°C)	85.5	74.3	74.5	74.5	74.1
Location of the peak temperature between drift	Between Drift #32 & #33	Between Drift #10 & #11	Between Drift #14 & #15	Between Drift #8 & #9	Between Drift #25 & #26

7.2.1.2 Case with Uncertainty Analysis with the Preclosure Period of 50 Years

Table 7.9 results of SRTA analysis along with uncertainty estimates for the temperatures at the drift wall. Based on the ninety-fifth percentile estimates, the thermal limit of 200˚C was never exceeded in any of the loading schemes. This indicates that the drift wall thermal limit is not of a concern for the given U.S. SNF inventory based on the average linear drift heat loads. As indicated in the following, the midway between the drifts temperature is to be noted in regards to the thermal limits.

Table 7.9: Results of Variable Drift Thermal Loading Analysis - Drift Wall Temperature with 50 Year Preclosure Period

	Drift Wall Temperature (˚C)			
Loading Scheme:	**Mean**	**Standard Deviation**	**90th %ile**	**95th %ile**
Scheme 1	129	13	146	152
Scheme 2	103	9	115	119
Scheme 3	102	9	114	118
Scheme 4	124	12	141	147
Scheme 5	137	14	156	164

There were three primary contributors to the uncertainty of the drift wall temperature. These contributors were the thermal conductivity of Tuff rock, specific heat of Tuff rock, and the density of the Tuff rock. Most of the other contributors had less impact on the overall uncertainty evaluation. Figure 7.5 provides the rank correlation of all the parameters that had uncertainty. Only Scheme 1 will be represented here due to the fact that the three main contributors are consistent for Schemes 1 through 5. The results for Schemes 2 through 5 can be found in Appendix D.

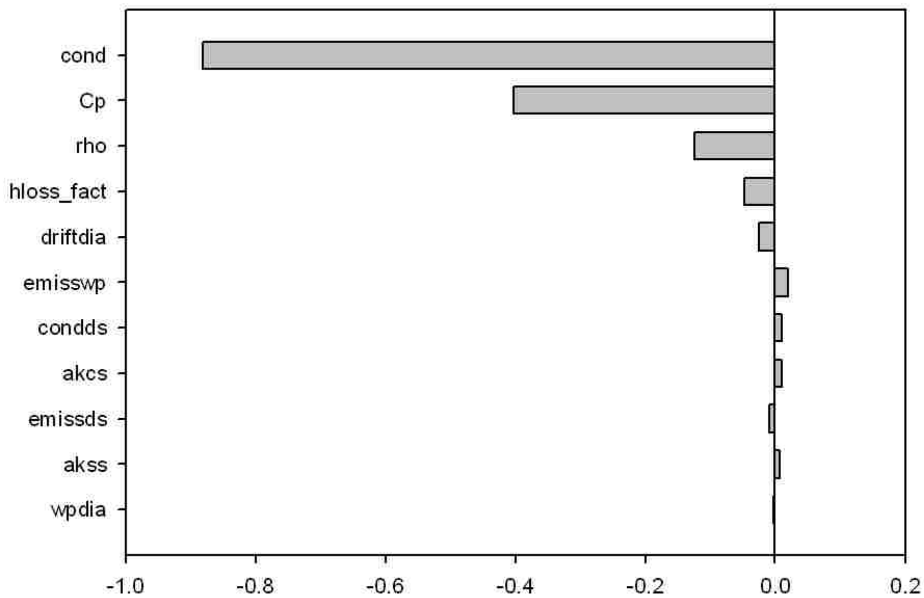

Figure 7.5: Results of Rank Correlation Analysis for Drift Wall Temperature (With Loading Scheme 1 – Sequential Loading Scheme, 50 Year Preclosure Period)

The results of SRTA calculations for the midway between the drifts temperature are given in Table 7.10. The ninetieth and ninety-fifth percentile give conservative estimates of the rock temperatures. Based on the ninety-fifth percentile estimates, loading Schemes 2 through 4 never exceeded the limit of 96˚C. However, loading Scheme 1 did violate the thermal limit. Results indicated that the capacity of the Yucca Mountain repository could be extended by implementing the proposed non-uniform loading Schemes 2 through 5.

Table 7.10: Results of Variable Drift Thermal Loading Analysis – Midway between the Drifts Temperature with 50 Year Preclosure Period

	Midway Between the Drifts Temperature (˚C)			
Loading Scheme:	**Mean**	**Standard Deviation**	**90th %ile**	**95th %ile**
Scheme 1	87	8	98	102
Scheme 2	76	7	85	88
Scheme 3	76	7	85	88
Scheme 4	76	7	85	88
Scheme 5	75	7	85	88

Again the rank correlation is presented in Figure 7.6 for the mid-drift. The three main contributors are the same as the drift wall however the order is slightly different. One can see that material properties of the Tuff rock; specific heat, thermal conductivity, and density are again very important in describing the uncertainty of the temperature calculation. The other parameters have little to no effect on the overall results and could be ignored.

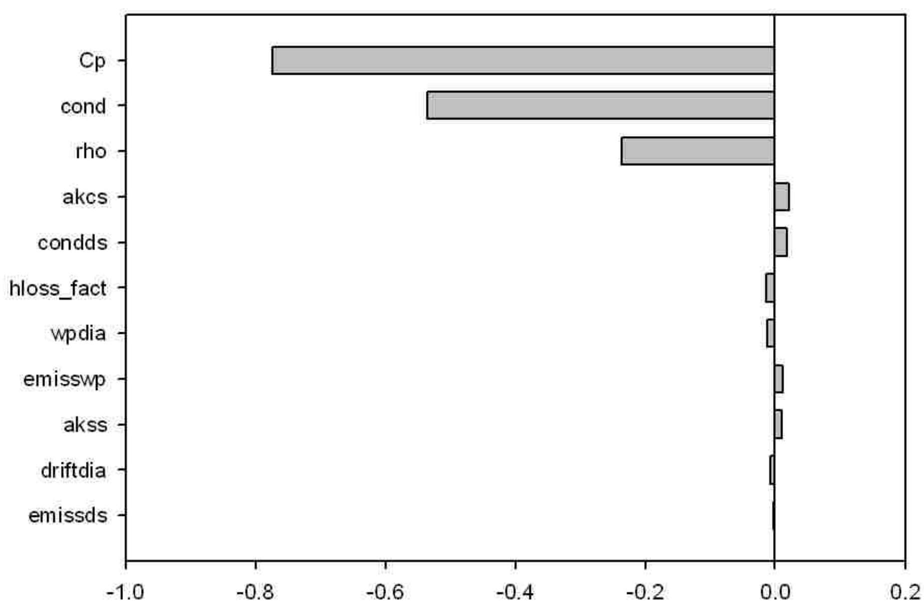

Figure 7.6: Results of Rank Correlation Analysis for Between Drift Temperature (With Loading Scheme 1 – Sequential Loading Scheme, 50 Year Preclosure Period)

7.2.1.3 Base Case with the Preclosure Period of 75 Years

Similar to the analysis in subsection 7.2.1.1 the five loading schemes were analyzed as a base case with a preclosure period of seventy-five years. Results are given in Table 7.11. Again the thermal design limits have not been exceeded in any of the loading schemes as can be seen in Table 7.11. This base case results indicate that the capacity of the repository can be increased by using the variable drift thermal loading schemes based on the average linear head load for each drift. Loading Scheme 2 was used to further analyze the uncertainties in the temperature calculations.

Table 7.11: Results of SRTA Calculations for the Variable Drift Thermal Loading Schemes (Base Case Input Values with 75 Year Preclosure Period)

Scheme:	1	2	3	4	5
Peak drift wall temperature (°C)	107.6	88.1	86.9	101.8	111.1
Location of the peak drift wall temperature	Drift #33	Drift #10	Drift #4	Drift #2	Drift #1
Peak rock temperature between drift (°C)	80.8	71.4	71.4	71.4	71.3
Location of the peak temperature between drift	Between Drift #32 & #33	Between Drift #10 & #11	Between Drift #14 & #15	Between Drift #8 & #9	Between Drift #25 & #26

7.2.1.4 Case with Uncertainty Analysis with the Preclosure Period of 75 Years

Table 7.12 provides the results of SRTA calculations along with uncertainty estimates for the temperatures at the drift wall. The drift wall thermal limit was never exceeded in any of the loading schemes even with the use of the ninety-fifth percentile estimates for the peak rock temperatures. The more limiting thermal limit was the thermal limit at the midway between the drifts.

Table 7.12: Results of Variable Drift Thermal Loading Analysis - Drift Wall Temperature with 75 Year Preclosure Period

	Drift Wall Temperature (˚C)			
Loading Scheme:	**Mean**	**Standard Deviation**	**90th %ile**	**95th %ile**
Scheme 1	109	10	123	127
Scheme 2	89	8	101	104
Scheme 3	88	8	98	102
Scheme 4	103	10	116	121
Scheme 5	113	11	127	132

As in the case of the fifty-year preclosure period there are three primary contributors to the uncertainty calculations of the drift wall. The contributors to the drift wall are the thermal conductivity of Tuff rock, specific heat of Tuff rock, and the density of the Tuff rock. The other contributors have less impact on the overall uncertainty evaluation. Figure 7.7 provides the rank correlation of all the parameters that contained uncertainty. Only Scheme 1 will be represented here due to the fact that the three main contributors are consistent for Schemes 1 through 5. Schemes 2 through 5 for the seventy-five year preclosure period can be found in Appendix E.

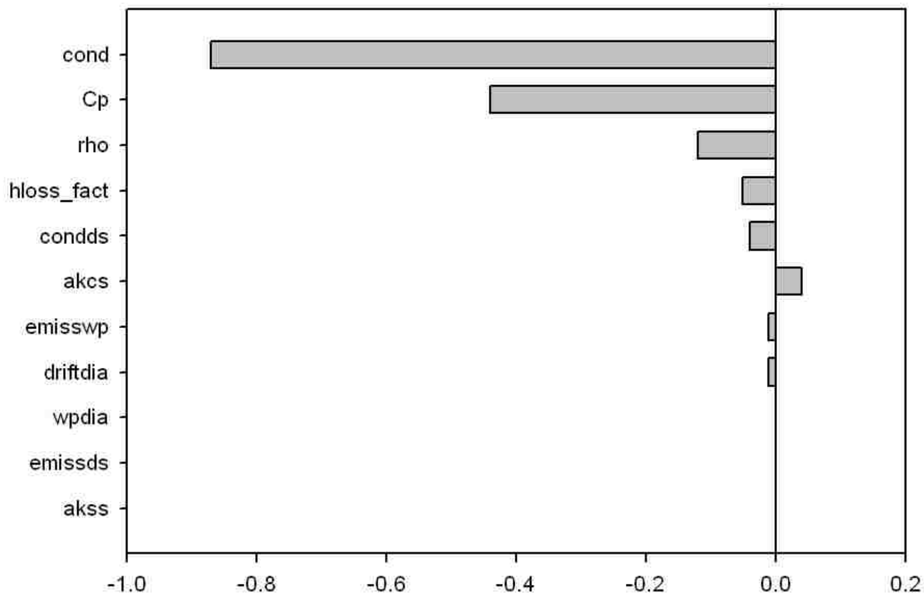

Figure 7.7: Results of Rank Correlation Analysis for Drift Wall Temperature (With Loading Scheme 1 – Sequential Loading Scheme, 75 Year Preclosure Period)

The results of SRTA calculations for the midway between the drifts temperature are summarized in Table 7.13. Based on the ninety-fifth percentile estimates, loading Schemes 2 through 4 never exceeded the limit of 96˚C. However, loading Scheme 1 did reach the limit for the ninety-fifth percentile. Based on loading Scheme 1 no further increase in capacity could be applied.

Table 7.13: Results of Variable Drift Thermal Loading Analysis – Midway between the Drifts Temperature with 75 Year Preclosure Period

	Midway Between the Drifts Temperature (˚C)			
Loading Scheme:	**Mean**	**Standard Deviation**	**90th %ile**	**95th %ile**
Scheme 1	82	8	92	96
Scheme 2	72	7	81	84
Scheme 3	72	6	81	84
Scheme 4	73	7	81	84
Scheme 5	72	6	80	84

Again the results of the rank correlation analysis are presented in Figure 7.8 for the rock temperature at the midway between the drifts. The three main contributors to the uncertainty of the temperature prediction were the same as at the drift wall with different order pf importance. One can see that material properties of the Tuff rock, i.e., specific heat, thermal conductivity, and density are again very important for the uncertainty of the temperature calculation. The other parameters have little to no effect on the overall results and could be ignored.

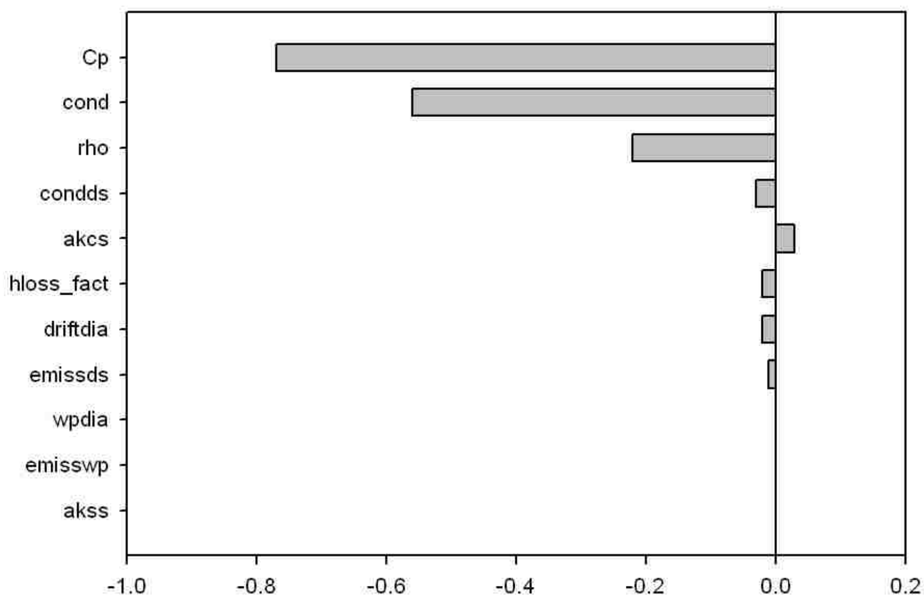

Figure 7.8: Results of Rank Correlation Analysis for Between Drift Temperature (With Loading Scheme 1 – Sequential Loading Scheme, 75 Year Preclosure Period)

7.2.1.5 Repository Capacity with the Implementation of Variable Drift Thermal Loading

Based on the results of calculation, the capacity of the repository is expected to be expandable due to that fact that the thermal limits were not exceeded for the assumed variable drift thermal loading scenarios (except for the 95th percentile estimate for loading Scheme 1). Table 7.14 and Table 7.15 provide the estimates of capacity expansion based on using the mean values of input parameters in Table 6.1.

Except for loading Scheme 1, all other loading schemes are expected to provide the similar benefit of capacity increase. Considering the margin in the drift wall temperature limit as discussed in Section 7.2.1.1 and 7.2.1.3, loading Schemes 2 and 3 are expected to be the best choice among the variable drift thermal loading options.

Table 7.14: Increase in Capacity for Variable Drift Thermal Loading for 35 Drifts (50 Year Preclosure Period)-Based on Mean

Scheme:	1*	2	3	4	5
Maximum Capacity per 35 drifts (MTU)	54254	65424	65187	65128	65750
Increase compared to 46757 MTU:	16.0%	39.9%	39.4%	39.3%	40.6%

*Mid-drift temperature was violated at the 95th %ile.

Table 7.15: Increase in Capacity for Variable Drift Thermal Loading for 35 Drifts (75 Year Preclosure Period)-Based on Mean

Scheme:	1	2	3	4	5
Maximum Capacity per 35 drifts (MTU)	58372	69158	69069	69158	69217
Increase compared to 46757 MTU:	24.8%	47.9%	47.7%	47.9%	48.0%

As far as decision making is concerned, which percentile value of the peak temperature distribution should be used as a basis for regulatory decisions is yet to be determined. If we select loading Scheme 2 as the best loading option, how much capacity increase is expected for loading Scheme 2 given the uncertainties in the results? In this study, the ninety-fifth percentile estimate was used as a conservative basis for discussion.

For a fifty-year preclosure period the estimated percent increase in the capacity with the implementation of loading Scheme 2 was 10.9% for the ninety-fifth percentile as seen in Table 7.16. For a preclosure period of seventy-five years the estimated percent increase in the capacity was 17.3%.

Table 7.16: Increase in Capacity for Variable Drift Thermal Loading for 35 Drifts (50 Year Preclosure Period)-Based on 95th %ile

Scheme:	2
Maximum Capacity per 35 drifts (MTU)	51861
Increase compared to 46757 MTU:	10.9%

Table 7.17: Increase in Capacity for Variable Drift Thermal Loading for 35 Drifts (75 Year Preclosure Period)-Based on 95th %ile

Scheme:	2
Maximum Capacity per 35 drifts (MTU)	54825
Increase compared to 46757 MTU:	17.3%

7.3 Sensitivity of the Estimated Capacity to the Uncertainty of Inputs

The sensitivity of the estimated capacity to the uncertainty of inputs is a subject of interest. If the results indicate a larger increase in the estimated capacity due to the reduction in uncertainty, the benefit of further investigations in reducing input parameter uncertainty can be warranted.

In this study, based on using the ninety-fifth percentile estimate, changes in the estimated capacity increase was noted when the uncertainty in input was reduced. A twenty percent reduction in the standard deviations for the major inputs was assumed for uncertainty reduction. The three main contributors to uncertainty, specific heat, conductivity, and density of Tuff rock were used in this investigation.

From Table 7.18 it can be seen that, under the variable drift spacing scenario, a twenty percent reduction in the uncertainty of all three parameters would result in the reduction in drift spacing from 78.5 to 70.1 meters.

Table 7.18: Capacity Increase Due to 20% Reduction in Uncertainty (95%-ile)-75 Years with Uniform Loading

Parameters	Drift Spacing (m)	Total MTU	% Increase
Density of Tuff Rock	74.4	80762.04	15.4%
Specific Heat of Tuff Rock	72.1	84154.74	20.2%
Thermal Conductivity of Tuff Rock	73.6	82229.58	17.5%
All Three Main Contributors	70.1	86687.43	23.8%

Under the variable drift thermal loading scenario (Scheme 2 with a preclosure period of 75 years), 20% reduction in uncertainty is estimated to result in an increase in capacity from 17.3% to 26.3% using the 95^{th} percentiles of the peak temperature distributions. This is shown in Table 7.19.

The estimate of HLW repository development cost ranges roughly between $60 billion and $100 billion (Shropshire, et. al., 2007). Increase of repository capacity by 10% means monetary gain in the order of billions. As the cost of reducing the uncertainty in major input parameters is expected to be much lower, the results indicate major benefits of uncertainty reduction of input parameters for the repository development. However, this observation is based on the use of ninety-fifth percentile estimates. If the decision is based on the mean estimates, there will be no benefit of uncertainty reduction assuming that the current mean values of the input parameters are well estimated and do not change with addition of new data.

Table 7.19: Capacity Increase Due to 20% Reduction in Uncertainty (95%-ile)-75 Years with Non-Uniform Loading

Parameters	MTU/Cask	Total MTU	% Increase*
Density of Tuff Rock	9.40	55713.80	19.2%
Specific Heat of Tuff Rock	9.57	56721.39	21.3%
Thermal Conductivity of Tuff Rock	9.49	56247.23	20.3%
All Three Main Contributors	9.96	59032.92	26.3%

*Based on 46757 MTU

8 Discussion

Demonstrated in this thesis is the increase in repository capacity that can result from modifying the SNF loading patterns. Based on the current discharge rate of nuclear reactors the total inventory of SNF in the U.S. will exceed the capacity of the Yucca Mountain repository by 2010. This leaves no room for future SNF discharged from the current nuclear fleet (including during the relicensed period) or future nuclear reactors that potentially will be built. Expansion of the capacity of the Yucca Mountain repository would provide a large economical benefit as siting and developing a second repository would expectedly be lengthy, contentious and expensive process.

Two different loading options were analyzed for this research; variable drift spacing and variable drift thermal loading. Analyses using these two loading options showed that by changing the design specifications of the repository (drift spacing), the amount of waste that could be emplaced in the drifts would be increased - the capacity of the repository would be expanded to accommodate future SNF discharges.

Assuming that the loaded spent fuel casks are directly disposed of at the Yucca Mountain, understanding how different cask loading schemes might affect the repository thermal design limits was of interest. COBRA-SFS was used to analyze the effect of nonuniform loading of spent nuclear fuels into the casks with respect to the peak clad temperature limit of 350˚C. Four different loading cases were analyzed for ambient temperatures of 17.2˚C and 200˚C on the outside of the cask. Results indicated that there is no concern with respect to the cladding surface temperature with the use of non-uniform loading of SNF in the cask over the range of SNF burnup, storage period, irradiation time and enrichment tested.

The burnup of spent fuel was analyzed using data from the DOE database. From this, the decay heat of the SNF was evaluated. Assuming that all the fuel was cooled for a twenty-five year period and that the repository would not be open until 2017, an average was taken to in order to determine the common decay heat profile for both PWR and BWR assemblies. It was determined that the average decay heat was 39,136 and 31,949 MWd/MTU for the PWR and BWR SNF assemblies respectively. In the future these values will most likely increase due to improvements in fuel manufacturing and management resulting in higher burnup fuels.

Using COMSOL Multiphysics the SRTA code was benchmarked with respect to its use for the analyses performed in this research. When compared to the results of the COMSOL conduction and convection models the SRTA code was found to be conservative.
The uncertainties in the input parameters of the model were also investigated for variable drift spacing under both uniform drift loading and variable drift thermal loading. Based on the results there were three main parameters that played important roles in the calculation of the temperatures in the repository. These are the thermal conductivity, specific heat, and the density of the Tuff rock. There exist multiple layers of Tuff rock in the system with varying material properties. The SRTA code is unable to account for different Tuff rock layers. In future investigations, it may be helpful to use a code capable of treating multi material layers.

This study showed that using variable drift spacing or variable drift thermal loading would help to increase the capacity of the Yucca Mountain repository. Based on the test case where the decay heat inventory was represented by an average PWR and BWR SNF, variable drift spacing was found to increase the capacity by about 40% using the mean rock temperature estimates. Although this amount of capacity increase does not represent the actual value due to the hypothetical nature of the test case, the result does indicate the benefit of using variable drift spacing.

In the case of variable drift thermal loading, the age-based mixed loading or decay heat-load based mixed loading would also result in a benefit of capacity increase by over 40%, based on the mean estimates. The number may be somewhat optimistic in this case as the heat flux from each drift was approximated in the model by the drift average value. If the possibility of local hot spots is considered, the estimated benefit would decrease. Nevertheless, the approach seems to have practical benefits in implementing waste loading schemes in the repository.

Uncertainty estimation in the calculation of rock temperatures was facilitated by the use of an efficient repository heat transfer model, SRTA. Although only parameter uncertainty was considered in this study, results showed that the uncertainty in temperature has a major impact in the determination of repository capacity. As the results indicate, the estimate of capacity increase was more than 25% different between the case based on the mean estimates and the case based on the 95th percentile-based estimates. This highlights the importance of reducing the uncertainty in the key input parameters such as thermal conductivity, specific heat, and density of the tuff rocks for the Yucca Mountain repository.

The study of the sensitivity in the uncertainty of density, conductivity, and specific heat of Tuff rock showed that the uncertainty in these parameters has a significant impact on capacity of the repository based on the comparison between the mean and the ninety-fifth percentile estimate cases. For variable drift spacing under uniform loading with a preclosure period of seventy-five years the capacity could be increased by as much as 42.6% based on the mean and 15% based on the ninety-fifth percentile. If the uncertainty in these three parameters is reduced by twenty percent the capacity of the repository will increase by as much as 23.8% based on the ninety-fifth percentile. Analyzing the sensitivity of the specific heat of Tuff rock alone increases the capacity by 20.2% based on the ninety-fifth percentile.

The sensitivity of uncertainties in the density and conductivity of Tuff rock have less impact on the increase of capacity; 15.4% and 17.5% respectively.

Sensitivity of uncertainties in the three parameters for variable drift thermal loading showed a similar result as for the variable drift spacing under uniform loading case. An increase in capacity of 47.9% based on the mean and 17.3% based on the ninety-fifth percentile for non-uniform loading was observed. A twenty percent reduction in uncertainty showed an increase in capacity to 26.3% for all three contributors based on the ninety-fifth percentile. Analyzing the sensitivity in uncertainty for specific heat, conductivity, and density of Tuff individually resulted in an increase in capacity of 21.3%, 20.3%, and 19.2% based on the ninety-fifth percentile. Based on the results of this sensitivity analysis it would be economically viable to analyze the material properties of the Tuff rock in more detail. The analysis of the specific heat alone would be the most beneficial to increasing the capacity of the repository based on the ninety-fifth percentile.

The study also found that the duration of ventilation period prior to the closure of the mountain would have a major impact in the determination of repository capacity; longer ventilation periods would result in an increased capacity. Varying the time of ventilation or preclosure period, however, needs to be justified with respect to the additional cost requirement for the increased repository operation period.

This study showed that the capacity of the Yucca Mountain repository could be increased if proper planning and implementation in the design of the repository was applied. The uncertainty in the model parameters was also of importance in order to investigate the change in the rock temperatures due to uncertainty. Overall this project demonstrates that the current limit of 70,000 MTU can be increased by optimizing the fuel-loading pattern. This is in addition to gains made by increasing the footprint of the repository or increasing the number of levels in the repository.

9 Future Work

Maximizing the repository capacity at Yucca Mountain is a complex issue. The SRTA code is a simplified model that doesn't take into account certain aspects such as cooling by infiltrating water flowing through the system. The hydrology of the mountain will play a role in determining the thermal response of the mountain under the presence of hot spent nuclear fuels. This aspect could not be analyzed using the analytical approach employed in the current study.

The SRTA code was modified from the original TPA code to include non-uniform loading. As discussed in this thesis the code's capability to analyze uniform loading cases was benchmarked but not for the non-uniform loading cases due to the complex nature of the problem. In the future, computer codes that are capable of modeling such complex problems should be used.

Future work could include the investigation of the effect of fluid flow through fractured media in the repository. From this the amount of heat removed from the system due to fluid cooling and the resulting changes in the thermal response of the Mountain can be estimated. Understanding the uncertainty in this estimation is also desirable.

During this research, only a few types of loading schemes were considered. Future work could include optimizing the loading strategies that yield the largest increase in capacity. For example, combining variable drift spacing and variable drift thermal loading is a possible SNF loading strategy. There are other ways to increase the capacity of the repository; including the idea of adopting a multiple-level repository and expanding the repository footprint. These ideas should be investigated further in combinations in order to optimize the capacity estimates for the Yucca Mountain repository.

10 References

Bechtel SAIC Company, LLC (Bechtel 2004). *Ventilation Model and Analysis Report*. ANL-EBS-MD-000030 REV 04. Las Vegas, Nevada: Bechtel SAIC, October 2004

Bechtel SAIC Company, LLC (Bechtel 2005). *Drift Scale THC Seepage Model*. MDL-NBS-HS-000001 REV 04. Las Vegas, Nevada: Bechtel SAIC. February 2005.

Birkholzer, J. T., et al. *Evaluating the Moisture Conditions in the Fractured Rock at Yucca Mountain: The Impact of Natural Convection Processes in Heated Emplacement Drifts*. Berkeley CA: Lawrence Berkley National Laboratory, November 20, 2006.

Buscheck, T.A., et al. *Thermohydrologic Behavior at the Potential Yucca Mountain Nuclear Waste Repository*. Livermore, CA: Lawrence Livermore National Laboratory, February 17, 2000.

Cheon, Myeongguk and Joonhong Ahn. *Expansion of Yucca Mountain Repository Capacity by ATW Fuel Cycle*. GLOBAL 2005 Tsukuba, Japan, 2005.

Claesson, Johan and Thomas Probert. "Temperature Field due to Time-Dependent Heat Sources in a Large Rectangular Grid – Derivation of Analytical Solution." Svensk Kärnbränslehantering AB, SKB TR-96-12, (January 1996): 7-10.

COMSOL, Inc., "*COMSOL Multiphysics 3.3a*", New England Executive Park Suite 350, Burlington, MA 01803, 2007

CRWMS M&O. *License Application Design Selection Report*. B00000000-01717-4600-00123 Las Vegas, Nevada: Civilian Radioactive Waste Management System, Management and Operating Contractor, August 30, 1999.

Decisioneering, Inc., "*Crystal Ball Risk Analysis Software & Solution,*" 2007

Electric Research Power Institute (EPRI 2006). *Program of Technology Innovation: Room at the Mountain – Analysis of the Maximum Disposal Capacity for Commercial Spent Nuclear Fuel in the Yucca Mountain Repository*. Palo Alto, CA: EPRI, May 2006.

Gaski, J., SINDA/G, Network Analysis Associates Inc., Fountain Valley, CA, 1987.

Glascoe, Lee G., et al. *Multiscale Thermohydrologic Model Analyses of Heterogeneity and Thermal-Loading Factors for a Proposed Nuclear Waste Repository*. Livermore, CA: Lawrence Livermore National Laboratory, January 12, 2004.

Itamura, Michael T., et al. *In-Drift Natural Convection Analysis of the Low Temperature Operating Mode (LTOM) Design*. Albuquerque, NM: Sandia National Laboratories, 2003

Johnson, Gary L. *Thermal Performance of a Buried Nuclear Waste Container Storing a Hybrid Mix of PWR and BWR Spent Nuclear Fuel Rods*. Lawrence Livermore National Lab, September 1998.

Li, Jun, et al. *Examining Repository Loading Options to Expand Yucca Mountain Repository Capacity*. Proceedings of GLOBAL 2007, pp. 519-525, 2007

Mansure, Arthur J. and Sharon Patney. *Determination of Equivalent Thermal Loadings as a Function of Waste Age and Burnup*. Albuquerque, NM Sandia National Laboratories, April 1991.

Michels, Walter C. and Sally Wilford. "The Physical Properties of Titanium. I. Emmisivity and Resistivity of the Commercial Metal." Journal of Applied Physics (June 28, 1949): 1223-1226

Michener, T.E., et al. *COBRA-SFS: A Thermal-Hydraulic Analysis Code for Spent Fuel Storage and Transportation Casks*. Pacific Northwest Laboratory. Richland, Washington, September 1995.

Nitao, J. J., Reference Manual for the NUFT Flow and Transport Code, Version 2.0, Lawrence Livermore National Laboratory Report No. UCRL-MA-130651, 1998.

Nuclear Regulatory Commision (NRC 2002). *Total System Performance Assessment (TPA) Version 4.0 Code: Module Descriptions and User's Guide*. Center for Nuclear Waste Regulatory Analyses. San Antonio, Texas, January 2002.

Pruess, K., C. Oldenburg and G. Moridis. TOUGH2 User's Guide, Version 2.0, Lawrence Berkeley National Laboratory Report LBNL-43134, Berkeley, CA, November 1999.

Shropshire, D. E., et al., Advanced Fuel Cycle Cost Basis, INL/EXT-07-12107, Idaho National Laboratory, April, 2007.

Stahala, Mike Peter. *High Level Nuclear Waste Repository Thermal Loading Analysis*. M.S. Thesis, Department of Nuclear Engineering, North Carolina State University, May 2006.

TOUGH2 Homepage (LBNL 2007). June 1, 2007. Lawrence Berkeley National Laboratory, June 25, 2007 <http://www-esd.lbl.gov/TOUGH2/>

U.S. Department of Energy (DOE 1999). *Design Feature Evaluation #12, Waste Package Spacing and Drift Spacing*. Office of Civilian Radioactive Waste Management, April 1999.

U.S. Department of Energy (DOE 2001). *Natural Convection Calculations of Waste Package Drift Emplacement*. Office of Civilian Radioactive Waste Management, September 26, 2001.

U.S. Department of Energy (DOE 2002a). *Yucca Mountain Science and Engineering Report*. Office of Civilian Radioactive Waste Management, February 2002.

U.S. Department of Energy (DOE 2002b). *Spent nuclear fuel discharges from US reactors 2002 RW859_2002.mdb*. Energy Information Administration U.S. Department of Energy, 2002.

U.S. Department of Energy (DOE 2004). *Igneous Intrusion Impacts on Waste Packages and Waste Forms*. Office of Civilian Radioactive Waste Management, April 19, 2004

U.S. Department of Energy (DOE 2007). April 28, 2006. Office of Civilian Radioactive Waste Management, February 26, 2007 <http://www.ocrwm.doe.gov/ym_repository/index.shtml>

Wigeland, Roald A. and Theodore H. Bauer. *Repository Benefits of Partitioning and Transmutation*. OECD/NEA 9th Information Exchange Meeting on Actinide and Fission Product Partitioning and Transmutation. Nimes, France, September 28, 2006.

Xu, T., E.L. Sonnenthal, N. Spycher, and K. Pruess, TOUGHREACT user's guide: A simulation program for non-isothermal multiphase reactive geochemical transport in variably saturated geologic media, Lawrence Berkeley National Laboratory Report LBNL-55460, Berkeley, California, 2004.

Appendices

Appendix A

COBRA-SFS Input

```
99999    0                                                                COBRA.1
    1    1     tn-24 horizontal helium  full-load validation analyses      COBRA.3
prop     6    5                                                           PROP.1
        1.        0.     100.0     .0780      1.24     83.33     .0410    PROP.3
        2.      200.     348.0     .0970      1.24    119.76     .0533
        3.      400.     596.0     .1150      1.24    156.25     .0641
        5.      600.     844.0     .1290      1.24    192.31     .0727
       10.      800.    1092.0     .1380      1.24    229.36     .0823
       15.     1000.    1340.0     .1380      1.24    265.25     .0907
    1 alum                         58.88                                  PROP.4
    2steel                           24.
    3rescu                         10.69
    4radme                        4.0000
    5stilt                         119.0
chan     7   12                                                           CHAN.1
     159.5      90.0                                                      CHAN.3
    1    1  136    0    0                                                 CHAN.5
    1    1    0    0    1                                                 CHAN.6
    1.0663.5750.1657    2.1984 .486                                       CHAN.7
    2.30041.226.6629    3.1410 .486    4.1984 .563
    3.0885.6630.6630    5.1410 .563
    4.30041.226.6629    5.1410 .486    7.1984 .563
    5.17701.3261.326    6.1410 .563    8.1410 .563
    6.0768.7115.4972    9.0790 .563
    7.30041.226.6629    8.1410 .486   11.1984 .563
    8.17701.3261.326    9.1410 .563   12.1410 .563
    9.15351.423.9943   10.0790 .563   13.1410 .563
   10.0768.7115.4972   14.1410 .563
   11.30041.226.6629   12.1410 .486   16.1984 .563
   12.17701.3261.326   13.1410 .563   17.1410 .563
   13.17701.3261.326   14.1410 .563   18.1410 .563
   14.17701.3261.326   15.1410 .563   19.1410 .563
   15.0768.7115.4972   20.0790 .563
   16.30041.226.6629   17.1410 .486   22.1984 .563
   17.17701.3261.326   18.1410 .563   23.1410 .563
   18.15351.423.9943   19.0790 .563   24.0790 .563
   19.15351.423.9943   20.1410 .563   25.0790 .563
   20.15351.423.9943   21.0790 .563   26.1410 .563
   21.0768.7115.4972   27.1410 .563
   22.30041.226.6629   23.1410 .486   29.1984 .563
   23.17701.3261.326   24.1410 .563   30.1410 .563
   24.15351.423.9943   25.0790 .563   31.1410 .563
   25.15351.423.9943   26.1410 .563   32.1410 .563
   26.17701.3261.326   27.1410 .563   33.1410 .563
   27.17701.3261.326   28.1410 .563   34.1410 .563
   28.0885.6630.6630   35.1410 .563
   29.30041.226.6629   30.1410 .486   37.1984 .563
   30.17701.3261.326   31.1410 .563   38.1410 .563
   31.17701.3261.326   32.1410 .563   39.1410 .563
   32.15351.423.9943   33.0790 .563   40.0790 .563
   33.15351.423.9943   34.1410 .563   41.0790 .563
   34.17701.3261.326   35.1410 .563   42.1410 .563
   35.17701.3261.326   36.1410 .563   43.1410 .563
   36.0768.7115.4972   44.0790 .563
```

37.30041.226.6629	38.1410	.486	46.1984	.563
38.17701.3261.326	39.1410	.563	47.1410	.563
39.17701.3261.326	40.1410	.563	48.1410	.563
40.15351.423.9943	41.0790	.563	49.1410	.563
41.15351.423.9943	42.1410	.563	50.1410	.563
42.17701.3261.326	43.1410	.563	51.1410	.563
43.17701.3261.326	44.1410	.563	52.1410	.563
44.15351.423.9943	45.0790	.563	53.1410	.563
45.0768.7115.4972	54.1410	.563		
46.30041.226.6629	47.1410	.486	56.1984	.563
47.17701.3261.326	48.1410	.563	57.1410	.563
48.15351.423.9943	49.0790	.563	58.0790	.563
49.15351.423.9943	50.1410	.563	59.0790	.563
50.17701.3261.326	51.1410	.563	60.1410	.563
51.17701.3261.326	52.1410	.563	61.1410	.563
52.17701.3261.326	53.1410	.563	62.1410	.563
53.17701.3261.326	54.1410	.563	63.1410	.563
54.17701.3261.326	55.1410	.563	64.1410	.563
55.0885.6630.6630	65.1410	.563		
56.30041.226.6629	57.1410	.486	67.1984	.563
57.17701.3261.326	58.1410	.563	68.1410	.563
58.15351.423.9943	59.0790	.563	69.1410	.563
59.15351.423.9943	60.1410	.563	70.1410	.563
60.15351.423.9943	61.0790	.563	71.0790	.563
61.15351.423.9943	62.1410	.563	72.0790	.563
62.17701.3261.326	63.1410	.563	73.1410	.563
63.17701.3261.326	64.1410	.563	74.1410	.563
64.17701.3261.326	65.1410	.563	75.1410	.563
65.17701.3261.326	66.1410	.563	76.1410	.563
66.0768.7115.4972	77.0790	.563		
67.30041.226.6629	68.1410	.486	79.1984	.563
68.17701.3261.326	69.1410	.563	80.1410	.563
69.17701.3261.326	70.1410	.563	81.1410	.563
70.17701.3261.326	71.1410	.563	82.1410	.563
71.15351.423.9943	72.1410	.563	83.0790	.563
72.15351.423.9943	73.1410	.563	84.1410	.563
73.17701.3261.326	74.1410	.563	85.1410	.563
74.15351.423.9943	75.0790	.563	86.0790	.563
75.15351.423.9943	76.1410	.563	87.0790	.563
76.17701.3261.326	77.1410	.563	88.1410	.563
77.15351.423.9943	78.0790	.563	89.1410	.563
78.0768.7115.4972	90.1410	.563		
79.30041.226.6629	80.1410	.486	92.1984	.563
80.17701.3261.326	81.1410	.563	93.1410	.563
81.15351.423.9943	82.0790	.563	94.0790	.563
82.15351.423.9943	83.1410	.563	95.0790	.563
83.17701.3261.326	84.1410	.563	96.1410	.563
84.15351.423.9943	85.0790	.563	97.0790	.563
85.15351.423.9943	86.1410	.563	98.0790	.563
86.15351.423.9943	87.0790	.563	99.1410	.563
87.15351.423.9943	88.1410	.563	100.1410	.563
88.15351.423.9943	89.0790	.563	101.0790	.563
89.15351.423.9943	90.1410	.563	102.0790	.563
90.17701.3261.326	91.1410	.563	103.1410	.563
91.0768.7115.4972	104.0790	.563		
92.30041.226.6629	93.1410	.486	106.1984	.563
93.17701.3261.326	94.1410	.563	107.1410	.563
94.15351.423.9943	95.0790	.563	108.1410	.563
95.15351.423.9943	96.1410	.563	109.1410	.563
96.17701.3261.326	97.1410	.563	110.1410	.563

```
 97.15351.423.9943   98.0790 .563  111.1410 .563
 98.15351.423.9943   99.1410 .563  112.1410 .563
 99.17701.3261.326  100.1410 .563  113.1410 .563
100.17701.3261.326  101.1410 .563  114.1410 .563
101.15351.423.9943  102.0790 .563  115.1410 .563
102.15351.423.9943  103.1410 .563  116.1410 .563
103.17701.3261.326  104.1410 .563  117.1410 .563
104.15351.423.9943  105.0790 .563  118.1410 .563
105.0768.7115.4972  119.1410 .563
106.30041.226.6629  107.1410 .486  121.1984 .563
107.17701.3261.326  108.1410 .563  122 .141 .486
108.17701.3261.326  109.1410 .563  123 .141 .486
109.17701.3261.326  110.1410 .563  124 .141 .486
110.17701.3261.326  111.1410 .563  125 .141 .486
111.17701.3261.326  112.1410 .563  126 .141 .486
112.17701.3261.326  113.1410 .563  127 .141 .486
113.17701.3261.326  114.1410 .563  128 .141 .486
114.17701.3261.326  115.1410 .563  129 .141 .486
115.17701.3261.326  116.1410 .563  130 .141 .486
116.17701.3261.326  117.1410 .563  131 .141 .486
117.17701.3261.326  118.1410 .563  132 .141 .486
118.17701.3261.326  119.1410 .563  133 .141 .486
119.17701.3261.326  120.1410 .563  134 .141 .486
120.0885.6630.6630  135 .141 .486
121.21091.321.3299  122.1984 .486
122.30041.226.6629  123.1984 .563
123.30041.226.6629  124.1984 .563
124.30041.226.6629  125.1984 .563
125.30041.226.6629  126.1984 .563
126.30041.226.6629  127.1984 .563
127.30041.226.6629  128.1984 .563
128.30041.226.6629  129.1984 .563
129.30041.226.6629  130.1984 .563
130.30041.226.6629  131.1984 .563
131.30041.226.6629  132.1984 .563
132.30041.226.6629  133.1984 .563
133.30041.226.6629  134.1984 .563
134.30041.226.6629  135.1984 .563
135.30041.226.6629  136.1984 .486
136.0663.5750.1657
  2    2   57    0    0                                                    CHAN.5
  1    1    0    0    1                                                    CHAN.6
  12.1699.1574.806    2.19844.427    8.19844.427    9.9870 .486            CHAN.7
  22.1699.1574.806    3.19844.427   10 .141 .486
  32.1699.1574.806    4.19844.427   11 .141 .486
  42.1699.1574.806    5.19844.427   12 .141 .486
  52.1699.1574.806    6.19844.427   13 .141 .486
  62.1699.1574.806    7.19844.427   14 .141 .486
  72.1699.1574.806    8.19844.427   15 .141 .486
  82.1699.1574.806   16.19844.427
  91.1518.6198.619   10.14101.971   16.14101.971   17.8460.5630
 101.1518.6198.619   11.14101.971   18 .141 .486
 111.1518.6198.619   12.14101.971   19 .141 .486
 121.1518.6198.619   13.14101.971   20 .141 .486
 131.1518.6198.619   14.14101.971   21 .141 .486
 141.1518.6198.619   15.14101.971   22 .141 .486
 151.1518.6198.619   16.14101.971   23 .141 .486
 161.1518.6198.619   24.8460.5630
 17.89137.6336.132   18 .0793.097   24.1984 .563   25.519 .563
 18.89137.6336.132   19 .0793.097   26 .519 .563
```

```
   19.89137.6336.132   20 .0793.097   27 .519 .563
   20.89137.6336.132   21 .0793.097   28 .519 .563
   21.89137.6336.132   22 .0793.097   29 .519 .563
   22.89137.6336.132   23 .0793.097   30 .519 .563
   23.89137.6336.132   24 .0793.097   31 .519 .563
   24.89137.6336.132   32 .519 .563
   25.71436.3074.806   26 .0792.534   32 .0792.534   33.502 .563
   26.71436.3074.806   27 .0792.534   34 .502 .563
   27.71436.3074.806   28 .0792.535   35 .502 .563
   28.71436.3074.806   29 .0792.534   36 .502 .563
   29.71436.3074.806   30 .0792.534   37 .502 .563
   30.71436.3074.806   31 .0792.534   38 .502 .563
   31.71436.3074.806   32 .0792.534   39 .502 .563
   32.71436.3074.806   40 .502 .563
   33.56084.8843.812   34 .0791.971   40.07901.971   41.361 .563
   34.56084.8843.812   35 .0791.971   42 .361 .563
   35.56084.8843.812   36 .0791.971   43 .361 .563
   36.56084.8843.812   37 .0791.971   44 .361 .563
   37.56084.8843.812   38 .0791.971   45 .361 .563
   38.56084.8843.812   39 .0791.971   46 .361 .563
   39.56084.8843.812   40 .0791.971   47 .361 .563
   40.56084.8843.812   48 .361 .563
   41.43083.3643.149   42 .0791.408   48 .0791.408   49.282 .563
   42.43083.3643.149   43 .0791.408   50 .282 .563
   43.43083.3643.149   44 .0791.408   51 .282 .563
   44.43083.3643.149   45 .0791.408   52 .282 .563
   45.43083.3643.149   46 .0791.408   53 .282 .563
   46.43083.3643.149   47 .0791.408   54 .282 .563
   47.43083.3643.149   48 .0791.408   55 .282 .563
   48.43083.3643.149   56 .282 .563
   49.26551.9891.989   50 .141.8445   56.1410.8445   57.1410 .563
   50.26551.9891.989   51 .141.8445   57 .141 .563
   51.26551.9891.989   52 .141.8445   57 .141 .563
   52.26551.9891.989   53 .141.8445   57 .141 .563
   53.26551.9891.989   54 .141.8445   57 .141 .563
   54.26551.9891.989   55 .141.8445   57 .141 .563
   55.26551.9891.989   56 .141.8445   57 .141 .563
   56.26551.9891.989   57 .141 .563
   57.61405.6923.977
    3    1  136    0    0                                                     CHAN.5
    1    1    0    0    1                                                     CHAN.6
    4    2   57    0    0                                                     CHAN.5
    1    1    0    0    1                                                     CHAN.6
    5    3    1    0    0                                                     CHAN.5
    1    1    0    0    1                                                     CHAN.6
    158.6932.15                                                               CHAN.7
    6    4    1    0    0                                                     CHAN.5
    1    1    0    0    1                                                     CHAN.6
    17.89918.68                                                               CHAN.7
    7    5    1    0    0                                                     CHAN.5
    1    1    0    0    1                                                     CHAN.6
    13.1896.641                                                               CHAN.7

rods     1    1    0    0    1                                                RODS.1
    1    1  120                                                               RODS.2
    1 .422   1.    1 .125    2  .25    3 .125                                 RODS.3
    2 .422   1.    2  .25    3  .25    4  .25    5  .25
    3 .422   1.    3 .125    5  .25    6 .125
    4 .422   1.    4  .25    5  .25    7  .25    8  .25
    5 .422   1.    5  .25    6  .25    8  .25    9  .25
```

6	.422	0.	6	.125	9	.25	10	.125		
7	.422	1.	7	.25	8	.25	11	.25	12	.25
8	.422	1.	8	.25	9	.25	12	.25	13	.25
9	.422	1.	9	.25	10	.25	13	.25	14	.25
10	.422	1.	10	.125	14	.25	15	.125		
11	.422	1.	11	.25	12	.25	16	.25	17	.25
12	.422	1.	12	.25	13	.25	17	.25	18	.25
13	.422	1.	13	.25	14	.25	18	.25	19	.25
14	.422	1.	14	.25	15	.25	19	.25	20	.25
15	.422	0.	15	.125	20	.25	21	.125		
16	.422	1.	16	.25	17	.25	22	.25	23	.25
17	.422	1.	17	.25	18	.25	23	.25	24	.25
18	.422	0.	18	.25	19	.25	24	.25	25	.25
19	.422	1.	19	.25	20	.25	25	.25	26	.25
20	.422	1.	20	.25	21	.25	26	.25	27	.25
21	.422	1.	21	.125	27	.25	28	.125		
22	.422	1.	22	.25	23	.25	29	.25	30	.25
23	.422	1.	23	.25	24	.25	30	.25	31	.25
24	.422	1.	24	.25	25	.25	31	.25	32	.25
25	.422	1.	25	.25	26	.25	32	.25	33	.25
26	.422	1.	26	.25	27	.25	33	.25	34	.25
27	.422	1.	27	.25	28	.25	34	.25	35	.25
28	.422	1.	28	.125	35	.25	36	.125		
29	.422	1.	29	.25	30	.25	37	.25	38	.25
30	.422	1.	30	.25	31	.25	38	.25	39	.25
31	.422	1.	31	.25	32	.25	39	.25	40	.25
32	.422	0.	32	.25	33	.25	40	.25	41	.25
33	.422	1.	33	.25	34	.25	41	.25	42	.25
34	.422	1.	34	.25	35	.25	42	.25	43	.25
35	.422	1.	35	.25	36	.25	43	.25	44	.25
36	.422	0.	36	.125	44	.25	45	.125		
37	.422	1.	37	.25	38	.25	46	.25	47	.25
38	.422	1.	38	.25	39	.25	47	.25	48	.25
39	.422	1.	39	.25	40	.25	48	.25	49	.25
40	.422	1.	40	.25	41	.25	49	.25	50	.25
41	.422	1.	41	.25	42	.25	50	.25	51	.25
42	.422	1.	42	.25	43	.25	51	.25	52	.25
43	.422	1.	43	.25	44	.25	52	.25	53	.25
44	.422	1.	44	.25	45	.25	53	.25	54	.25
45	.422	1.	45	.125	54	.25	55	.125		
46	.422	1.	46	.25	47	.25	56	.25	57	.25
47	.422	1.	47	.25	48	.25	57	.25	58	.25
48	.422	0.	48	.25	49	.25	58	.25	59	.25
49	.422	1.	49	.25	50	.25	59	.25	60	.25
50	.422	1.	50	.25	51	.25	60	.25	61	.25
51	.422	1.	51	.25	52	.25	61	.25	62	.25
52	.422	1.	52	.25	53	.25	62	.25	63	.25
53	.422	1.	53	.25	54	.25	63	.25	64	.25
54	.422	1.	54	.25	55	.25	64	.25	65	.25
55	.422	1.	55	.125	65	.25	66	.125		
56	.422	1.	56	.25	57	.25	67	.25	68	.25
57	.422	1.	57	.25	58	.25	68	.25	69	.25
58	.422	1.	58	.25	59	.25	69	.25	70	.25
59	.422	1.	59	.25	60	.25	70	.25	71	.25
60	.422	0.	60	.25	61	.25	71	.25	72	.25
61	.422	1.	61	.25	62	.25	72	.25	73	.25
62	.422	1.	62	.25	63	.25	73	.25	74	.25
63	.422	1.	63	.25	64	.25	74	.25	75	.25
64	.422	1.	64	.25	65	.25	75	.25	76	.25
65	.422	1.	65	.25	66	.25	76	.25	77	.25

```
 66 .422   0.   66 .125   77  .25   78 .125
 67 .422   1.   67  .25   68  .25   79  .25   80  .25
 68 .422   1.   68  .25   69  .25   80  .25   81  .25
 69 .422   1.   69  .25   70  .25   81  .25   82  .25
 70 .422   1.   70  .25   71  .25   82  .25   83  .25
 71 .422   1.   71  .25   72  .25   83  .25   84  .25
 72 .422   1.   72  .25   73  .25   84  .25   85  .25
 73 .422   1.   73  .25   74  .25   85  .25   86  .25
 74 .422   0.   74  .25   75  .25   86  .25   87  .25
 75 .422   1.   75  .25   76  .25   87  .25   88  .25
 76 .422   1.   76  .25   77  .25   88  .25   89  .25
 77 .422   1.   77  .25   78  .25   89  .25   90  .25
 78 .422   1.   78 .125   90  .25   91 .125
 79 .422   1.   79  .25   80  .25   92  .25   93  .25
 80 .422   1.   80  .25   81  .25   93  .25   94  .25
 81 .422   0.   81  .25   82  .25   94  .25   95  .25
 82 .422   1.   82  .25   83  .25   95  .25   96  .25
 83 .422   1.   83  .25   84  .25   96  .25   97  .25
 84 .422   0.   84  .25   85  .25   97  .25   98  .25
 85 .422   1.   85  .25   86  .25   98  .25   99  .25
 86 .422   1.   86  .25   87  .25   99  .25  100  .25
 87 .422   1.   87  .25   88  .25  100  .25  101  .25
 88 .422   0.   88  .25   89  .25  101  .25  102  .25
 89 .422   1.   89  .25   90  .25  102  .25  103  .25
 90 .422   1.   90  .25   91  .25  103  .25  104  .25
 91 .422   0.   91 .125  104  .25  105 .125
 92 .422   1.   92  .25   93  .25  106  .25  107  .25
 93 .422   1.   93  .25   94  .25  107  .25  108  .25
 94 .422   1.   94  .25   95  .25  108  .25  109  .25
 95 .422   1.   95  .25   96  .25  109  .25  110  .25
 96 .422   1.   96  .25   97  .25  110  .25  111  .25
 97 .422   1.   97  .25   98  .25  111  .25  112  .25
 98 .422   1.   98  .25   99  .25  112  .25  113  .25
 99 .422   1.   99  .25  100  .25  113  .25  114  .25
100 .422   1.  100  .25  101  .25  114  .25  115  .25
101 .422   1.  101  .25  102  .25  115  .25  116  .25
102 .422   1.  102  .25  103  .25  116  .25  117  .25
103 .422   1.  103  .25  104  .25  117  .25  118  .25
104 .422   1.  104  .25  105  .25  118  .25  119  .25
105 .422   1.  105 .125  119  .25  120 .125
106 .422   1.  106  .25  107  .25  121  .25  122  .25
107 .422   1.  107  .25  108  .25  122  .25  123  .25
108 .422   1.  108  .25  109  .25  123  .25  124  .25
109 .422   1.  109  .25  110  .25  124  .25  125  .25
110 .422   1.  110  .25  111  .25  125  .25  126  .25
111 .422   1.  111  .25  112  .25  126  .25  127  .25
112 .422   1.  112  .25  113  .25  127  .25  128  .25
113 .422   1.  113  .25  114  .25  128  .25  129  .25
114 .422   1.  114  .25  115  .25  129  .25  130  .25
115 .422   1.  115  .25  116  .25  130  .25  131  .25
116 .422   1.  116  .25  117  .25  131  .25  132  .25
117 .422   1.  117  .25  118  .25  132  .25  133  .25
118 .422   1.  118  .25  119  .25  133  .25  134  .25
119 .422   1.  119  .25  120  .25  134  .25  135  .25
120 .422   1.  120 .125  135  .25  136 .125
  2    2  105                                                      RODS.2
  1 .422   1.    13.000    93.000                                  RODS.3
  2 .422   1.    23.000   103.000
  3 .422   1.    33.000   113.000
  4 .422   1.    43.000   123.000
```

5	.422	1.	53.000	133.000		
6	.422	1.	63.000	143.000		
7	.422	1.	73.000	153.000		
8	.422	1.	83.000	163.000		
9	.422	1.	92.500	172.500		
10	.422	1.	102.500	182.500		
11	.422	1.	112.500	192.500		
12	.422	1.	122.500	202.500		
13	.422	1.	132.500	212.500		
14	.422	1.	142.500	222.500		
15	.422	1.	152.500	232.500		
16	.422	1.	162.500	242.500		
17	.422	.75	172.000	252.000		
18	.422	.75	182.000	262.000		
19	.422	.75	192.000	272.000		
20	.422	.75	202.000	282.000		
21	.422	.75	212.000	292.000		
22	.422	.75	222.000	302.000		
23	.422	.75	232.000	312.000		
24	.422	.75	242.000	322.000		
25	.422	1.	251.500	331.500		
26	.422	1.	261.500	341.500		
27	.422	1.	271.500	351.500		
28	.422	1.	281.500	361.500		
29	.422	1.	291.500	371.500		
30	.422	1.	301.500	381.500		
31	.422	1.	311.500	391.500		
32	.422	1.	321.500	401.500		
33	.422	1.	331.000	411.000		
34	.422	1.	341.000	421.000		
35	.422	1.	351.000	431.000		
36	.422	1.	361.000	441.000		
37	.422	1.	371.000	451.000		
38	.422	1.	381.000	461.000		
39	.422	1.	391.000	471.000		
40	.422	1.	401.000	481.000		
41	.422	1.	410.500	490.500		
42	.422	1.	420.500	500.500		
43	.422	1.	430.500	510.500		
44	.422	1.	440.500	520.500		
45	.422	1.	450.500	530.500		
46	.422	1.	460.500	540.500		
47	.422	1.	470.500	550.500		
48	.422	1.	480.500	560.500		
49	.422	1.	10.375	80.375	90.125	160.125
50	.422	1.	10.250	20.250	90.250	100.250
51	.422	1.	20.375	30.375	100.125	110.125
52	.422	1.	30.250	40.250	110.250	120.250
53	.422	1.	40.375	50.375	120.125	130.125
54	.422	1.	50.250	60.250	130.250	140.250
55	.422	1.	60.375	70.375	140.125	150.125
56	.422	1.	70.250	80.250	150.250	160.250
57	.422	1.	80.375	90.375	160.125	170.125
58	.422	1.	90.250	100.250	170.250	180.250
59	.422	1.	100.375	110.375	180.125	190.125
60	.422	1.	110.250	120.250	190.250	200.250
61	.422	1.	120.375	130.375	200.125	210.125
62	.422	1.	130.250	140.250	210.250	220.250
63	.422	1.	140.375	150.375	220.125	230.125
64	.422	1.	150.250	160.250	230.250	240.250

```
   65 .422   0.   160.375   170.375   240.125   250.125
   66 .422   1.   170.250   180.250   250.250   260.250
   67 .422   0.   180.375   190.375   260.125   270.125
   68 .422   1.   190.250   200.250   270.250   280.250
   69 .422   0.   200.375   210.375   280.125   290.125
   70 .422   1.   210.250   220.250   290.250   300.250
   71 .422   0.   220.375   230.375   300.125   310.125
   72 .422   1.   230.250   240.250   310.250   320.250
   73 .422   1.   240.375   250.375   320.125   330.125
   74 .422   0.   250.250   260.250   330.250   340.250
   75 .422   1.   260.375   270.375   340.125   350.125
   76 .422   0.   270.250   280.250   350.250   360.250
   77 .422   1.   280.375   290.375   360.125   370.125
   78 .422   0.   290.250   300.250   370.250   380.250
   79 .422   1.   300.375   310.375   380.125   390.125
   80 .422   0.   310.250   320.250   390.250   400.250
   81 .422   0.   320.375   330.375   400.125   410.125
   82 .422   1.   330.250   340.250   410.250   420.250
   83 .422   0.   340.375   350.375   420.125   430.125
   84 .422   1.   350.250   360.250   430.250   440.250
   85 .422   0.   360.375   370.375   440.125   450.125
   86 .422   1.   370.250   380.250   450.250   460.250
   87 .422   0.   380.375   390.375   460.125   470.125
   88 .422   1.   390.250   400.250   470.250   480.250
   89 .422   1.   400.375   410.375   480.125   490.125
   90 .422   1.   410.250   420.250   490.250   500.250
   91 .422   1.   420.375   430.375   500.125   510.125
   92 .422   1.   430.250   440.250   510.250   520.250
   93 .422   1.   440.375   450.375   520.125   530.125
   94 .422   1.   450.250   460.250   530.250   540.250
   95 .422   1.   460.375   470.375   540.125   550.125
   96 .422   1.   470.250   480.250   550.250   560.250
   97 .422   1.   490.375   560.375   570.250
   98 .422   1.   490.250   500.250   570.500
   99 .422   1.   500.375   510.375   570.250
  100 .422   1.   510.250   520.250   570.500
  101 .422   1.   520.375   530.375   570.250
  102 .422   1.   530.250   540.250   570.500
  103 .422   1.   540.375   550.375   570.250
  104 .422   1.   550.250   560.250   570.500
  105 .422   0.   571.000
    3    1  120                                                              RODS.2
    4    2  105                                                              RODS.2
    5    0    0                                                              RODS.2
    6    0    0                                                              RODS.2
    7    0    0                                                              RODS.2
  3.0 .059 655. .366  10.  0.1 409..02431000. .422                          RODS.4
slab    20   18   51                                                         SLAB.1
    1                       3344.3      0.00                                 SLAB.2
    2                          3.4      0.00
    3                        185.6      0.00
    4                       2954.7      0.00
    5                        247.5    29.878  0.5  .887.715
    6                        202.9      0.00
    7                         88.1      0.00
    8                        361.6      0.00
    9                         68.7      0.00
   10                        332.2      0.00
   11                         3.60      0.00
   12                       161.39      0.00
```

```
13                          356.69      0.00
14                          194.48      0.00
15                          353.45
16                          303.43
17                           95.22
18                          713.38
19                          388.96
20                         6217.60
 1     10.858                1     2    18                                          SLAB.3
 2     10.858                1     3    19
 3     10.078                2     4    14     7    19
 4     11.715                1     5    13
 5     11.715                1     6    14
 6     10.078                1    12    14
 7     10.858                1     8    18
 8     10.858                1     9    19
 9     10.078                2    10    14    18    19
10     11.715                1    11    13
11     11.715                1    14    14
12     11.715                1    13    13
13     11.715                1    14    14
14     10.155                2    15    14    24    14
15     11.715                1    16    13
16     11.715                1    17    14
17     10.078                1    26    12
18     10.858                1    19    18
19     10.858                1    20    19
20     10.078                2    21    17    22    14
21     10.151                1    28    20
22     11.715                1    23    16
23     11.280
24     11.715                1    25    15
25     11.684                1    29    20
26     11.397                2    27    11    31    20
27     11.048
28     215.64                2    29    10    32     9
29     215.64                2    30    10    33     9
30     215.64                2    31    10    34     9
31     215.64                1    35     9
32     217.03                2    33     8    36     7
33     217.03                2    34     8    37     7
34     217.03                2    35     8    38     7
35     217.03                1    39     7
36     238.21                2    37     6    40     5
37     238.21                2    38     6    41     5
38     238.21                2    39     6    42     5
39     238.21                1    43     5
40     343.41                2    41     4    44     3
41     343.41                2    42     4    45     3
42     343.41                2    43     4    46     3
43     343.41                1    47     3
44     23.459                2    45     1    48     2
45     23.459                2    46     1    49     2
46     23.459                2    47     1    50     2
47     23.459                1    51     2
48     2
49     2
50     2
51     2
 1      34.65     5.545                                                             SLAB.5
```

```
  2     69.29     2.806
  3     85.38     4.009
  4     140.6     1.386
  5     99.61     1.531
  6     2.032     4.295
  7     1.206     3.665
  8     1.369    4.3505
  9     14.55    0.4094
 10     10.58     0.563
 11     1.394    4.2716
 12     1.834    3.2480
 13     2.181    1.4700
 14     1.369    4.3250
 15     1.369    4.3615
 16     1.369    5.2730
 17     34.65    6.0450
 18     1.369    4.3913
  1    8    1    1    9    1    2   10    1    4   10    1    7   10          SLAB.6
            1   11   10    1   16   10    1   22   10    1   29   10          SLAB.7
  2    8    1   37   10    1   46   10    1   56   10    1   67   10          SLAB.6
            1   79   10    1   92   10    1  106   10    1  121    9          SLAB.7
  4    9    1  121    9    1  122   10    1  123   10    1  124   10          SLAB.6
            1  125   10    1  126   10    1  127   10    1  128   10          SLAB.7
            2    1    8
  5    9    1  129   10    1  130   10    1  131   10    1  132   10          SLAB.6
            1  133   10    1  134   10    1  135   10    1  136    9          SLAB.7
            2    2    8
  7    1    2    8    8                                                      SLAB.6
  8    1    2    7    8
 10    2    2    6    8    4    1    8
 11    2    2    5    8    4    2    8
 12    9    2    3    8    3    1    9    3    2   10    3    4   10          SLAB.6
            3    7   10    3   11   10    3   16   10    3   22   10          SLAB.7
            3   29   10
 13    9    2    4    8    3   29   10    3   46   10    3   56   10          SLAB.6
            3   67   10    3   79   10    3   92   10    3  106   10          SLAB.7
            3  121    9
 15    9    3  121    9    3  122   10    3  123   10    3  124   10          SLAB.6
            3  125   10    3  126   10    3  127   10    3  128   10          SLAB.7
            5    1   15
 16    9    3  129   10    3  130   10    3  131   10    3  132   10          SLAB.6
            3  133   10    3  134   10    3  135   10    3  136    9          SLAB.7
            5    1    8
 18    1    4    8    8                                                      SLAB.6
 19    1    4    7    8
 21    1    6    1   13
 22    2    4    6    8    6    1   18
 23    2    4    5    8    6    1   16
 24    2    4    3    8    5    1    8
 25    2    4    4    8    5    1   14
 26    1    5    1    7
 27    1    7    1    6
 28    1    6    1   17
 29    3    4    5    4    5    1    5    6    1    3
 30    1    5    1    1
 31    2    5    1    2    7    1    2

radg       7    2    3                                                     RADG.1
  1    5                                                                   RADG.2
  11.470  .8    1.0191    2.4664    3.0576    4.0478    5.4091           5 RADG.3
```

```
    26.045   .9    1.1134    2.0431    3.0000    4.2402    5.6033              5
    34.009   .9    1.0211    2.0000    3.0374    4.9158    5.0257              5
    45.273   .8    1.0133    2.2754    3.6962    4.0151    5.0000              5
    54.391   .8    1.1369    2.8305    3.0235    4.0       5.0091              5
    2    8                                                                       RADG.2
    14.351   .8    1.0000    2.0000    3.0163    4.2583    5.1317    6.2192    8 RADG.3
                   7.0928    8.2817                                              RADG.4
    24.325   .8    1.0000    2.0000    3.2078    4.4189    5.0677    6.1126    8 RADG.3
                   7.1105    8.0825                                              RADG.4
    31.531   .9    1.0463    2.5870    3.0000    4.0000    5.0000    6.0503    8 RADG.3
                   7.1092    8.2072                                              RADG.4
    45.545   .9    1.2026    2.3267    3.0000    4.0000    5.0000    6.0339    8 RADG.3
                   7.1900    8.2468                                              RADG.4
    52.806   .9    1.2042    2.1044    3.0000    4.0000    5.0000    6.1895    8 RADG.3
                   7.3127    8.1892                                              RADG.4
    63.665   .8    1.2602    2.1329    3.0210    4.0513    5.1450    6.0000    8 RADG.3
                   7.3051    8.0845                                              RADG.4
    74.351   .8    1.0928    2.1098    3.0384    4.2422    5.2017    6.2571    8 RADG.3
                   7.0000    8.0580                                              RADG.4
    84.362   .8    1.2810    2.0818    3.0727    4.3139    5.1217    6.0710    8 RADG.3
                   7.0579    8.0000                                              RADG.4
    3    2                                                                       RADG.2
    14.295   .8    1.3139    2.6861                                            2 RADG.3
    22.994   .9    1.9843    2.0157                                            2
    1    1    4    1    2    4    5                                              RADG.10
    2    2    8    4    5   12   13   11   10    8    7
    3    1    4   12   13   15   16
    4    2    8   10   11   24   25   23   22   19   18
    5   -2    8   24   25   29   30   31   26   16   15
    6   -1    5   21   28   29   23   22
    7   -3    2   27   31
heat     1    0    1                                                             HEAT.1
                3.66                3.66                                         HEAT.2
  1.0  1.0  1.0  1.0  1.0                                                        HEAT.4
drag     1    5                                                                  DRAG.1
 100. -1.0                100. -1.0                                              DRAG.2
    1   18    0                                                                  DRAG.3
    7    5   120.0388   2..1919   2..3562   2..5204   2..6846   2..8488   2.     DRAG.4
                .9657   2.                                                       DRAG.5
    7    2     2.0388   1..1919   1..3562   1..5204   1..6846   1..8488   1.     DRAG.4
                .9657   1.                                                       DRAG.5
    7    3     4.0388   1..1919   1..3562   1..5204   1..6846   1..8488   1.     DRAG.4
                .9657   1.                                                       DRAG.5
    7    6     7.0388   1..1919   1..3562   1..5204   1..6846   1..8488   1.     DRAG.4
                .9657   1.                                                       DRAG.5
    7   10    11.0388   1..1919   1..3562   1..5204   1..6846   1..8488   1.     DRAG.4
                .9657   1.                                                       DRAG.5
    7   15    16.0388   1..1919   1..3562   1..5204   1..6846   1..8488   1.     DRAG.4
                .9657   1.                                                       DRAG.5
    7   21    22.0388   1..1919   1..3562   1..5204   1..6846   1..8488   1.     DRAG.4
                .9657   1.                                                       DRAG.5
    7   28    29.0388   1..1919   1..3562   1..5204   1..6846   1..8488   1.     DRAG.4
                .9657   1.                                                       DRAG.5
    7   36    37.0388   1..1919   1..3562   1..5204   1..6846   1..8488   1.     DRAG.4
                .9657   1.                                                       DRAG.5
    7   45    46.0388   1..1919   1..3562   1..5204   1..6846   1..8488   1.     DRAG.4
                .9657   1.                                                       DRAG.5
    7   55    56.0388   1..1919   1..3562   1..5204   1..6846   1..8488   1.     DRAG.4
                .9657   1.                                                       DRAG.5
    7   66    67.0388   1..1919   1..3562   1..5204   1..6846   1..8488   1.     DRAG.4
```

```
              .9657   1.                                                        DRAG.5
    7   78   79.0388   1..1919   1..3562   1..5204   1..6846   1..8488   1.     DRAG.4
              .9657   1.                                                        DRAG.5
    7   91   92.0388   1..1919   1..3562   1..5204   1..6846   1..8488   1.     DRAG.4
              .9657   1.                                                        DRAG.5
    7  105  106.0388   1..1919   1..3562   1..5204   1..6846   1..8488   1.     DRAG.4
              .9657   1.                                                        DRAG.5
    7  120  135.0388   1..1919   1..3562   1..5204   1..6846   1..8488   1.     DRAG.4
              .9657   1.                                                        DRAG.5
    7    1    1.0388   .5.1919   .5.3562   .5.5204   .5.6846   .5.8488   .5     DRAG.4
              .9657   .5                                                        DRAG.5
    7  136  136.0388   .5.1919   .5.3562   .5.5204   .5.6846   .5.8488   .5     DRAG.4
              .9657   .5                                                        DRAG.5
    2    2    0                                                                 DRAG.3
    7    9   57.0388   2..1919   2..3562   2..5204   2..6846   2..8488   2.     DRAG.4
              .9657   2.                                                        DRAG.5
    7    1    8.0388   1..1919   1..3562   1..5204   1..6846   1..8488   1.     DRAG.4
              .9657   1.                                                        DRAG.5
    3    1    0                                                                 DRAG.3
    2    1    10.001  1.5.9999  1.5                                             DRAG.4
    4    1    0                                                                 DRAG.3
    2    1    10.001  1.5.9999  1.5                                             DRAG.4
    5    1    0                                                                 DRAG.3
    2    1    10.001  1.5.9999  1.5                                             DRAG.4
bdry    19    1    4    2                                                       BDRY.1
    1   5.24e-8   3.66e+2 0.3333333  .88                                        BDRY.2
    2   4.73e-5
    3   4.60e-5
    4   1.32e-9   7.74e+7 0.3333333  .88
    5   1.89e-6
    6   3.26e-5
    7   1.15e-8   9.85e+4 0.3333333  .88
    8   2.82e-5
    9   9.36e-5
   10   3.94e-6       1.0       .25
   11   2.24e-8
   12   1.89e-7
   13   4.57e-4
   14   5.70e-9   8.02e+5 0.3333333  .88
   15   9.36e-5
   16   6.56e-5
   17   7.05e-5
   18   7.14e-5
   19   1.44e-4
    1    2   0.   63.   1.  63.                                                   BDRY.3
   48    18.820    1                                                            BDRY.5
    1   1.    1   1.    1                                                       BDRY.6
   49    18.820    1                                                            BDRY.5
    1   1.    1   1.    1                                                       BDRY.6
   50    18.820    1                                                            BDRY.5
    1   1.    1   1.    1                                                       BDRY.6
   51    18.820    1                                                            BDRY.5
    1   1.    1   1.    1                                                       BDRY.6
    131.05322.2    7    4  63.  63.                                             BDRY.8
    110.39    8    0                                                            BDRY.9
    20.649   15    0
    3  1.0   16    0
    4  2.0   17    0
    5  3.0   18    0
    6 3.75   19   12   28    2      8.02   29    2      8.02   30    2      8.02 BDRY.9
```

```
                       31    2      8.02   32    2      8.02   33    2      8.02 BDRY.10
                       34    2      8.02   35    2      8.02   36    2      8.02
                       37    2      8.02   38    2      8.02   39    2      8.02
    712.90   14    0                                                              BDRY.9
    1  1.0    8    0                                                              BDRY.11
    2  1.0    9   27    1    4      1.50    2    4      1.50    3    4      1.50 BDRY.11
                        4    4      1.50    5    4      1.50    6    4      1.50 BDRY.12
                        7    4      1.50    8    4      1.50    9    4      1.50
                       10    4      1.50   11    4      1.50   12    4      1.50
                       13    4      1.50   14    4      1.50   15    4      1.50
                       16    4      1.50   17    4      1.50   18    4      1.50
                       19    4      1.50   20    4      1.50   21    4      1.50
                       22    4      1.50   23    4      1.50   24    4      1.50
                       25    4      1.50   26    4      1.50   27    5      1.50
    3  1.0    9    0                                                              BDRY.11
    4  1.0   10    0
    212.85322.2    3    3  63.   63.                                              BDRY.8
    1 1.00    5    0                                                              BDRY.9
    211.31    6   12   28    2      5.61   29    2      5.61   30    2      5.61 BDRY.9
                       31    2      5.61   32    2      5.61   33    2      5.61 BDRY.10
                       34    2      5.61   35    2      5.61   36    2      5.61
                       37    2      5.61   38    2      5.61   39    2      5.61
    315.50    7    0                                                              BDRY.9
    1 1.00    2    0                                                              BDRY.11
    2 1.00    3    0
    3 1.00    4    0
    0                                                                             BDRY.13
calc     1                                                                        CALC.1
  0.0.0001.0001.0001.0001                                                         CALC.2
     500                                                                          CALC.3
oper     1         3    1                                                 1      OPER.1
  00.           145.     1.e-4.001435400      185.  -.000001       0.0           OPER.2
    1    1    1    1                                                              OPER.8
   14                                                                             OPER.16
   0.  0.0.0001  0.0.0002 0.32.0627 0.79.1254 1.04.1881 1.10                      OPER.17
.2508 1.10.5643 1.10.6897 1.10.7524 1.05.8150 0.80.9404 0.18
.9405  0.01.000  0.0
outp 1101                                 2                                       OUTP.1
endd
```

Appendix B

Distributions used in Crystal Ball 7.

Assumption: akcs

Normal distribution with parameters:

Mean	15.486
Std. Dev.	4.2144

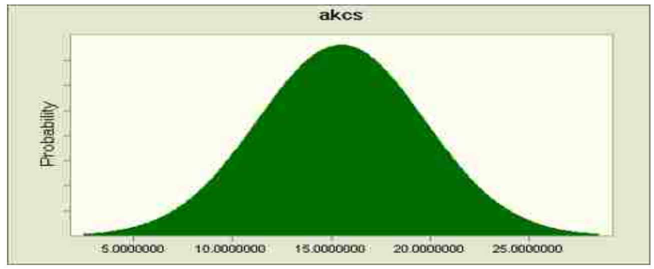

Assumption: akss

Normal distribution with parameters:

Mean	16.615
Std. Dev.	2.0991

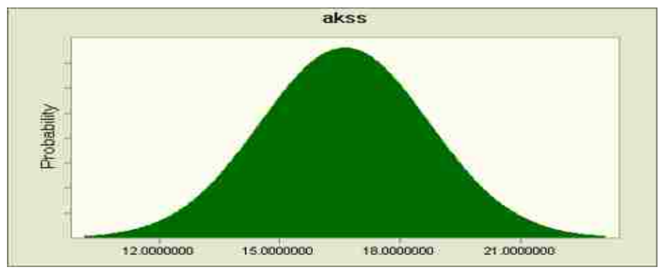

Assumption: cond

Normal distribution with parameters:

Mean	2.603
Std. Dev.	0.3413

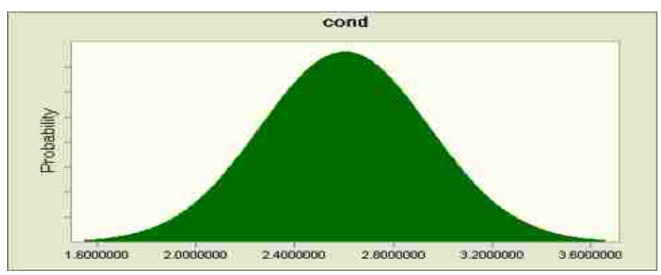

Assumption: condds

Normal distribution with parameters:

Mean	20.002
Std. Dev.	0.7705

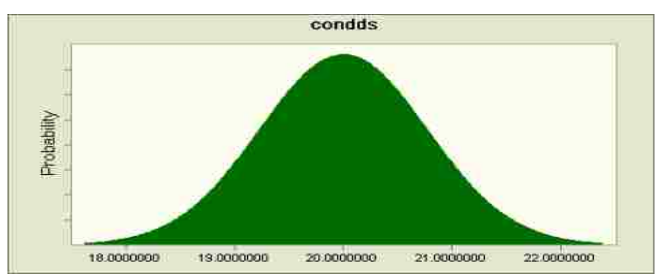

Assumption: Cp

Normal distribution with parameters:

Mean	930
Std. Dev.	170

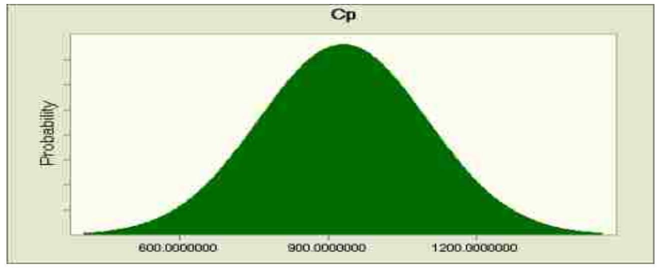

Assumption: driftdia

Normal distribution with parameters:

Mean	5.0
Std. Dev.	0.089

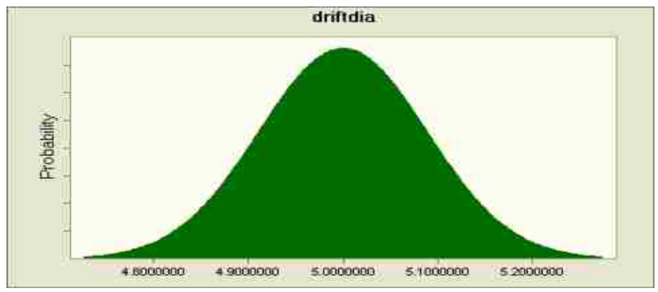

Assumption: emissds

Normal distribution with parameters:

Mean	0.64375
Std. Dev.	0.0472

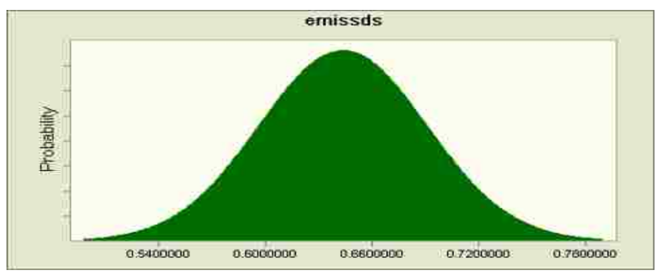

Assumption: emisswp

Normal distribution with parameters:

Mean	0.87
Std. Dev.	0.0232

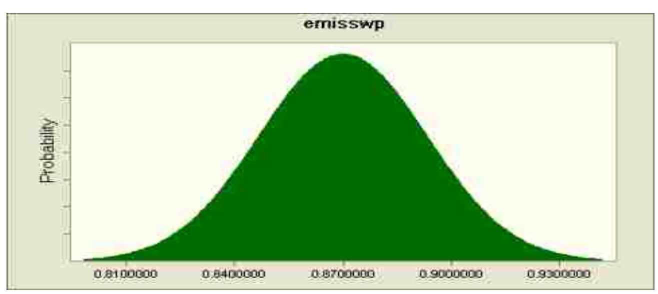

Assumption: hloss_fact

Normal distribution with parameters:

Mean	0.88
Std. Dev.	0.01

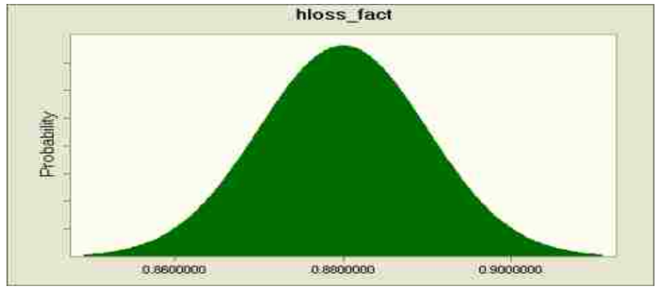

Assumption: rho

Normal distribution with parameters:

Mean	2593
Std. Dev.	138

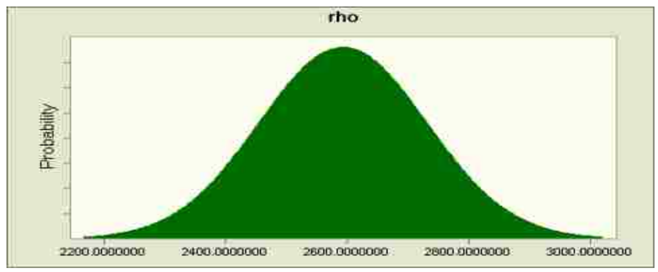

Appendix C

Loading Scheme 1

BWR:	PWR:
0.357	0.643

Drift #	BWR (W/MTU)	PWR (W/MTU)	# WP's	MTU/Cask	Length (m)	Linear Heat Load (kW/m)
1	179.628	362.152	180	7.89	1057	0.40
2	285.775	478.966	181	7.89	1061	0.55
3	320.218	533.738	181	7.89	1066	0.61
4	410.57	584.204	182	7.89	1070	0.70
5	457.216	623.895	183	7.89	1074	0.76
6	461.127	622.863	184	7.89	1079	0.76
7	503.564	660.995	184	7.89	1083	0.81
8	554.84	665.165	185	7.89	1087	0.84
9	538.118	673.453	186	7.89	1092	0.84
10	498.991	731.148	187	7.89	1096	0.87
11	441.28	730.64	187	7.89	1101	0.84
12	506.223	770.11	188	7.89	1105	0.91
13	539.221	738.976	189	7.89	1109	0.90
14	475.887	850.036	190	7.89	1114	0.96
15	562.615	847.677	190	7.89	1118	1.00
16	606.434	909.771	191	7.89	1122	1.08
17	699.513	875.122	192	7.89	1127	1.09
18	698.186	979.456	190	7.89	1116	1.18
19	740.803	1022.064	187	7.89	1098	1.24
20	813.478	1028.916	184	7.89	1079	1.28
21	852.447	1068.016	180	7.89	1060	1.33
22	876.682	1075.645	177	7.89	1042	1.35
23	882.947	1054.18	174	7.89	1023	1.33
24	934.659	1032.438	171	7.89	1004	1.34
25	929.814	1116.023	168	7.89	986	1.41
26	996.252	1217.838	165	7.89	968	1.53
27	1002.31	1229.655	162	7.89	950	1.55
28	980.046	1312.003	159	7.89	932	1.61
29	1070.406	1289.087	151	7.89	887	1.63
30	1118.015	1333.958	143	7.89	842	1.68
31	1122.981	1355.51	135	7.89	796	1.70
32	1176.543	1400.29	128	7.89	751	1.78
33	1193.558	1422.781	120	7.89	705	1.80
34	1290.641	1368.472	112	7.89	660	1.80
35	1159.616	1475.416	61	7.89	614	1.07

Loading Scheme 2

BWR:	PWR:
0.357	0.643

Drift #	BWR (W/MTU)	PWR (W/MTU)	# WP's	MTU/Cask	Length (m)	Linear Heat Load (kW/m)
1	604.812	1094.927	180	7.89	1057	1.24
2	673.129	1036.946	181	7.89	1061	1.22
3	662.409	871.401	181	7.89	1066	1.07
4	745.803	1010.838	182	7.89	1070	1.23
5	668.552	922.449	183	7.89	1074	1.12
6	797.296	960.192	184	7.89	1079	1.21
7	769.369	979.421	184	7.89	1083	1.21
8	719.6	971.42	185	7.89	1087	1.18
9	764.769	947.305	186	7.89	1092	1.19
10	741.498	1036.501	187	7.89	1096	1.25
11	715.44	881.403	187	7.89	1101	1.10
12	698.874	941.199	188	7.89	1105	1.15
13	789.8	887.258	189	7.89	1109	1.15
14	756.141	961.853	190	7.89	1114	1.20
15	762.586	929.44	190	7.89	1118	1.17
16	750.426	847.706	191	7.89	1122	1.09
17	662.571	819.708	192	7.89	1127	1.03
18	765.87	827.264	190	7.89	1116	1.08
19	691.345	944.42	187	7.89	1098	1.15
20	644.505	863.801	184	7.89	1079	1.06
21	748.513	925.864	180	7.89	1060	1.16
22	633.632	889.11	177	7.89	1042	1.07
23	684.852	883.61	174	7.89	1023	1.09
24	679.942	906.317	171	7.89	1004	1.11
25	672.43	909.499	168	7.89	986	1.11
26	631.731	852.264	165	7.89	968	1.04
27	709.243	883.228	162	7.89	950	1.11
28	688.201	873.293	159	7.89	932	1.09
29	689.848	899.951	151	7.89	887	1.11
30	605.723	863.649	143	7.89	842	1.03
31	657.422	853.743	135	7.89	796	1.05
32	697.62	903.549	128	7.89	751	1.12
33	595.619	909.551	120	7.89	705	1.07
34	687.215	902.782	112	7.89	660	1.11
35	753.426	845.206	61	7.89	614	0.64

Loading Scheme 3

BWR:	PWR:
0.357	0.643

Drift #	BWR (W/MTU)	PWR (W/MTU)	# WP's	MTU/Cask	Length (m)	Linear Heat Load (kW/m)
1	83.85	1539.359	180	7.89	1057	1.37
2	335.402	1289.002	181	7.89	1061	1.28
3	351.579	1278.947	181	7.89	1066	1.27
4	430.995	1239.555	182	7.89	1070	1.28
5	478.212	1129.706	183	7.89	1074	1.21
6	531.649	1042.823	184	7.89	1079	1.16
7	587.925	1018.191	184	7.89	1083	1.16
8	631.003	988.376	185	7.89	1087	1.16
9	689.336	966.689	186	7.89	1092	1.17
10	691.521	1005.357	187	7.89	1096	1.20
11	724.96	978.251	187	7.89	1101	1.19
12	722.406	952.838	188	7.89	1105	1.17
13	744.234	981.437	189	7.89	1109	1.21
14	748.221	937.573	190	7.89	1114	1.17
15	781.865	934.225	190	7.89	1118	1.18
16	780.814	912.847	191	7.89	1122	1.16
17	804.283	888.586	192	7.89	1127	1.15
18	801.167	850.148	190	7.89	1116	1.12
19	795.894	816.823	187	7.89	1098	1.09
20	804.089	791.259	184	7.89	1079	1.07
21	813.454	762.831	180	7.89	1060	1.05
22	805.366	782.439	177	7.89	1042	1.06
23	811.23	759.608	174	7.89	1023	1.04
24	819.79	751.607	171	7.89	1004	1.04
25	828.776	744.414	168	7.89	986	1.04
26	830.507	740.127	165	7.89	968	1.04
27	831.141	724.856	162	7.89	950	1.03
28	828.243	725.988	159	7.89	932	1.03
29	836.833	722.095	151	7.89	887	1.02
30	834.157	718.039	143	7.89	842	1.02
31	836.539	724.589	135	7.89	796	1.02
32	838.427	719.946	128	7.89	751	1.03
33	832.952	729.415	120	7.89	705	1.03
34	840.31	722.103	112	7.89	660	1.02
35	838.218	725.108	61	7.89	614	0.60

Loading Scheme 4

BWR:	PWR:
0.357	0.643

Drift #	BWR (W/MTU)	PWR (W/MTU)	# WP's	MTU/Cask	Length (m)	Linear Heat Load (kW/m)
1	179.628	362.152	180	7.89	1057	0.40
2	1194.544	1406.474	181	7.89	1061	1.79
3	333.846	479.545	181	7.89	1066	0.57
4	1025.51	1418.882	182	7.89	1070	1.72
5	465.124	534.986	183	7.89	1074	0.69
6	1002.114	1361.371	184	7.89	1079	1.66
7	554.872	583.638	184	7.89	1083	0.77
8	981.939	1329.331	185	7.89	1087	1.62
9	589.721	627.165	186	7.89	1092	0.83
10	917.566	1296.755	187	7.89	1096	1.56
11	602.82	623.9	187	7.89	1101	0.83
12	802.811	1251.968	188	7.89	1105	1.47
13	650.556	641.757	189	7.89	1109	0.87
14	887.111	1233.371	190	7.89	1114	1.49
15	634.202	696.465	190	7.89	1118	0.90
16	868.468	1139.138	191	7.89	1122	1.40
17	593.211	672.542	192	7.89	1127	0.87
18	841.235	1044.922	190	7.89	1116	1.31
19	578.786	705.802	187	7.89	1098	0.89
20	840.518	1049.785	184	7.89	1079	1.31
21	570.614	747.786	180	7.89	1060	0.92
22	785.345	1085.638	177	7.89	1042	1.31
23	516.854	785.336	174	7.89	1023	0.93
24	792.201	1057.913	171	7.89	1004	1.29
25	586.67	741.964	168	7.89	986	0.92
26	769.153	1030.067	165	7.89	968	1.26
27	553.348	810.189	162	7.89	950	0.97
28	761.716	1029.013	159	7.89	932	1.26
29	603.276	876.223	151	7.89	887	1.05
30	704.638	991.27	143	7.89	842	1.19
31	590.308	832.943	135	7.89	796	1.00
32	660.893	924.662	128	7.89	751	1.12
33	621.844	935.334	120	7.89	705	1.11
34	698.776	872.807	112	7.89	660	1.09
35	727.277	953.747	61	7.89	614	0.68

Loading Scheme 5

BWR:	PWR:
0.357	0.643

Drift #	BWR (W/MTU)	PWR (W/MTU)	# WP's	MTU/Cask	Length (m)	Linear Heat Load (kW/m)
1	1343.72	1603.721	180	7.89	1057	2.03
2	147.015	261.002	181	7.89	1061	0.30
3	1131.244	1478.338	181	7.89	1066	1.82
4	323.887	350.344	182	7.89	1070	0.46
5	1008.725	1406.51	183	7.89	1074	1.70
6	415.928	426.766	184	7.89	1079	0.57
7	935.354	1354.47	184	7.89	1083	1.62
8	492.893	508.007	185	7.89	1087	0.67
9	878.54	1307.488	186	7.89	1092	1.55
10	538.956	549.914	187	7.89	1096	0.73
11	847.217	1264.037	187	7.89	1101	1.50
12	578.404	586.306	188	7.89	1105	0.78
13	809.309	1230.071	189	7.89	1109	1.45
14	611.562	622.419	190	7.89	1114	0.83
15	778.668	1193.76	190	7.89	1118	1.40
16	636.919	652.197	191	7.89	1122	0.87
17	758.268	1154.508	192	7.89	1127	1.36
18	654.514	685.3	190	7.89	1116	0.91
19	740.062	1120.331	187	7.89	1098	1.32
20	661.538	720.255	184	7.89	1079	0.94
21	718.658	1082.64	180	7.89	1060	1.28
22	664.913	749.264	177	7.89	1042	0.96
23	722.525	1059.066	174	7.89	1023	1.26
24	657.058	777.088	171	7.89	1004	0.99
25	721.192	1019.989	168	7.89	986	1.23
26	646.628	807.409	165	7.89	968	1.01
27	716.685	993.02	162	7.89	950	1.20
28	653.18	825.752	159	7.89	932	1.03
29	706.764	955.737	151	7.89	887	1.16
30	647.448	849.691	143	7.89	842	1.04
31	697.268	933.826	135	7.89	796	1.14
32	654.672	868.454	128	7.89	751	1.07
33	689.48	912.459	120	7.89	705	1.12
34	661.994	884.628	112	7.89	660	1.08
35	674.773	899.248	61	7.89	614	0.64

Appendix D

Rank correlation for non-uniform loading with a preclosure period of 50 years.

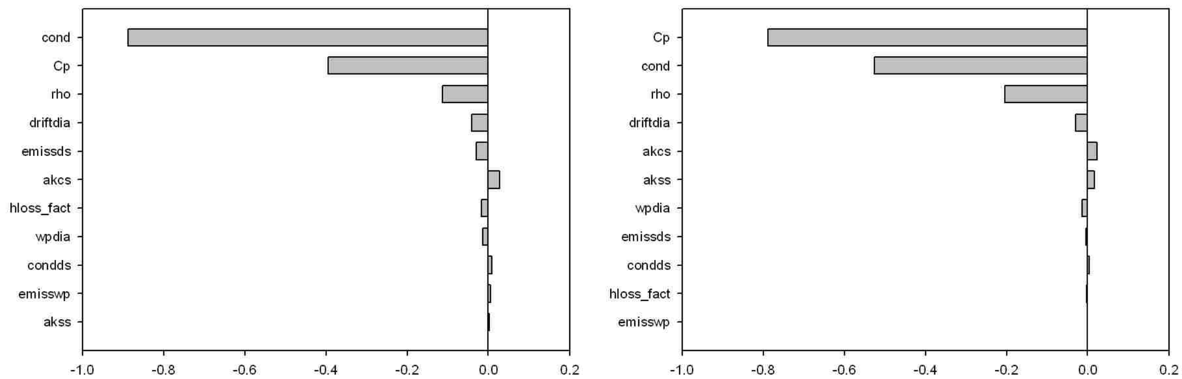

(a) (b)

Loading Scheme 2: (a) Drift Wall (b) Between Drift

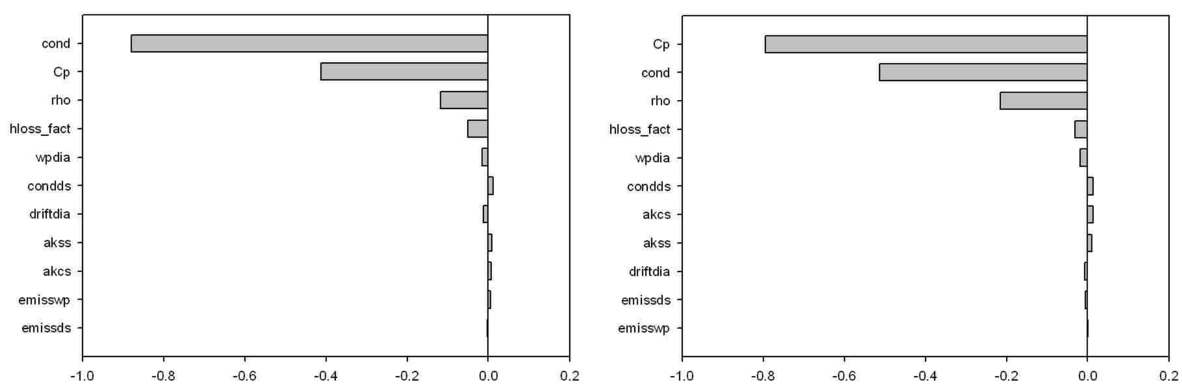

(a) (b)

Loading Scheme 3: (a) Drift Wall (b) Between Drift

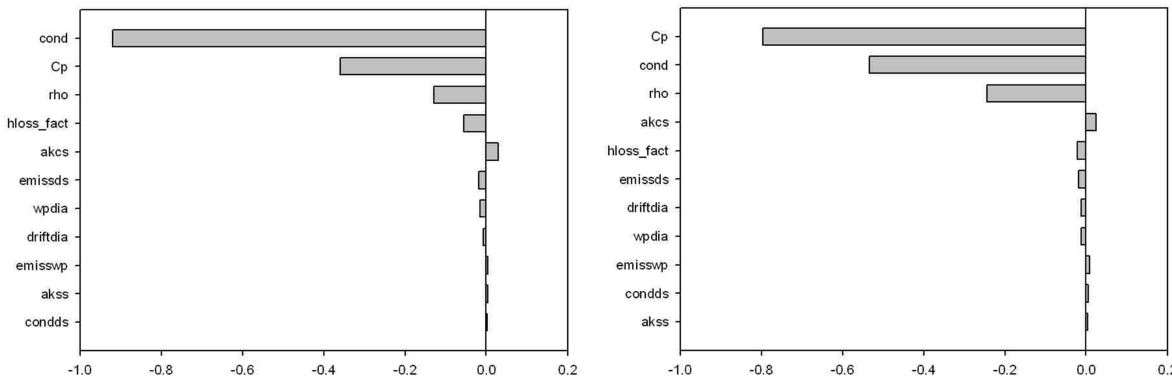

(a) (b)

Loading Scheme 4: (a) Drift Wall (b) Between Drift

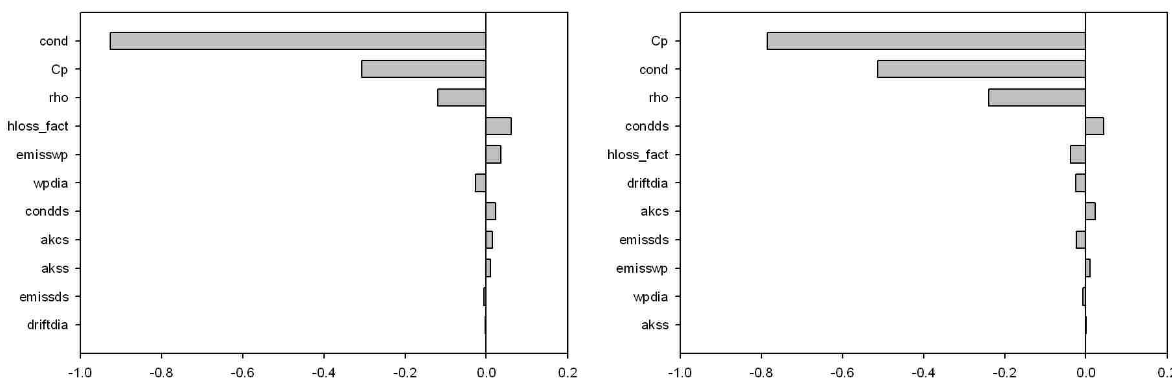

(a) (b)

Loading Scheme 5: (a) Drift Wall (b) Between Drift

Appendix E

Rank correlation for non-uniform loading with a preclosure period of 75 years.

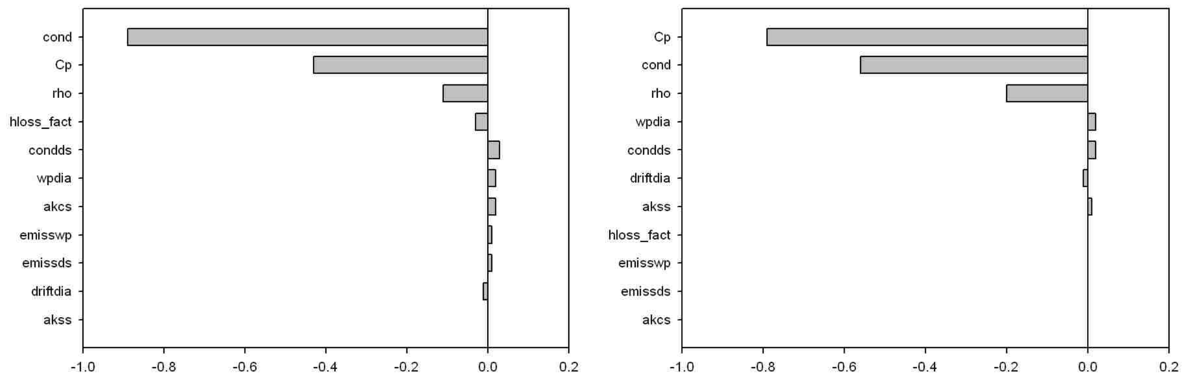

(a) (b)

Loading Scheme 2: (a) Drift Wall (b) Between Drift

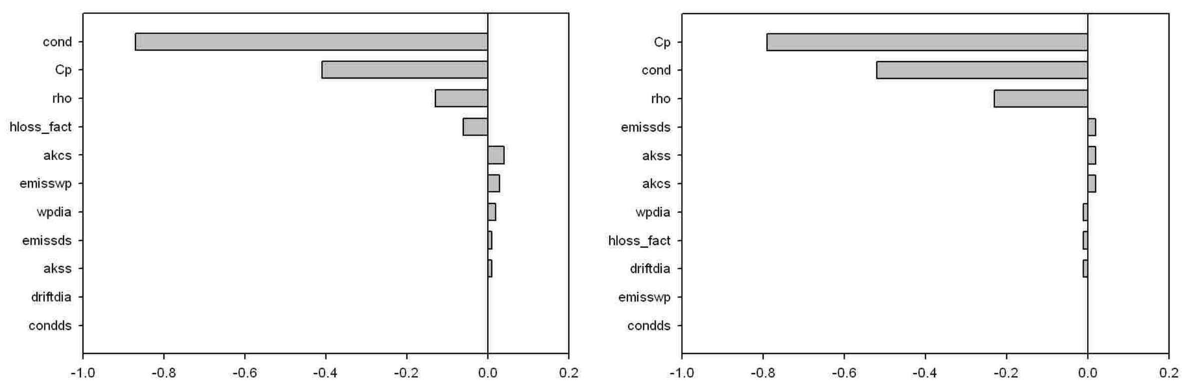

(a) (b)

Loading Scheme 3: (a) Drift Wall (b) Between Drift

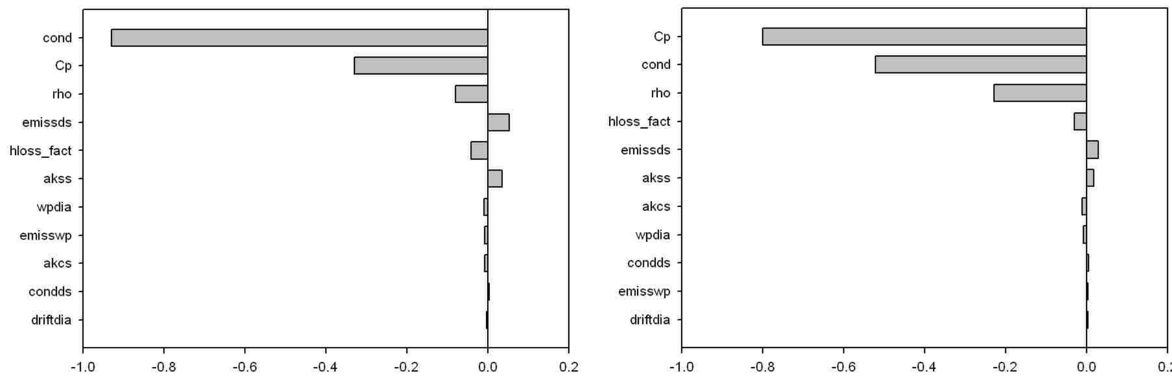

(a) (b)

Loading Scheme 4: (a) Drift Wall (b) Between Drift

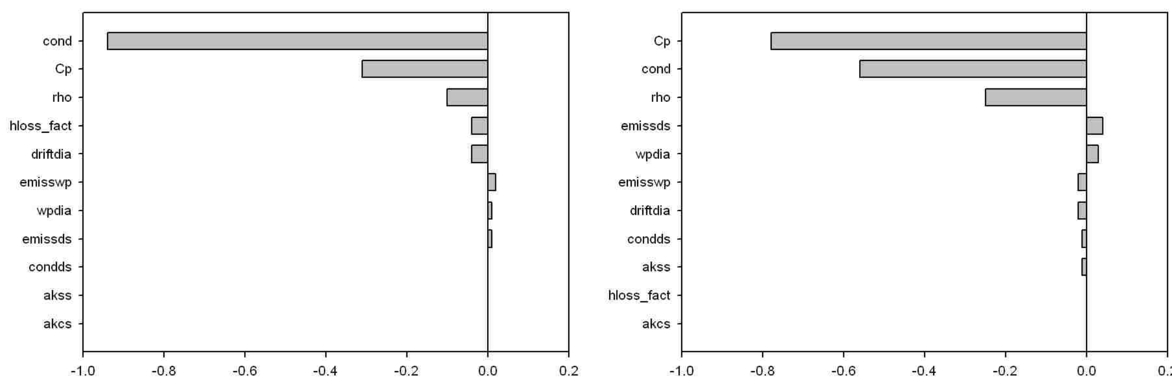

(a) (b)

Loading Scheme 5: (a) Drift Wall (b) Between Drift